Open Research Online

The Open University's repository of research publications
and other research outputs

Subaqueous basaltic magmatic explosions trigger phreatomagmatism: a case study from Askja, Iceland

Journal Item

How to cite:

Graettinger, Alison H.; Skilling, Ian; McGarvie, Dave and Höskuldsson, Ármann (2013). Subaqueous basaltic magmatic explosions trigger phreatomagmatism: a case study from Askja, Iceland. Journal of Volcanology and Geothermal Research, 264 pp. 17–35.

For guidance on citations see FAQs.

© 2013 Elsevier B.V.

Version: Accepted Manuscript

Link(s) to article on publisher's website:
http://dx.doi.org/doi:10.1016/j.jvolgeores.2013.08.001
http://www.scopus.com/inward/record.url?eid=2-s2.0-84883863002&partnerID=40&md5=8dde60368d7cf231fff4b0a9b3bcf5a3

Copyright and Moral Rights for the articles on this site are retained by the individual authors and/or other copyright owners. For more information on Open Research Online's data policy on reuse of materials please consult the policies page.

oro.open.ac.uk

Elsevier Editorial System(tm) for Journal of Volcanology and Geothermal Research
Manuscript Draft

Manuscript Number: VOLGEO4033R1

Title: Subaqueous basaltic magmatic explosions trigger phreatomagmatism: a case study from Askja, Iceland

Article Type: Research Paper

Keywords: magma fragmentation; phreatomagmatic explosions; basalt; subaqueous eruption

Corresponding Author: Dr. Alison H. Graettinger, PhD

Corresponding Author's Institution: University at Buffalo

First Author: Alison H. Graettinger, PhD

Order of Authors: Alison H. Graettinger, PhD; Ian P Skilling; Dave W McGarvie; Armann Hoskuldsson

Abstract: Sequences of basaltic pillow lavas that transition upwards with systematic gradation from pillow fragment breccias to fluidal bomb-bearing breccia to bomb-bearing lapilli tuffs are common at Askja volcano, Iceland. Based on the detailed textural investigation of three of these sequences, we argue that they record temporally continuous transition from effusive to explosive products that were erupted from and deposited at or near a single subaqueous vent. The recognition of such sequences is important as they provide evidence for controls on the onset of explosive activity in subaqueous environments. Such investigations are complicated by the interplay of magmatic gas expansion, phreatomagmatic and mechanical granulation fragmentation mechanisms in the subaqueous eruptive environment.

All of the sequences studied at Askja have textural, componentry and sedimentological characteristics suggestive of a close genetic and spatial relationship between the pillow lavas and all of the overlying glassy clastic deposits. The identification of magma fragmentation signatures in pyroclasts was accomplished through detailed textural studies of pyroclasts within the full range of grain sizes of a given deposit i.e. bomb/blocks, lapilli and fine ash. These textural characteristics were compared and evaluated as discriminators of fragmentation in pyroclastic deposits. The presence of angular vitric clasts within the breccia and lapilli tuff displaying fragile glassy projections indicates little or no post-depositional textural modification. A shift in vesicle and clast textures between the pillow lavas and the large concentration of fluidal bombs in the breccia indicate that the phreatomagmatic explosions were initially triggered by magmatic vesiculation. The initial magmatic gas expansion may have been triggered by depressurization caused by the drainage of the ice-confined lake surrounding Askja. The Fuel Coolant Interactions (FCI) of the more efficient phreatomagmatic explosion was enabled by the increase in the surface area to volume ratio of the fluidal bombs in the water, producing a premix of magma and water. The onset and increasing influence of phreatomagmatic fragmentation is preserved in the presence of very fine blocky ash particles and diminished presence of larger particles such as fluidal bombs. The textural, sedimentological and environmental characteristics of these deposits suggest that phreatomagmatic explosions can be triggered by initial magmatic gas expansion, but that it is likely one of many mechanisms for triggering such explosions.

June 24, 2013

Journal of Volcanology and Geothermal Research

Revisions

Dear Dr. Wilson-

Enclosed is my revision of my submission to JVGR. I have attempted to address the issues/comments made by the reviewers throughout the manuscript. Comments regarding the revisions occur in the 'revision notes' portion of the revised submission. In general these adjustments removed redundancies and therefore shortened the manuscript length.

Please note that I completed this work at the University at Pittsburgh, but my current location is the University at Buffalo. I would like the affiliations in the ms to reflect this.

Thank you for the timely and thoughtful reviews of this manuscript. If there are any questions please feel free to contact me.

Scincerely,

Alison Graettinger

Center for Geohazard Studies

University at Buffalo

Buffalo, NY 14260

agraettinger@gmail.com

Revision NotesJVGR.docx
Click here to download Response to Reviewers: Revision NotesJVGR.docx

Revision Notes:

Reviewer 1

The reviewer's comments about repetition in the manuscript, particularly in sections 3-4 have been addressed through some reorganization and deletion of repetitive phrasing. Section three now addresses the specific lithologies first and then addresses the dimensions and variables of the individual deposits. This removes the need for the 'overview' section.

The changes noted in the 'Revision, changes marked' manuscript focus on rewording or major reorganization and does not have all minor grammatical corrections or formatting changes included (i.e. changing table numbers).

The Abstract has been shortened by removing unnecessary detail and a comment referencing the summary of the large table was included.

Consequently, the ms is now roughly 600 words and 3 tables shorter.

Table 2 was removed due to repetition with information in figure 7.

Table 4 was removed because of repetition from text and Figure 7.

Table 5 was removed and paraphrased in text (lines 896-901).

Figure 6: Field images of clast types were included with the schematics to highlight the different morphologies.

Figure 7: Additional notation was included to indicate the percentage type in the figure and the caption was rewritten to address each grain size dataset included in the figure.

Figure 8: Brightness and contrast were adjusted on field images of fluidal bombs to help highlight the clast shape. If this is insufficient annotation of the image may further resolve this issue. The missing labels have been restored.

Table 3 (now 2) was expanded to include a Limu section. And the additional suggested references were included.

Specific comments from the annotated PDF: All comments were addressed to some degree. In particular all grammatical suggestions were incorporated.

The volatile data analysis referenced in the paper is sourced from Cameron unpublished data. This is noted in the text (section 3.0), and later references to this data set reference back to the section which describes it.

Points of ‘careful wording’ were revised as suggested i.e. magmatic volatiles and external water were used exclusively instead of previous more confusing terms (section 4) .

Reviewer 2

Sample numbers were added to SEM analyses for the purpose of highlighting uncertainty. Line 335-336.

All references to percent were annotated with appropriate vol. or wt. or abundance. Measurements based on 2D and 3 D analysis were clarified.

Highlights

1) Textural investigation of subaqueous basaltic effusion to explosion transition.
2) Example of subaqueous magmatic explosions triggering phreatomagmatism.
3) Evaluation of textures for identifying basaltic fragmentation mechanisms.

EFFrevisions.final.docx
Click here to view linked References

Subaqueous basaltic magmatic explosions trigger phreatomagmatism: a case study from Askja, Iceland

Alison H. Graettinger[1], Ian Skilling[2], Dave McGarvie[3], Ármann Höskuldsson[4]

1Alison H. Graettinger (corresponding author)
University of Pittsburgh, 200 SRCC, Pittsburgh PA, 15260
*Currently:
University at Buffalo, Center for Geohazard Studies, 411 Cooke Hall, Buffalo, NY 14260
Telephone: +17166454286
agraettinger@gmail.com

2Ian P. Skilling
University of South Wales, Pontypridd, RCT, CF37 4BD, UK
Telephone: +44 1443 654151
ipskilling@gmail.com

3Dave W. McGarvie
The Open University in Scotland, 10 Drumsheugh Gardens, Edinburgh, EH3 7QJ, UK
Telephone: +44 (0) 131 226 3851
Dave.mcgarvie@open.ac.uk

4Ármann Höskuldsson
The University of Iceland, Askja, Sturlagata 7, 101 Reykjavik, Iceland
Telephone +354-5254215
armh@hi.is

Abstract

Sequences of basaltic pillow lavas that transition upwards with systematic gradation from pillow fragment breccias to fluidal bomb-bearing breccia to bomb-bearing lapilli tuffs are common at Askja volcano, Iceland. Based on the detailed textural investigation of three of these sequences, we argue that they record temporally continuous transition from effusive to explosive products that were erupted from and deposited at or near a single subaqueous vent. The recognition of such sequences is important as they provide evidence for controls on the onset of explosive activity in subaqueous environments. Such investigations are complicated by the interplay of magmatic gas expansion, phreatomagmatic and mechanical granulation fragmentation mechanisms in the subaqueous eruptive environment.

All of the sequences studied at Askja have textural, componentry and sedimentological characteristics suggestive of a close genetic and spatial relationship between the pillow lavas and all of the overlying glassy clastic deposits. The identification of magma fragmentation signatures in pyroclasts was accomplished through detailed textural studies of pyroclasts within the full range of grain sizes of a given deposit i.e. bomb/blocks, lapilli and fine ash. These textural characteristics were compared and evaluated as discriminators of fragmentation in pyroclastic deposits. The presence of angular vitric clasts within the breccia and lapilli tuff displaying fragile glassy projections indicates little or no post-depositional textural modification. A shift in vesicle and clast textures between the pillow lavas and the large concentration of fluidal bombs in the breccia indicate that the phreatomagmatic explosions were initially triggered by magmatic vesiculation. The initial magmatic gas expansion may have been triggered by depressurization caused by the drainage of the ice-confined lake surrounding Askja. The Fuel Coolant Interactions

(FCI) of the more efficient phreatomagmatic explosion was enabled by the increase in the surface area to volume ratio of the fluidal bombs in the water, producing a premix of magma and water. The onset and increasing influence of phreatomagmatic fragmentation is preserved in the presence of very fine blocky ash particles and diminished presence of larger particles such as fluidal bombs. The textural, sedimentological and environmental characteristics of these deposits suggest that phreatomagmatic explosions can be triggered by initial magmatic gas expansion, but that it is likely one of many mechanisms for triggering such explosions.

Keywords: magma fragmentation; phreatomagmatic explosions; basalt; subaqueous eruption

1.0 Introduction

The question of what controls the transition of basaltic effusive to explosive activity in water-rich environments, has been a matter of debate over the last 20 years (Houghton and Nairn 1991; Houghton and Schmincke 1989; Mastin et al. 2004; White 1996; Wohletz 1986; Wohletz 2002; Wohletz 2003; Zimanowski et al. 1997; Zimanowski et al. 2003). The answer to this question has important implications for modeling volcanic hazards, such as the potential for explosions or the grain size distribution, height and duration of ash plumes in wet environments. Submarine exploration technology has advanced our ability to describe subaqueous explosive volcanic deposits from the submarine environment (Clague et al. 2003; Clague and Davis 2003; Clague et al. 2009; Eissen et al. 2003). However, the study of explosively generated deposits formed in an ice-confined (glaciovolcanic) environment offers much more accessible deposits that are commonly well preserved in three-dimensions. We argue that such centers preserve sequences that record in situ transitions from effusive to explosive activity at a single vent. The detailed

textural and stratigraphic study of such sequences offers the best opportunity for understanding the onset of explosive activity and the interplay of fragmentation mechanisms in natural subaqueous settings.

The focus of this study is three ca. 30 m thick, glass-rich, incipiently palagonitized basaltic pyroclastic deposits that directly overlie pillow lavas from Askja volcano, Iceland (Fig. 1). All three clastic sequences are massive but display a systematic and continuous fining upward from pillow-fragment breccia to fluidly-shaped bomb-bearing breccia and then into vitric lapilli tuff. Ostensibly similar sequences of pillow lavas overlain by breccias, containing pillow fragments, capped by vitric lapilli tuffs, have been described from many areas, including ophiolite sequences (Carlisle 1963), Archean basalt provinces (Dimroth et al. 1978), ocean island settings (Fujibayashi and Sakai 2003) and several glaciovolcanic sequences (Jones 1970; Skilling 2009; Werner and Schmincke 1999). Such sequences could clearly be derived through many processes. Common interpretations for these sequences can be divided into those where the clastic deposits are (1) erupted from a different vent than that which produced the lavas, (2) were produced by the same vent that produced the lavas but not as part of a temporally continuous eruption, (3) or were erupted from the same vent as lavas and were part of a continuous eruption. Mechanisms that produce unrelated sequences of pillow lavas and clastic deposits include deposition of density currents from nearby vents or post-emplacement collapse of deposits on top of the pillows. Similar sequences produced from the same vent without continuous eruption include flow related collapse (autoclastic breccias), intrusion of pillowed dikes into clastic deposits, or explosive activity instigated under already solidified lava. Based on a detailed textural analysis of the sequences from the Austurfjöll massif of Askja, we argue that the

deposits were produced from the same vent over a brief eruption that transitioned from effusive activity to magmatic explosive, and then to phreatomagmatic explosive eruptive activity.

The interpretation of such clastic deposits relies heavily on the distinction of the influence of different fragmentation mechanisms in the formation of subaqueous basaltic pyroclasts along the contact between facies within the transitional sequences. Evidence for the mechanisms of fragmentation, transportation and deposition are preserved in the textures of subaqueous pyroclasts over the full range of grain sizes, including bombs, lapilli and fine ash, though most research has focused on fine ash textures (Büttner et al. 1999; De Rosa 1999; Dellino et al. 2001; Dellino and Liotino 2002; Durig et al. 2012; Ersoy et al. 2006; Heiken 1971; Mattox and Mangan 1997). These textural data can then be used to make inferences on the controls of the onset of subaqueous explosive activity and specifically phreatomagmatic activity. In this study we present data on textural characteristics of fine ash to block-sized clasts that could be used to help distinguish phreatomagmatic from magmatic fragmentation, and argue that the phreatomagmatic eruptions in our study area were generated following an initial mingling (premixing) of magma and water driven by magmatic fragmentation. It is not clear how important or common initial mingling by magmatic fragmentation might be in basaltic phreatomagmatic sequences elsewhere, and is likely only one mechanism for instigating such eruptions. The uniquely dynamic nature of the ice-confined lakes may play a role in the initiation of magmatic gas expansion through depressurization caused by lake drainage. Nevertheless, similar textural investigations may be used to identify the mechanisms during the onset of exposivity in other basaltic phreatomagmatic systems.

1.1 Eruption setting

Basaltic glaciovolcanic systems under thick ice (>400 m) typically evolve into ice-confined lacustrine centers (Allen et al. 1982; Gudmundsson 2003; Gudmundsson et al. 1997; Werner and Schmincke 1999). Within the ice-confined lake the water level may change rapidly and repeatedly through time (Bjornsson 2002; Gudmundsson et al. 1997; Höskuldsson et al. 2006; Smellie et al. 2008). Simplified models of such centers include initial subaqueously emplaced effusive products, dominated by pillowed lavas, followed by a shift towards more explosive activity with deposition of glassy fragmental deposits (Allen 1980; Jones 1970; Moore et al. 1995; Werner et al. 1996). Within this model it is assumed that there is a decreasing fragmentation and dispersal of subaqueous eruptions as confining pressure or water depth increases, particularly above 400 m (Allen 1980; Clague et al. 2003; Zimanowski and Büttner 2003). However, investigations of submarine basaltic deposits are revealing the presence of explosively derived deposits at depths up to 3 km (Clague and Davis 2003; Fujibayashi and Sakai 2003; Helo et al. 2011; Portner et al. 2010; Schipper and White 2010; Schipper et al. 2010; Schipper et al. 2011; Sohn et al. 2008; Wohletz 2003). This uncertainty over the importance of controls other than confining pressure (Mastin et al. 2009; Schipper et al. 2011; White 1996) on the triggering of subaqueous explosions emphasizes the importance for detailed studies of natural deposits that may record the onset of basaltic explosions in water.

1.2 Field area

Askja is one of the largest and best-exposed formerly ice-confined volcanoes on Earth. Most research to date has been on its Holocene (ice-free) evolution. It comprises a complex of basaltic glaciovolcanic massifs that are dominated by pillow lavas and subaqueously emplaced vitric lapilli tuff deposits. These massifs are cut by at least three calderas and surrounded by Holocene

subaerial lava flows (Fig. 1). The greatest volume of glaciovolcanic deposits at Askja is the eastern mountain massif, Austurfjöll, which is truncated by the two youngest calderas. Austurfjöll has been described briefly by Brown et al. (1991), Sigvaldason, (1968 and 2002) and more recently in detail by Graettinger et al. (2012).

Austurfjöll is incised on its eastern side by large gullies that extend up to 3 km into the massif. The vertical exposure within the gullies is between 10 and 100 m. These exposures are dominated by pillow lava sheets, lava breccias and vitric lapilli tuff. Three of these gullies contain well-exposed sequences that display gradual transitions up section between effusive pillow lavas at their base, to an upward fining pillow fragment and bomb-bearing breccia and vitric lapilli tuff sequence. The sequences have lateral continuity of tens of meters and can be traced in multiple directions. The three gullies from north to south are named, Drekagil, Nautagil and Rosagil (Fig. 1).

2.0 Methods

This study is based on field work conducted over two seasons at Austurfjöll. The three sequences of basaltic pillow lava, pillow-fragment breccia, fluidal bomb-bearing breccia and vitric lapilli tuffs were identified in 2010 and revisited in 2011 for more detailed sampling and study. Samples were collected from the top of the basal pillow units, the lowermost breccia at the contact with the pillow lavas and then progressively up through the section of overlying breccias and vitric lapilli tuffs, with an average sample interval of two meters. At each location a sample of matrix (lapilli and any ash present) and an outsized clast was collected. Outsized clasts are defined here as the largest clasts that exceed the visually estimated median grain size at a particular stratigraphic level. Measurements were taken of the average clast size and the outsized

clasts. Measurements were limited to the longest axis of the largest outsized clasts with intact glassy chill rinds around their entire margins. Field measurements of vesicularity percentages of the core and glassy rim of outsized clasts were supported by measurements of field photographs. A minimum of five measurements of such clasts were taken at each site. If a secondary size mode of outsized clast was present, the largest clasts representative of both modes were studied.

A binocular microscope with mounted digital camera was used to estimate the vesicularity percentage of partially disaggregated matrix and clasts. Additional observations of vesicle shape, distribution, alignment and coalescence were recorded. These observations were also used to estimate the mean matrix grain sizes. The partial consolidation, high friability and fragile clast morphologies precluded full granulometric analyses. Digital images of thin sections were also used to quantify 2D vesicularity percentages and dimensions using ImageJ software. Vesicle number density (Nv) was calculated based on methods outlined in Shea et al. (2010). In addition to vesicle textures, the presence of microlites and rare phenocrysts, tachylite, sideromelane and mixed tachylite-sideromelane fragments were documented across matrix and clast samples. Values represent 2D volume percent of each parameter calculated from image analysis.

Detailed logging of sedimentary structures and X-ray fluorescence (XRF) analyses of outsized clasts and pillows were completed for each sequence to investigate the genetic relationships between the facies of the sequence. XRF bulk rock major element analyses were conducted at Washington State University GeoAnalytical lab from pillow lavas, fluidal bombs in the breccia and outsized clasts in the lapilli tuff.

Textural analysis, using secondary electron images collected on a JEOL JSM-5900 at Dickinson College, of the fine ash fraction included study of grain mounts of loose grains, coated

in carbon. Samples were sieved to isolate particles <50 μm to target potential 'active' particles (<130 μm) of fuel coolant interaction (FCI) experiments (Büttner, 2002). Textures described include ash morphology (blocky and equant, chips and blades, or spines and needles), conchoidal fracture, the presence of intact or broken vesicles, abrasion features (scalloped edges), coatings and adhering particles. Textures were recorded in a per grain basis, so percentages represent the abundance of a given texture, not volumetric presence of vesicles within the ash particles.

3.0 Overview of lithofacies

All three sequences are exposed in steep walled gullies incised into the base of the eastern margin of the 750 m high Austurfjöll massif of Askja volcano (Fig.1). The sequences have basal pillow lavas overlain by pillow-fragment and fluidal bomb-bearing breccias and capped by vitric lapilli tuffs. Fluidal bombs also occur within the lapilli tuff sequences, but decrease in abundance up section. The transition from breccia to lapilli tuff is defined as the point where the fluidal bomb presence is less than 30 vol.% of the deposit. The clastic deposits range from 15-35 m in thickness and display gradational transitions between each lithofacies. Geomorphologic evidence, particularly the thickness of subaqueous sequences at Austurfjöll (700 m), and volatile saturation pressure data indicate the eruption of the basal lavas occurred in water ca. 700 m deep, or beneath some combination of water, ice and sediment with a confining pressure of ca. 7.7 MPa (Cameron, B. unpublished data). There is no structural or textural evidence that these three sequences include subaerially emplaced deposits.

Pillow lava flows at Askja can be subdivided into two main lithofacies, named Pl1 and Pl2. The distinction between the two lithofacies is the variability in the dimensions of the pillow tubes and the frequency of transitions into non-pillowed lavas. Pl1 lavas are comprised of highly

220 regular tubes, both in shape and cross-sectional dimension with average diameters of 50 cm and
221 a range of <20 cm in diameter per within a pillow lava sheet. Pl2 lavas contain a much greater
222 diversity of pillow dimensions, with cross-sectional diameters ranging from 50–200 cm. They
223 also commonly display transitions to columnar, curvi-columnar and blocky-jointed subaqueously
224 emplaced lava flows without pillow forms. Pl2 lavas also have more distended pillow shapes and
225 display less regular stacking (Fig. 5). Pillows measured in the basal lava of the three transitional
226 sequences and apparently intact pillows in the lowermost pillow breccia, fall within observed
227 range of the massif, where cross-sectional diameters are typically 60 cm and core vesicularities
228 around 50 vol.%. Their internal variability and common occurrence of transitions to non-
229 pillowed lavas means that the basal lavas of all three sequences described here are classed as Pl2
230 facies.

231 In all three sequences the breccia that immediately overlies the pillow lavas is initially
232 entirely clast-supported, composed of apparently intact pillows and pillow fragments, with
233 decreasing occurrence of obvious pillow forms (intact or otherwise) within 1-2 meters of the
234 contact. Clasts in the breccia become progressively more isolated in the vitric lapilli matrix (30-
235 70 vol.% of the breccia) up section and pillow fragments are replaced by fluidal bombs within
236 one meter of the pillow lava to breccia contact.

237 Pillows are distinguished by their regular, ellipsoidal cross-sectional shape and
238 occasional presence of keels. Typical pillows exhibit vesicle bands and pipe vesicles (Fig. 6).
239 Pillows typically have regular glassy rinds between 0.1 and 1.5 cm thick. Vesicles are typically
240 round and undeformed in the vesicle bands that dominate the outer few cm of the pillow. Pillow
241 cores may display coalesced vesicle morphologies and radial pipe vesicles are common at the
242 core and rim of the pillow (Edwards et al. 2009; Fujibayashi and Sakai 2003; Höskuldsson et al.

2006). Pillow fragments display partial glassy quench rinds, interrupted vesicle bands, pipe vesicles and incomplete pillow forms. Fluidal bombs on the other hand display a wider range of cross-sectional morphologies, with convolute clast shapes and an irregular distribution of irregular vesicles. When not intact, bombs display a jig-saw fit fracture pattern. The average fluidal bomb vesicularity is on the order of 25% but can be as much as 60 %. Fluidal bombs have glassy rinds between 0.1 and 2 cm in diameter. Vesicles are also typically coalesced and polylobate, with an abundance of elongate vesicles parallel to the glassy rim. Radial pipe vesicles are absent. The distribution of vesicles within the bombs is irregular. Vesicle morphology within the bombs displays an increase in coalescence up section (Fig. 7). The breccia matrix comprises coarse, glassy and angular vitric lapilli (0.5-2 cm). All the vitric clasts within the breccias and lapilli tuffs except fluidal bombs are highly angular with fragile shapes.

The vitric lapilli tuff makes up the bulk of the sequences. The change from breccia into lapilli tuff is characterized by a gradual decrease in the abundance of fluidal bombs with height in all three sequences, from 30 vol.% in the top of the breccia unit to 5 vol.% at the top of lapilli tuff (Fig. 2-4). Weak sub-parallel bedding develops only in the upper 3 m of the lapilli tuff in two of the sequences, NG and RG. The diameter of the bombs peaks in the lower portion of the lapilli tuff, frequently within 5-10 m of the facies transition (Fig. 7) and then decreases rapidly up section. Lapilli are 1-3 cm are dominantly equant and angular, but may have partial fluidal margins and display no systematic change in size up section. Vesicles in the vitric lapilli display a wide range of morphologies that include isolated ellipsoidal to irregularly shaped vesicles, high degrees of interconnectedness, and the presence of tube vesicle morphologies (Fig. 8). Lapilli vesicularity is internally consistent between 20-40% depending on the sequence. The microlite content of bombs increases up-section from 2% up to nearly 10%. The microlite content of lapilli

however, peaks in the breccia, and remains low in the lapilli tuff <10%. Clasts greater than 2 cm have sideromelane rims that can reach up to 1 cm thick and microlite-bearing tachylite cores. Fragments below 2 cm in diameter are dominated by sideromelane. Consequently, the overall ratio of sideromelane to tachylite in the deposit increases up-section. Ash and lapilli are typically very angular with delicate spines and margins preserved (Fig. 8). The clasts display no rounding or removal of fragile spines from fine ash and the deposits exhibit no traction current structures, slump structures or other evidence of remobilization or lateral transport. While palagonitized deposits are common within Austurfjöll, the deposits described here have very limited and impersistent occurrence of palagonite.

The bulk rock chemistry for the sequences of the basal pillows, fluidal bombs of the breccia and lapilli tuff and lapilli clasts were analyzed for major and trace element abundances. The deposits are all tholeiitic basalts with limited internal variability between clast types in given sequence as highlighted in Table 1.

Fourteen fine ash samples were selected for SEM micro-textural analysis from the uppermost breccias and through the overlying lapilli tuff unit of the Drekagil and Nautagil localities. Between 100 and 180 grains <50 microns were counted for each sample and values are reported as abundance of grains with a target texture. Individual particles may display multiple textures. Less than 25% of the fine ash particles had any obvious vesicles (Fig. 9). Of the vesicles present, only about 3% had clast margins dominated by the presence of a vesicle (where the vesicle influences the shape of 40% or greater of the margin. The bulk of vesicles observed at this scale were small, round and isolated within significantly larger grains and dissected by planar or obviously stepped conchoidal fracture surfaces. Vesicle sizes recorded in the fine ash were mostly between 5 and 100 microns in diameter. A significant portion of fine ash grain

shapes (35-40%) were chips (one small dimension, two equal dimensions), blade (one small, one long dimension), or needle-like (two small and one long dimension) (Fig. 9). Approximately 45% of fine ash grains were blocky and roughly equant or prismatic in shape (all dimensions are similar; Fig. 9A). The fine ash samples also include minor occurrences of tube vesicle rich clasts (<10 %) and limu o Pele (<5 %). Limu o Pele are thin (μm to mm) curved lenses of sideromelane glass (Fig. 9D). These curved sheets of glass are significantly thinner than the chips described above. The curvature of the limu o Pele suggests they were derived from vesicles with a diameter greater than the typical vesicles preserved (>60 μm) at this grain size. There are no crystals in the fine ash component of any of the sequences.

Fine ash particles with sharp edges showed evidence of minor abrasion, including rounding and scalloping (Fig. 9H), on less than 10% of all fine ash grains studied. In contrast convolute and fragile shapes, including thin spines of glass (Fig. 9A,D,E), were present on an average of 12% of the fine ash grains. The fine ash fraction of the NG and DG sections displays some minor discoloration from a grey brown to yellow brown, commonly associated with palagonatization. Other evidence for chemical alteration of the fine ash fraction includes pitting of fracture surfaces and flakey coatings. Adhering finer particles are common on 50% of the fine ash grains, but rarely obscure the complete grain. Some particles have thin (micron) skins or coatings that are cracked and flaking away from the grain.

3.1 Individual sequences

The three sequences studied occur within deep gullies called Drekagil, Nautagil and Rosagil (Fig. 1). The sequence in Drekagil (DG) is exposed in a near vertical cliff within a 50 m deep

east-west trending gully. Laterally, the sequence overlies a sharp erosional contact of the top of a sequence of well-bedded lapilli and ash tuffs that display significant palaeotopography on their upper surface (Fig. 2). The pillow lavas occur as a thick (30 m) valley-filling pillow lava sheet that abuts and overtops a paleo-cliff of ash and lapilli tuff. Due to the steep nature of the modern gully, sampling of the pillow unit was limited to the margins of the lensoid unit. The corresponding stratigraphic log follows a diagonal path from the margin of the transitional sequence to its center to access the lapilli tuff directly overlying the greatest thickness of the pillow unit (Fig. 2). The pillow unit is well exposed in the vertical wall, directly below the lapilli tuff. The breccia that overlies the pillow lavas is ca. 5 m thick and initially clast supported with intact and fragmented pillow clasts preserved in the basal 1 m. The clasts are replaced by fluidal bombs with increasing lapilli matrix presence (transitioning from 30-70 vol.% of the breccia) in the upper 4 m. The lapilli tuff has a thickness of 14 m with fluidal bombs throughout. Maximum bomb sizes are 50 cm, but are predominantly between 20-30 cm in the lapilli tuff. . The sequence is capped by a convolute bedded ash that is overlain by a feldspar-phyric non-pillowed sheet lava. The contact between the lapilli tuff and the ash tuff is sharp, but there is no evidence of significant erosion. The sequence at Drekagil is the only one of the three studied that contains accidental lithics in the lapilli tuff, namely subangular porphyritic tholeiite lava lapilli (< 5 cm in diameter), which comprise <1 vol.% of the deposit and are too infrequent to have any obvious trend in occurrence.

Nautagil (NG) contains the thickest of the sequences (35 meters) where it forms the entire southern wall of the gully (Fig. 3). The thickness of the basal pillow lava unit is uncertain as the pillows are partially covered by unconsolidated deposits of pumice from the 1875 eruption of Askja and local talus, but the pillow lavas are at least 2 m thick. The overlying breccia is 7 m

thick with pillow fragments dominating the lowest 2 m giving way to fluidal bombs and increasing (up to 60 vol.%) lapilli matrix the upper 5 m. This breccia is overlain by 24 meters of lapilli tuff. In the upper 3 m of the lapilli tuff a weak parallel ca. 10^0 bedding dipping to the northeast (away from Austurfjöll) develops. Laterally, the deposit displays some palagonitization, but typically displays only incipient palagonitization along the sampled southern wall of the valley. This sequence is cut by a basaltic dike that is one of the type examples of coherent margined volcaniclastic dikes (CMVDs) described from Askja and interpreted as having formed by dike emplacement into ice-cemented volcaniclastic sediments (Graettinger et al. 2012).

The exposure in Rosagil (RG) makes up a large portion of the southern wall of the gully, with a total thickness of 16 m. The basal pillow lava exposure is limited due to talus, but has a minimum thickness of 2 m (Fig. 4). The breccia is 4 m thick with pillow fragments dominating the lower 1 m and fluidal bombs occurring in the upper 3 m. The breccia is overlain by ten meters of lapilli tuff. A weak parallel and shallow (10^0 dipping northeast, away from the summit of Austurfjöll) stratification develops in the upper meter of the tuff. The upper 1 m of the deposit is also locally more intensely palagonitized than the rest of the deposit. Laterally (2-5 away from sampling area) this sequence is intruded by pillowed intrusions with meter-wide peperitic margins.

4.0 Interpretation of deposits

Sequences of pillow lava, to pillow fragment and fluidal bomb breccias, to lapilli tuff sequences are not uncommon in subaqueous basaltic sequences (Carlisle 1963; Dimroth et al. 1978; Fujibayashi and Sakai 2003; Jones 1970; Skilling 2009; Werner and Schmincke 1999). Their

gross similarities between these pillow lava, breccia, and tuff sequences belie the range of mechanisms that can produce outwardly similar deposits. The following discussion will use detailed stratigraphic and textural studies of the facies present at Askja to identify the eruptive history of these deposits.

The structure and components of the Austurfjöll sequences are indicative of a wholly subaqueous environment, including pillowed lavas, sideromelane dominate clastic deposits and the absence of bomb sags, oxidation, or other emergent textures. The morphology of the massif and dominance of subaqueous deposits up to 700 m above the local base and volatile analyses (see section 3.0) from pillow glass rinds indicate that the depth of water was likely on the order of 750 m. The sequences of pillowed lavas, to pillow fragment and fluidal bomb breccia to fluidal bomb-bearing lapilli tuff show consistent internal bulk rock geochemistry suggestive of a co-genetic origin for the pillows and clastic components of the deposits (Table 1). The vesicle morphology of the lapilli is highly similar to that of the fluidal bombs supporting the related genesis of the pyroclasts.

The dominant feature of the three sequences is the massive nature of the lithofacies associated with a progressive upward fining from pillow breccia, through fluidal bomb breccia, to lapilli tuff. The lapilli show fairly consistent dimensions throughout the sequence. The transitions between the facies are gradational and show no sedimentary structures indicative of hiatuses in the eruption.

The gradational upward fining, associated poor sorting and random clast orientation of these sequences is likely the result of high sediment fallout rates possibly from direct deposition from subaqueous convective plumes (Maicher et al. 2000). Grading of outsized clasts may result from Stokes settling of larger particles before smaller particles; however, the lack of sorting

present in the lapilli and ash sized particles, and initial increase in bomb size, does not support this mechanism for bomb distribution in these deposits. A weak parallel bedding is present only in the upper few meters of two of the three deposits. This bedding may be due to time gaps in deposition or delayed gravitational settling in the water column of the finer deposits in this case lapilli and fine ash late in the eruption. Loading structures, traction currents, slump structures and other structures suggesting lateral transport of the deposit are not present (Maicher et al. 2000; White 2000). The apparent lack of remobilization is also supported by the lack of alteration of sharp grain edges (Solgevik et al. 2007) and the preservation of fragile glassy spines and limu o Pele (Fig. 9A,D,E) that would be easily damaged if mobilized in any granular flow or slump (Sohn 1995). The massive nature and systematic grading of coarser clasts through the deposit supports continuous deposition of pyroclasts. This observation, the presence of significant bombs and the limited lateral extent of the deposits suggest that they are vent proximal.

If the deposits are interpreted as primary and vent proximal, it would imply that the sequence represents the inverse of what was expelled from the vent, suggesting that the eruption initially produced large and abundant blocks and bombs, that progressively decreased in size and abundance through the eruption, until a lapilli dominated deposit of consistent grain-size was formed. Based on the lack of remobilization, co-genetic origin and structureless nature of the deposits we interpret the sequences to represent in situ temporally continuous eruptions from a single vent that display a transition from effusive to explosive basaltic activity.

The identification of fragmentation mechanisms in subaqueous pyroclasts remains a challenging task, dependent on the presence of multiple collaborating pieces of evidence. Previous pyroclastic studies have put emphasis on VND and fine ash textures (Ersoy et al. 2006; Lautze et al. 2012; Murtagh et al. 2011; Shea et al. 2010), but these features are not consistent

indicators of fragmentation (Mattsson 2010; Ross and White 2012). The basaltic pyroclastic textures useful for such studies are summarized in Table 2 and evaluated for the relative strength of different textural parameter historic uses.

4.1 Pillow lava

Pillow lava sheets of both Pl1 and Pl2 type are the dominant morphology of subaqueous lavas at Askja. The relationship between subaqueous lava flow morphology and effusion rate is established based on three major groups with pillow lavas representing the lowest effusion rate, lobate pillow-free lavas an intermediate effusion rate and sheet flows (highest effusion rate)(Gregg and Fink 1995; Gregg and Smith 2003; Griffiths and Fink 1992). Lava flow morphology can also be a factor of slope angle (Gregg and Fink 1995; Gregg and Keszthelyi 2004), but as the large pillow sheet flows at Askja occur on shallow slopes, except where they abut paleotopography, slope effects can be ignored here. Pl1 lavas, that display regular pillow forms and stacking, are interpreted as the lowest effusion rate end-member of subaqueous lava flows. Pl2 lavas have a more complex internal structure and locally display textures of lobate subaqueous lava flows, including blocky and columnar jointing domains mingled with large irregular pillow lava tubes. These structures suggest that Pl2 lavas represent an intermediate step between low effusion rate pillow lavas and moderate effusion rate lobate flows (Bear and Cas 2007; Dimroth et al. 1978; Griffiths and Fink 1992; Walker 1992). All three sequences described here have these higher effusion rate pillowed lavas at their base.

4.2 Pillow fragments and fluidal bombs

426 The breccias that immediately overlie the pillow lavas are dominated by three main types
427 of block-sized components: isolated intact pillow forms, pillow fragments and fluidal bombs.
428 Pillows can become isolated or appear to be isolated in clastic matrix through an influx of
429 fragmental material during effusion without significant interaction with the lava (Carlisle 1963;
430 Dimroth et al. 1978; Schipper et al. 2011), intrusion of pillowed dikes through fragmental
431 deposits (Carlisle 1963; Edwards et al. 2009; Gorny et al. 2012), by gravitational detachment and
432 deposition away from the main lava flow (Bevins and Roach 1979; Dimroth et al. 1978; Gorny et
433 al. 2012; Moore 1975), or as ballistic blocks into clastic deposits (Staudigel and Schmincke
434 1984). Well incised exposures, like at Askja, are useful to determine if pillow clasts are truly
435 isolated, or if they can be traced to an intrusion or pillow lava tube. In the Askja deposits, intact
436 isolated pillows are the least common block-sized component, and while intrusions are present,
437 sampling was preferentially collected away from exposed intrusions. Consequently, at
438 Austurfjöll apparently intact pillows in the breccias are interpreted as isolated clasts.
439 Angular pillow fragments can be formed through gravitational collapse of an advancing
440 flow (Jones 1970; Moore 1975), or any other brittle break-up of partially or fully cooled pillow
441 lavas such as slumping (Cas et al. 2003; Jones 1970) or through explosive disruption of an
442 existing flow (Smellie and Hole 1997). Differentiation of these processes requires detailed
443 investigation of the clast morphologies and three dimensional exposures of the deposit structure.
444 The breccia clasts at Askja were described in detail and are dominated by apparently intact
445 pillows, and within a few meters, fluidal bombs. Angular pillow fragments do occur along the
446 contact with the pillow lavas, but are notably rare higher in the clastic sequences.
447 The deposits described here have significant lateral continuity and do not display any
448 bedding, including slump structures, nor do they display any transitions into competent lava

449 flows. Flow-generated “autoclastic” breccias are frequently observed within large pillow sheets
450 at the Askja complex, but they occur as lenses between multiple lava flows and have both lateral
451 and vertical gradational contacts with coherent pillowed lavas with a dominance of angular
452 pillow fragment clasts. The Austurfjöll deposits however, contain an abundance of fragile glass
453 features, including glassy rinds, complex fluidal shapes, spines on fine ash and the lack of
454 sedimentary structures indicating lateral transport, all of which suggest that they are not
455 reworked Additionally, if the deposit experienced collapse or transport a greater proportion of
456 angular blocks would be expected rather than the dominance of fluidal bombs with intact rinds as
457 observed at Askja. The componentry, fragile grain edges, and structureless upward fining of the
458 transitional sequences of DG, NG and RG are suggestive of an explosive origin for the breccia
459 with high rates of settling through a water column.

460 Fluidal bombs display convolute shapes reflecting ductile fragmentation of liquid magma
461 (Houghton and Gonnermann 2008; Houghton and Nairn 1991; Houghton and Schmincke 1989;
462 Walker and Croasdale 1971). Similar clasts have been described in submarine sequences, where
463 they have been misnamed “pillows” (Portner et al. 2010; Staudigel and Schmincke 1984) but
464 have also been recognized as juvenile fluidal bombs in some sequences (Cole et al. 2001;
465 Simpson and McPhie 2001; Sorrentino et al. 2011; Staudigel and Schmincke 1984). The fluidal
466 bombs from Austurfjöll share significant similarities in morphology, vesicularity and
467 coalescence of vesicles to the examples attributed to subaqueous fire fountaining (Cas et al.
468 2003; Simpson and McPhie 2001; Staudigel and Schmincke 1984). Bombs in subaerial
469 Strombolian and Hawaiian and Surtseyan deposits can have fluidal shapes including fusiform,
470 ribbon, or cow-pie morphologies that all result from the ductile disruption of liquid magma
471 (Houghton and Gonnermann 2008; Houghton and Schmincke 1989; Murtagh et al. 2011;

Sorrentino et al. 2011; Walker and Croasdale 1971). Fluidal shapes in subaerial environments are most commonly associated with fire fountaining (Cas et al. 2003; Houghton and Gonnermann 2008; Houghton and Schmincke 1989). The fluidal bombs at Austurfjöll are distinct from the angular blocks that are common in Surtseyan sequences (Brown et al. 1994; Sohn 1995; Sorrentino et al. 2011), which are derived from solidified lava, e.g. from cooled lava flows, larger fragmented bombs, vent walls, or intrusions. Unlike typical Surtseyan eruption deposits, fluidal bombs dominate the breccias and lower lapilli tuff of the Askja sequences and angular bombs (pillow fragments) are limited to absent. Juvenile bombs are also frequently subordinate in abundance to such accidental lithics in Surtseyan eruption deposits (Murtagh et al. 2011; Sohn 1995; Walker and Croasdale 1971). Descriptions of bombs are notably absent in numerous characterizations of deep submarine explosive eruptions, which may in part be due to sampling logistics (Clague et al. 2003; Clague and Davis 2003). However, the presence of these fluidal bombs, and the observation of fluidal ejecta in FCI experiments (Büttner et al. 2002; Grunewald et al. 2007; Ross and White 2012; Zimanowski et al. 1997), have not yet been incorporated into models of fragmentation. Consequently, the fluidal bombs within the Austurfjöll sequences are interpreted as juvenile products of subaqueous explosive magmatic fragmentation, based on their initial abundance, morphology, intact glass rinds and distinctive vesicle pattern from the pillow lavas at the base of the sequence.

Subaerial Strombolian and Hawaiian bombs typically display a range of vesicularity of 30-60 and 60-90 vol.% respectively (Brown et al. 1994; Houghton and Schmincke 1989). These values are higher than what is observed at Askja (20-60 vol.%) or typical Surtseyan eruptions (5-40 vol.%)(Brown et al. 1994; Cas et al. 2003; Head and Wilson 2003; Murtagh et al. 2011; Sorrentino et al. 2011). Head and Wilson (2003) suggest that the vesicularity required for deep

495 subaqueous explosive eruptions is 75%, but values are commonly reported significantly lower at
496 mid-ocean ridges (Clague and Davis 2003). The boundaries between eruptions that are described
497 as “Surtseyan” and “Strombolian” are fuzzy and both behaviors have been described within a
498 single eruption (Houghton and Gonnermann 2008; Houghton and Nairn 1991; Houghton and
499 Schmincke 1989). Similarly, the recognition of bombs or clasts generated in wetter versus drier
500 environments can be difficult without contrasting textures revealing interaction with air
501 (oxidization) vs. water (thick glassy rinds) within the same deposit (Brown et al. 1994;
502 Sorrentino et al. 2011) and indeed the presence or absence of water in the environment does not
503 automatically dictate the fragmentation style (Table 2). Bomb vesicularity is frequently one of
504 the few characteristics used to differentiate between subaerial and phreatomagmatic eruption
505 deposits, where typical Surtseyan bombs have lower average vesicularities than typical
506 Strombolian bombs (Houghton and Gonnermann 2008). Fluidal bombs from Askja have low
507 vesicularites (20-60%), thick glassy rinds (0.2-1.5 cm) and no apparent oxidization showing the
508 greatest similarity to Surtseyan bombs, but having irregular vesicle distributions and polylobate
509 shapes typical of Strombolian subaerial bombs. The frequent presence of the bombs indicates a
510 low efficiency of fragmentation relative to that of phreatomagmatic explosions low in the
511 sequence.
512
513 **4.3 Lapilli and coarse ash**
514 Lapilli dominate the bulk of the deposit from the matrix of the breccia to the top of the lapilli
515 tuff. The dominant lapilli size range is from 1 to 3 cm with vesicle morphologies and shapes
516 similar to vesicles found in the fluidal bombs. The bulk of lapilli are equant in size and serve as
517 matrix for the larger blocks and bombs in the upper breccia and lapilli tuff. The lapilli are

518 interpreted as the products of the breakup of larger globules of melt (like fluidal bombs) and the
519 disruption of melt directly at the vent. Fragmentation of the lapilli reflects a combination of
520 magmatic degassing, quench granulation and brittle fragmentation from interaction with other
521 particles or the conduit during transport and deposition. The low percentage of microlites and
522 dominance of sideromelane glass are indicative of rapid cooling of smaller juvenile fragments,
523 suggesting that there is greater primary fragmentation influencing lapilli formation.
524
525 **4.4 Fine Ash**
526 Fine ash first occurs within the sequences in the lapilli tuffs and progressively increases in
527 abundance up section. In order to use fine ash textures to infer primary fragmentation
528 mechanisms, it must be assumed that they are the result of molten magma break up, not post-
529 explosive mechanical fragmentation (Mattox and Mangan 1997) an assumption supported by
530 their very fine and blocky nature and preserved fragile textures. The fine ash component of the
531 DG and NG tuffs are dominated by chips, blades and needle shapes that are associated with
532 mechanical granulation in experimental magma-water interactions (Büttner et al. 1999) (Fig. 9).
533 Particles with these textural signatures of quench fragmentation are abundant (up to 40%) in the
534 fine ash fraction of the breccia and lapilli sequences. Evidence of the entrapment of external
535 water within the melt, is preserved in the presence of a small percentage (5%) of limu o Pele,
536 representing local ductile deformation in the formation of a large bubble wall fragment (Maicher
537 et al. 2000; Schipper et al. 2013; Schipper and White 2010; Schipper et al. 2011).
538 Blocky, equant fine ash grains with stepped features and an absence of significant vesicle
539 influence are frequently called ‘active particles’ (<130 microns) of FCI (Büttner et al. 2002;
540 Wohletz 2003; Zimanowski and Wohletz 2000). Blocky textures can also be produced in non-

541 explosive interactions with water and wet sediment, but the resulting grain size are coarse ash to
542 fine lapilli (Mastin et al. 2009; Schipper et al. 2011). These particles are all the product of rapid
543 thermal transfer from the particles to a coolant, resulting in the brittle fragmentation of the
544 magma.

545 Blocky/equant fine ash particles make up on average 45% of the fine ash fraction of the
546 Austurfjöll sequences. Lapilli within the breccias and tuffs of the sequence between 2-20 mm
547 also display blocky equant shapes, but have vesicularities up to 25 vol.% and crystal contents up
548 to 10 vol.%, whereas the blocky fine ash fraction are crystal free. The fine ash particles that do
549 contain vesicles were counted separately and display a much lower presence of vesicles in
550 general and notably fewer fracture surfaces that are clearly influenced by vesicle walls than
551 similarly sized particles from a purely magmatic eruption (Houghton and Gonnermann 2008). As
552 a result of the particle size investigated the vesicles preserved in the fine ash are much smaller
553 than were preserved in the lapilli and fluidal bombs. It is nevertheless important to acknowledge
554 the similarity in morphology of the fine ash particles with coarser grain fractions in the
555 sequences at Askja as well as with those in non-explosive thermal granulation experiments.
556 Scalloped edges, characterized by small ~1-2 micron curved gashes along the margins of grains
557 (Fig. 9H) and rounding of fine ash particles are indicative of physical alteration of fine ash
558 particles (Solgevik et al. 2007), but were only found on 10% of fine ash grains studied at
559 Austurfjöll. Fragile shapes, including thin spines of glass, were present on an average 12% of the
560 fine ash grains, such delicate features would be difficult to preserve in the event of any
561 remobilization of the deposit. Flakey coatings probably indicate minor alteration post-
562 fragmentation along with the orange discoloration of fine ash these indicate weak hydration,
563 incipient palagonatization, of the deposits (Büttner et al. 2002; Büttner et al. 1999; Harpel et al.

2008; Nemeth and Cronin 2011). Fine ash particles are a critical grain size for unraveling the fragmentation mechanisms of the eruptions as they represent the most efficient fragmentation and require the greatest energy to produce. The size of these grains means that they only preserve the last stage of fragmentation, as interacting fragmentation mechanisms may destroy much of the earlier evidence of less efficient fragmentation mechanisms. Such particles are also limited as they do not make up more than 10% of the total deposit volume at any stratigraphic level. The finest grains must be studied in the context of detailed analysis of the whole deposit including larger pyroclasts, eruption, transport and depositional processes and their environments.

Mechanisms of magma fragmentation clearly impart textural characteristics to glass particles at all scales. Vesicle size, shape and alignment and interconnectedness reflect magmatic volatile exsolution, fragmentation and quenching with implications for the relative timing of all of these processes (Murtagh et al. 2011; Stovall et al. 2011). Quench rind thickness, sideromelane vs. tachylite ratios and microlite presence indicate the relative rate of cooling (Schipper et al. 2011). However, the signatures of initial fragmentation can be altered by subsequent fragmentation and shape modification during transport, deposition and chemical alteration. The final deposition of subaqueous volcaniclastic material is commonly the result of lateral transport mechanisms such as density currents (Maicher et al. 2000; Smellie and Hole 1997; White 2000), the collapse of over-steepened deposits (Jones 1970; Sohn 1995), or suspension settling (Eissen et al. 2003; Maicher et al. 2000). Remobilization can cause additional fragmentation and/or impart textures such as the chipping of edges or rounding through abrasion (Solgevik et al. 2007), muting or destroying textural signatures of initial fragmentation. The introduction of accidental clasts during transport also complicates interpretations. Recycling of clasts has been noted as a common process in subaerial and emergent/near surface

phreatomagatic eruptions, but has not been discussed much in the subaqueous literature (Houghton and Smith 1993; Rosseel et al. 2006). Although numerous textures have been used to distinguish magmatic from phreatomagmatic eruption products no one texture can be used in isolation (Table 2). A full interpretation of the textures displayed by glassy pyroclasts should include magma state prior to fragmentation, fragmentation, eruption mechanism(s), transport, deposition, environment and any subsequent post-depositional changes (Harpel et al. 2008).

4.5 Vesicle textures as a record of fragmentation mechanism

Vesicles textures are the product of a combination at least six processes: nucleation, diffusive growth, decompressive expansion, coalescence, collapse, deformation and escape (Schipper et al. 2010). The overall vesicularity of the deposits described here (25-60 vol.%) is comparable to subaqueous to emergent (i.e. phreatomagmatic) basaltic deposits (10-60 vol.%) (Houghton and Gonnermann 2008; Houghton and Schmincke 1989; Murtagh et al. 2011; Schipper et al. 2011; Simpson and McPhie 2001). The dominance of coalescence and vesicle growth in the lapilli and fluidal bombs is suggestive of decoupled gas within the magma (Schipper et al. 2011), rather than continuous nucleation and exsolution.

The differences observed in vesicularity between the three grain size groups (ash, lapilli and blocks/bombs) are clearly influenced by the size of vesicles that can be observed, and the method of calculating vesicularity. The vesicularity of bombs and lapilli were calculated both in the field and with image analysis using ImageJ, both methods are two dimensional. These values are assumed to be of representative of three dimensional distributions. The vesicularity of fine ash was not calculated as a vesicle percent, but rather a binary value of presence of vesicles in part due to the small size and low abundance of vesicles at this grain size. Vesicle textures can be

610 described as young (pre-fragmentation) textures or mature (post-fragmentation) textures. Young
611 textures are small, sub-spherical and abundant vesicles. Rim to core vesicle coarsening is a sign
612 of post-fragmentation vesiculation in subaerial and subaqueous bombs (Moitra et al. 2013;
613 Parcheta et al. 2013; Schipper et al. 2011; Stovall et al. 2011). This mature texture results from a
614 residence time of the melt in a shallow chamber or the conduit for gases to exsolve and be
615 distributed through the melt (Schipper et al. 2011). In the case of mature textures in pillow lavas,
616 the distribution of large coalesced vesicles is typical found at the center of the pillow, away from
617 rapidly cooling and apparently young vesicle textured rims.

618 The overall distribution of the vesicles in fluidal bombs indicates that they are not post-
619 fragmentation bubble textures, or at least the process of coalescence had commenced prior to
620 fragmentation as they are well distributed throughout the bombs. Smaller vesicles are also
621 present, but a consistent alignment or distribution is absent, and thus no evidence of continued
622 nucleation of vesicles after bomb formation. Stretched vesicles along the bomb margins may be
623 ellipsoidal in morphology and represent deformation of pre-fragmentation vesicles during and
624 after bomb formation. Vesicle textures in pillows and fluidal bombs can be compared to reveal
625 the relative timing of vesicle coalescence to fragmentation. The pillows are early stage eruption
626 products with rounded vesicles (pre-fragmentation) and including radial pipe vesicles and an
627 inward coarsening of vesicle diameter (post-fragmentation), which are also preserved in pillow
628 fragments.

629 Lapilli vesicle morphology and distribution is nearly identical to that of the fluidal bombs
630 suggesting the vesicles of both grain sizes have the same pre-fragmentation origin. In very fine
631 ash, those vesicles observed isolated within a particle and smaller than the fracture planes formed
632 prior to fragmentation. The <50 μm size of fine ash particles studied precludes the preservation

633 of vesicles larger than 100 μm. Those vesicles that are present, however, are indicative of pre-
634 fragmentation vesiculation.

635 The similarity of vesicle coalescence and other textures between bomb and lapilli clasts
636 suggests that similar processes were controlling vesicle formation in the breccia and lapilli tuff.
637 However, a comparison of initial pillow lava vesicle textures with fluidal bombs and lapilli
638 suggests a change in the behavior of magmatic gasses during the eruption. The vesicles in the
639 bombs display increased coalescence relative to the uppermost pillow lava flows and minor (~5-
640 10%) increase in vesicularity, indicating an increase in gas exsolution within the melt, and
641 suggest that the bombs were formed by explosive magmatic gas expansion (Fig. 7). The fluidal
642 morphology of the bombs also indicates ductile deformation during transport through the vent
643 and the overlying water column, which is in agreement with a magmatic, rather than
644 phreatomagmatic origin for the generation of the bombs. While fluidal bombs are observed in
645 some phreatomagmatic deposits, they do not occur with the concentration observed at Askja or
646 other subaqueous magmatic settings (Simpson and McPhie 2001). However, the more complex
647 textures of the lapilli and ash indicate multiple fragmentation mechanisms were contributing to
648 the formation of these finer particles including FCI and mechanical granulation (Fig.7).

649

650 **5.0 Magma fragmentation at the onset of basaltic phreatomagmatic explosions**

651 The kinetic disruption of a magma is accomplished in two main ways: ductile deformation of the
652 melt and brittle deformation of the cooling glass/lava. Ductile, or inertial fragmentation, is the
653 breakup of magma during decompression in the form of inertial stretching and breakup of the
654 liquid magma (Houghton and Gonnermann, 2008; and references within). Basaltic magmatic
655 explosions predominantly involve the ductile disruption of the melt through the nucleation and

growth and buoyant rise of vesicles (Parfitt and Wilson 2009; Zimanowski et al. 2003). The fluidal texture of bombs, with elongate vesicles in the glassy rim and convolute vesicle morphologies is a result of the ductile deformation of magma driven by the expansion and coalescence of magmatic water (Büttner et al. 1999; Eissen et al. 2003; Kokelaar 1986; Mastin et al. 2009; Parcheta et al. 2013; Zimanowski and Büttner 2003; Zimanowski and Wohletz 2000). Vesicle morphologies and distributions are distinct in the pillow lavas and pillow lava fragments, relative to the later pyroclasts (fluidal bombs and lapilli), and suggest coalescence of magmatic gas bubbles prior to the formation of the pyroclasts but not during pillow extrusion. This accumulation of magmatic gas could lead to the initial formation of fluidal bombs and possibly some lapilli, generated by expansion of these bubbles (Fig. 7 & 8). There is, however, limited evidence of ductile deformation preserved in the fine ash scale in the form of tube vesicles and rare fine ash with large vesicle walls preserved along fractures. This supports the evidence that magmatic gas expansion is recorded in the large polylobate vesicles representing existing degassing pathways, and not nucleation of new vesicles.

While it is reasonable to indicate the onset of magmatic gas expansion driven explosivity in these deposits it is exceedingly difficult to identify when, if at all, the magmatic gas expansion stops. Rather, the fragmentation mechanism that dominates pyroclast formation changes, and may then mask the signature of magmatic fragmentation. The polylobate highly coalesced vesicles of are also present in the lapilli tuff, but the influence of magmatic fragmentation becomes less evident with the rapid decrease in fluidal bombs within a meter or so of the top of the breccia, suggesting a more effective fragmentation mechanism.

Brittle fragmentation of magma occurs when the material fails as a solid. In order for liquid magma to deform in a brittle fashion the strain rate must be high enough to prevent liquid

679 relaxation of the melt (Büttner et al. 2002; Büttner et al. 1999; Dellino et al. 2001; Zimanowski
680 et al. 2003). Fragmentation of basaltic magma by brittle processes include: FCI, quench
681 granulation and other mechanical fracture through impact upon landing or transportation
682 (Maicher et al. 2000). Most studies that distinguish between phreatomagmatic and magmatic
683 fragmentation focus on the fine ash grain size fraction (<64 μm) as it records the most efficient
684 fragmentation mechanism involved in the creation of the deposit, i.e. the mechanism that
685 requires the greatest energy (Büttner et al. 1999; Dellino and La Vope 1996; Durig et al. 2012;
686 Heiken 1971; Mattsson and Tripoli 2011; Zimanowski et al. 2003). Phreatomagmatic explosions
687 driven by FCI occur where vapor is produced through the rapid heating of the water interacting
688 with the surface of the melt. This vapor film must be disrupted to bring the melt in direct contact
689 with the water. The disruption of the vapor film can be an internal or external process, where
690 changes in the system, including other mechanisms of melt fragmentation, can initiate FCI
691 explosions. (Kokelaar 1986; Schipper et al. 2013; Wohletz 1986; Wohletz 2003; Zimanowski
692 and Büttner 2003; Zimanowski and Wohletz 2000). The resulting explosion can then create
693 pressure variations and fragment country rock or cooling crusts and result in the exposure of
694 fresh magma to the system. The violence of these interactions produces deposits that are
695 characterized by lithic blocks and abundant fine ash. Disruption of melt by FCI shockwaves can
696 result in the rapid depressurization of a degassing melt and encourage magmatic explosivity.
697 Similarly magmatic explosions can engender the formation of a fuel coolant premix and enable a
698 phreatomagmatic interaction. The dynamic interplay of pressure, heat and coolant can result in a
699 feedback loop where one or both of these fragmentation mechanisms may engender the
700 conditions required to trigger the other. Simultaneously, both of these mechanisms result in the
701 exposure of new melt which subsequently cools and contracts resulting in quench granulation.

This complex interplay of magma fragmentation mechanisms only highlights the challenge of interpreting sequences like those at Austurfjöll.

Quench granulation is due to contraction during cooling and the brittle failure of the outer contracted layers of melt that is accentuated in wet environments (Cas et al. 2003; Schipper et al. 2010; Wohletz 1986; Wohletz 2003). This secondary fracture occurs at a variety of scales including jig-saw fit bombs, angular blocks and chip and needle-shaped fine ash particles. Lapilli that have incomplete sideromelane rims reflect the brittle fragmentation of cooled melt. Particles associated with this type of fragmentation are typically dominated by wholly sideromelane clasts. Quench granulation only releases 10% of the thermal energy available (Schmid et al. 2010) and creates larger particles (coarse ash and lapilli) than FCI. Additional fragmentation can occur through clast to clast interaction, impact with the ground and during transportation. The preservation of large fluidal clasts and intact glassy margins on lapilli and bombs indicate that these secondary fragmentation mechanisms, including post-depositional transport, are limited. Fine ash grain textures also support this lack of transportation through the preservation of fragile spines and limited grain abrasion.

The role of ductile deformation in FCI explosions is poorly understood. Ductiley deformed clasts are observed in limited quantities in phreatomagmatic deposits, including limu o Pele (Clague et al. 2009; Maicher et al. 2000; Schipper and White 2010) and fluidal bombs (Mattsson and Tripoli 2011; Ross et al. 2011). The formation of limu o Pele involves the ductile deformation of melt as a result of trapping external water within the melt. The trapped water rapidly expands as vapor stretching the melt into a thin film (bubble wall), in a processes documented in littoral, submarine and subglacial environments (Clague et al. 2009; Maicher et al. 2000; Schipper and White 2010). Limu o Pele are not a dominant feature within the Askja

deposits (never more than 4 vol %), but are frequent enough (Fig. 9) to indicate that trapping of external water by molten magma did occur in this fully subaqueous environment, further indicating the complexity of subaqueous melt water interactions.

It is very important to note that none of these fragmentation processes occur in isolation, as each individual mechanism disrupts the magma and may enable the decompression of internal volatiles, increase the surface area for interaction with external water and disrupt insulating vapor films (Maicher et al. 2000) triggering other mechanisms of fragmentation enabling feedback loops between magmatic and phreatomagmatic explosions. Quench granulation, in particular, can occur in any wet eruptive environment and contributes to all subaqueous eruptions (Cas et al. 2003; Mastin et al. 2009; Schipper et al. 2010; Wohletz 1986; Wohletz 2003).

The interpretation of pillow, fluidal bomb, lapilli and fine ash particle textures from the three transitional sequences at Askja clearly reflect a complex interplay of several fragmentation mechanisms that evolve throughout the eruption sequence. The shape of clasts and fine particles reflect the ductile or brittle nature of these mechanisms. The interrelated nature of mechanisms of fragmentation results in the modification, overprinting and even destruction of earlier textural signatures of the fragmentation (Ersoy et al. 2006). It is therefore, critical to use multiple parameters, such as sedimentary structures, vesicularity, grain size and grain shape at multiple grain sizes to reconstruct the mechanisms of fragmentation for pyroclastic deposits generated in wet environments. For the sequences described here, we suggest that the evolution of the fragmentation mechanisms producing the deposits started with initial magmatic fragmentation in a subaqueous environment which then enabled more efficient FCI explosions. This progressive shift does not imply that magmatic fragmentation was shut down by the onset of phreatomagmatic activity, rather the more effective process rapidly dominated the production of

748 pyroclasts with magmatic gas expansion becoming a subordinate process. At the same time
749 fragmentation by mechanical process (dominantly quench granulation) and the entrapment of
750 external water (limu o Pele) accompanied the more dominant fragmentation mechanisms (Fig.
751 10).
752
753 **5.1 What triggers explosive activity in subaqueous eruptions?**
754 Potential triggers for a transition from effusive to explosive activity in a subaqueous environment
755 include: depressurization by a decrease in confining pressure, access/infiltration of water to the
756 rising magma, and internal dynamics of the magma due to changes in the magma flux, volatile
757 content or crystallization. In a glaciovolcanic setting a reduction of confining pressure can result
758 from a decrease in the overburden, such as water or ice or wet sediment due to the dynamic
759 nature of the environment. Ice-confined lake water levels are highly dynamic and can drain
760 slowly or rapidly during and after an eruption (Bjornsson 1985; Höskuldsson et al. 2006; Skilling
761 et al. 2009; Smellie 2001; Smellie and Hole 1997). Decompression would also occur as a result
762 of increasing the elevation of a vent relative to the water level through the construction of a
763 massif (Edwards et al. 2009; Moore and Calk 1991; Zimanowski and Büttner 2003). A sudden
764 collapse of the growing massif or collapse of the vent itself could also result in rapid
765 decompression over the vent area (Fujibayashi and Sakai 2003; Scott et al. 2003; Wohletz 2003).
766 The initiation of external water-magma interaction may further instigate decompression
767 and facilitate further explosive activity (White 1996; Wohletz 1986; Wohletz 2002). This may be
768 accomplished through the trapping of external water under an advancing flow over wet
769 sediments, or between pillows, or the infiltration of water into the vent, or fractured lava flow
770 crusts (Brown et al. 1994; Clague et al. 2009; Eissen et al. 2003; Maicher et al. 2000; Schipper

771 and White 2010; White 1996; Zimanowski and Büttner 2002). In the case of the completely
772 subaqueous sequence at Askja, ample volumes of water are available for interaction with
773 erupting magma indicating that the volume of water was not a limiting variable for triggering the
774 explosions. The presence of effusive pillow lavas during the early phase of the eruption indicates
775 that melt was interacting with abundant water, but conditions were not conducive for melt/water
776 pre-mix generation and FCI explosions (Wohletz 2002; Zimanowski et al. 1997). The pillow
777 fragment breccia indicates that the pillow lava was partially mechanically disrupted, likely
778 through the onset of explosive magmatic activity which formed juvenile fluidal bombs that then
779 progressively dominate the breccia up-section. Vesicle morphologies and their distribution in the
780 fluidal bombs points to an increase in magmatic volatile expansion and accumulation of vesicles
781 through coalescence after pillow formation and during bomb formation. During the initial
782 explosive phase lapilli were also produced in small quantities to form the matrix of the breccia.
783 As the eruption continued lapilli became the dominant pyroclast size, producing a massive lapilli
784 tuff. This upward fining of the deposit, as expressed by the increase in ash presence and decrease
785 in outsized clasts and the accompanying increasing abundance of very fine blocky ash particles
786 indicates that conditions became more favorable for FCI explosions. The initial magmatic
787 fragmentation enabled the dynamic mingling of magma and water to enable FCI and increased
788 quench granulation. The threshold between passive and explosive fragmentation in these cases is
789 loosely constrained by laboratory scale experiments defining a range of the greatest potential for
790 explosive interaction, where the mass ratios of coolant to magma is between $1>R>0.1$ (Wohletz
791 2002). However, this mass ratio does not occur in isolation and the other variables, including
792 confining pressure, and magma viscosity have not been sufficiently investigated. In this case the
793 increased surface area to volume ratio of the 20-50 cm bombs needed to occur with sufficient

794 volume to maintain a mass ratio of water to magma below 1. Based on the 4-7 m of fluidal
795 bomb-bearing breccia it seems feasible that the ratio of heat to coolant in the resulting mix was
796 favorable to trigger a FCI explosion. This then suggest that explosive magmatic fragmentation
797 can facilitate explosive fuel coolant interactions that dominate pyroclast formation for the
798 remainder of the eruption. While not the only mechanism to instigate FCI explosions, this may
799 represent a common mechanism for FCI initiation. If this model is valid, one important question
800 still remains, namely what controlled the initial increase in magmatic gas expansion for the
801 Austurfjöll eruptions?

802 Variations of internal eruption dynamics could initiate magmatic explosive activity
803 through an increase in eruption rate (Clague et al. 2009; Fujibayashi and Sakai 2003), changes in
804 volatile content, or viscosity (composition or crystallization) (Fowler et al. 2002; Wohletz 2003).
805 The abundance of crystals within a melt will also directly affect the gross vesicularity and play a
806 role in the potential explosivity of a melt (Houghton and Gonnermann 2008).

807 The presence of textures reflecting magmatic gas expansion and coalescence in the
808 Austurfjöll deposits indicates that internal volatiles play a critical role in the first stages of
809 fragmentation, and thus it is reasonable to consider internal drivers for the initiation of
810 explosivity, such as eruption rate. The presence of pillow lavas of Pl2 type at the base of the
811 Austurfjöll sequences indicates that effusion occurred at a higher rate than would form typical
812 (i.e. Pl1) pillow lava forms. Deformed sideromelane glass quenched particles and elongated
813 vesicles on clast rims in the overlying breccias/lapilli tuffs suggest a high strain rate that is also
814 associated with a high eruption rate (Parcheta et al. 2013). This may suggest that the onset of
815 explosivity coincided with an increased eruption rate from pillowed lavas to magmatic gas
816 driven jetting of magma globules into the water column. Other internal factors such as melt

viscosity and volatile saturation pressures do not seem to change dramatically between the pillows and the bombs. The crystal content of the lapilli and bomb samples is below 10 vol.% This suggests that the formation of crystals is not a significant contributor behavior of the melt. Additionally the chemistry of the pillows and clastic samples shows a high degree of internal consistency.

Alternatively, the shift in eruptive behavior may have been due to factors external to the melt where the increase in internal volatile expansion and coalescence between the pillow lavas and the fluidal bombs could have been the result of decompression from a reduction of confining pressure over the vent. Investigations of glaciovolcanic deposits have sought geologic textures that preserve the evidence of rapid syn-eruptive decompression through environmental changes, and suggest that dramatic changes in bulk vesicularity may be a key to identifying this process (Höskuldsson et al. 2006). The first fluidal bombs at Austurfjöll have different morphology and distribution of vesicles from the underlying lavas, reflecting an increase in vesicle coalescence, not an increase in nucleation as might be expected during a decompression event. However, there is geologic evidence within nearby areas of Austurfjöll massif for voluminous drainage of water, as indicated by deeply eroded channels in similar lapilli tuffs that are infilled with stream flow and debris flow deposits. Such a large drainage event may have rapidly decreased the lake level volume, resulting in a rapid pressure change over the massif. The timing and duration of such an event is not well constrained, but at least one drainage event is stratigraphically correlated within the same eruptive unit as the NG transitional sequence (Graettinger unpublished data). Large ice sheets like would have been present at Askja are less susceptible to rapid drainage events than thinner, more localized ice bodies; however, the volume of water drained may not need to be

significant to influence eruptive conditions of an actively degassing magma, particularly if the eruption rate was already high as evidenced by the presence of Pl2 lavas.

The internal compositional and textural consistency of the sequences at Askja suggests that there was little change in melt properties during the eruption of these deposits. While a change in mass flux at the vent may be responsible for the onset of magmatic gas decompression at all three sites, in similar fashions, it seems more likely that environmental conditions would produce such similar processes at different vents. Drainage events are frequent at glaciovolcanic centers (Bennett et al. 2006; Carrivick et al. 2004; Gudmundsson et al. 1997; Höskuldsson et al. 2006), and are a likely the strongest candidate to trigger the onset of explosive activity at an actively effusing vent.

5.2 Eruption Style

The discussion of eruption mechanics in fully subaqueous environments is complicated by the terminology, particularly with regard to comparisons that are often made with subaerial eruption styles. Comparisons with Strombolian (Clague and Davis 2003; Clague et al. 2009; Deardorff et al. 2011; Head and Wilson 2003; Schipper et al. 2011) and Hawaiian (Cas et al. 2003; Head and Wilson 2003; Schipper et al. 2010), eruption styles typically are focused on the decoupled or coupled nature of magmatic gas, but belies the underlying complexity of subaqueous fragmentation. Deep (ca. 1 km), gas-coupled submarine eruptions have also recently been given the term Poseidic (Schipper et al. 2010) to highlight some of the variations present in subaqueous eruptions. Surtseyan eruptions are considered to be the 'wet' equivalent of Strombolian eruptions, but the term is predominantly applied to emergent or limited water environments, not

861 fully subaqueous systems (Brand and Clarke 2009; Skilling 2009; Sohn 1995; Sorrentino et al.
862 2011; White and Ross 2011).

863 Fluidal bombs have been used to suggest the occurrence of submarine basaltic fire
864 fountaining at ocean islands (Simpson and McPhie 2001), but the nature of vesicles in the
865 Austurfjöll deposits is more suggestive of decoupled gas, that is characteristic of Strombolian
866 eruptions (Clague and Davis 2003; Clague et al. 2009; Polacci et al. 2008; Schipper et al. 2011;
867 Schipper et al. 2010). The vesicularity of Hawaiian eruption deposits is typically high, and
868 pyroclasts are dominated by ragged clasts with uniformly distributed vesicles, suggested that the
869 gas bubbles are coupled to the magma during eruption and a more continuous eruption.
870 Strombolian eruptions of basaltic magma have a variety of fluidal and ragged clasts are that are
871 produced in a non-continuous 'unsteady' eruption, but occur as discrete eruptions, due to the
872 decoupled gas (Houghton and Gonnermann 2008). Surtseyan eruptions can display discrete
873 bursts and continuous uprush behavior. The Askja deposits lack some of the more distinctive
874 Surtseyan deposit characteristics including lithic blocks, bomb sags and stratigraphy indicative of
875 pulsatory behavior. The sequences at Austurfjöll are predominantly massive with a gradual
876 upward fining and weak bedding only in the upper meters of the larger deposits. This indicates a
877 more continuous eruptive behavior resulting in continuous deposition.

878 The erosional history and complex overlapping facies of adjacent fissure eruptions at
879 Askja make the identification of exact vent locations for each sequence very difficult. Without
880 sufficient exposure vent position is estimated to be roughly located within the deposit itself, and
881 therefore within 10-50 m of sample location based on the scope of the deposit and the lack of
882 evidence for remobilization. Deposit volume is calculated from lateral extent, estimated by
883 observation of the three-dimensional dissection of the deposit and from lithofacies mapping of

884 DK, NG and RG. Original volume estimates are clearly approximate due to the degree of deposit
885 overlap and erosion. The estimated volume of the individual deposits is between 0.0004-0.003
886 km^3. Typical Strombolian eruptions and Icelandic fissure eruptions have extrusion rates between
887 10 and 100 m^3/s (Parfitt and Wilson 2009). These explosive eruptive rates are also similar in
888 range to the values estimated for subaqueous lobate lava flows (Griffiths and Fink 1992).
889 Estimates for eruption duration can be established from these values to be minutes to a few hours
890 for each sequence.

891 We have suggested above that the first formation of fluidal bombs is the result of rapid
892 extrusion of magma driven by internal volatiles, jetting the magma into the water column. The
893 shear stress imparted on the surface of the magma exceeds the surface tension causing a
894 separation into magma globules, forming the fluidal bombs (Cas et al. 2003; Head and Wilson
895 2003; Wohletz 2003). The presence of pillow fragments mixed with fluidal bombs suggests that
896 the pillows were disrupted during the onset of explosivity, but the absence of frothy pillows or
897 pillow fragments suggests that the transition occurred in the vent and not in a growing pillow
898 tube. The coalescence of vesicles and vesicle size indicate decoupled volatile behavior (Clague
899 and Davis 2003; Head and Wilson 2003; Schipper et al. 2011). The ejection of this first globule
900 then exposes a greater surface area of magma to interact with external water. The bomb-bearing
901 lapilli tuff is interpreted as representing the shift from subaqueous magmatic fragmentation to
902 FCI fragmentation. The increased efficiency of the fragmentation is recorded in the overall
903 decreasing grain size of the deposits through the increase in the proportion of lapilli and ash. The
904 sequences described here would be insufficiently characterized by only one grain size faction
905 due to the limitations of each particle type to record the interplay of fragmentation mechanisms
906 observed through this more comprehensive textural study.

907 The interplay of phreatomagmatic fragmentation (FCI) with magmatic fragmentation is
908 not unique to fully submerged eruptions (Houghton and Schmincke 1989; Skilling 2009;
909 Solgevik et al. 2007; White 1996). However, the initiation of a phreatomagmatic eruption by a
910 decoupled gas magmatic eruption has not yet been described in a completely subaqueous
911 environment. Deposits preserving a magmatic trigger for FCI explosions at Askja likely do not
912 represent an exclusive series of events, but instead represents the dynamic nature of subaqueous
913 explosive eruptions and reinforces the potential for feedback loops of basaltic magma
914 fragmentation mechanisms.
915
916 **6.0 Conclusion**
917 Pyroclast textures in three subaqueous basaltic sequences from Askja reveal the interaction of
918 magmatic and FCI fragmentation mechanisms as the eruption transitioned from effusive to
919 explosive behavior. The identification of the signature of different fragmentation mechanisms in
920 natural subaqueous phreatomagmatic eruptions remains a challenge. However, the comparison of
921 textures in multiple grain sizes across important facies transitions as in this study can reveal
922 subtle changes in internal volatile expansion and fragment cooling history as preserved in vesicle
923 morphology, distribution and size as well as glass type and microlite abundances. By using an
924 integrated approach it is possible to compensate for challenges such as textural overprinting and
925 limited sedimentary structures. We propose an eruption history for the three sequences described
926 here where the initial disruption of the effusively erupting magma by decoupled magmatic
927 volatile expansion was the result of decompression that may have been the result of drainage or
928 partial drainage of overlying water in the ice-confined lake. This magmatic explosive behavior
929 subsequently enabled FCI, as well as minor trapping of external water and quench granulation.

All of these fragmentation mechanisms influenced the final grain size distribution and pyroclast textures of the sequences. The initial disruption of the magma that was driven by volatile expansion is preserved in the form of the fluidal bombs up to 50 cm in diameter and the large, irregularly distributed, polylobate vesicles of the lapilli and bombs that were no present in the underlying pillows. The role of phreatomagmatic explosions is recorded predominantly in the fine ash fraction of the deposit in the form of blocky, vesicle free grains and the increase and dominance of sideromelane dominated lapilli and fine ash up section. The combination of low efficiently magmatic fragmentation and FCI explosions in the same eruptive sequence highlights the complexity of magma water interactions in wet environments. Given the close genetic and spatial relationship between the pillows and clastic deposits we suggest that the deposits were produced through the continuous eruption of effusive to transitionally explosive behavior. The recognition of such transitional sequences is important as they provide evidence for controls on the onset of explosive activity in subaqueous environments. It is critical to continue to investigate the conditions and triggers of fuel coolant interactions to better model violent phreatomagmatic eruptions.

7.0 Acknowledgments

This work was made possible by a National Science Foundation grant to IPS, DG and AH. Our gratitude goes to Háskóli Íslands, NORVOLK and the Vatnajökull National Park, for field logistics and permits. Dickinson College is acknowledged for the use of the SEM and Robert Dean should be thanked for his assistance using the equipment. Field assistance from R. Wham, R. Lee, A. Lema and M. Ellis was invaluable. This manuscript was improved greatly by two anonymous reviewers.

8.0 References

Allen CC (1980) Icelandic subglacial volcanism: thermal and physical studies The Journal of Geology 88:108-117

Allen CC, Jercinovic MJ, Allen JSB (1982) Subglacial volcansim in North-Central British Columbia and Iceland The Journal of Geology 90:699-715

Bear AN, Cas RAF (2007) The complex facies architecture and emplacement sequene of a Miocene submarine mega-pillow lava flow system, Muriwai, North Island, New Zealand. Journal of Volcanology and Geothermal Research 160:1-22

Bennett MR, Huddart D, Waller RI (2006) Diamict fans in subglacial water-filled cavities- a new glacial environment. Quaternary Science Reviews 25:3050-3069

Bevins RE, Roach RA (1979) Pillow lava and isolated-pillow breccia of rhyodacite composition from the Fishguard Volcanic Group, Lower Ordovician, S.W. Wales, United Kingdom. The Journal of Geology 87(2):193-201

Bjornsson A (1985) Dynamics of crustal rifting in NE Iceland. Journal of Geophysical Research 90:10151-10162

Bjornsson H (2002) Subglacial lakes and jokulhlaups in Iceland. Global and Planetary Change 35:255-271

Brand BD, Clarke AB (2009) The architecture, eruptive history, and evolution of the Table Rock Complex, Oregon: From a Surtseyan to an energetic maar eruption. Journal of Volcanology and Geothermal Research 180:203-224

Brown SJA, Smith RT, Cole JW, Houghton BF (1994) Compositional and textural characteristics of the strombolian and surtseay K-Trig basalts, Taupo Volcanic Centre, New Zealand: Imlications for eruption dynamics. New Zealand Journal of Geology and Geophysics 37:113-126

Büttner R, Dellino P, La Volpe L, Lorenz V, Zimanowski B (2002) Thermohydraulic explosions in phreatomagmatic eruptions as evidenced by the comparison between pyroclasts and products from Molten Fuel Cooland Interaction experiments. Journal of Geophysical Research 107:2277

Büttner R, Dellino P, Zimanowski B (1999) Identifying magma-water interaction from the surface features of ash particles. Nature 401:688-690

Carlisle D (1963) Pillow breccias and their aquagene tuffs, Quadra Island, British Columbia. The Journal of Geology 71(2):48-71

Carrivick JL, Russell AJ, Tweed FS (2004) Geomorphological evidence for jokulhlaups from Kverkfjoll volcano, Iceland. Geomorphology 63:81-102

Cas RAF, Yamagishi H, Moore L, Scutter C (2003) Miocene submarine fire fountain deposits, Ryugazaki Headland, Oshoro Peninsula, Hokkaido, Japan: implications for submarine fountain dynamics and fragmentation processes. In: White JDL, Smellie JL, Clague DA (eds) Subaqueous Explosive Volcanism AGU Washington DC, pp 299-316

Clague DA, Batiza R, Head JW, Davis AS (2003) Pyroclastic and hyrdoclastic deposits on Loihi Seamount, Hawaii. In: White JDL, Smellie JL, Clague DA (eds) Explosive subaqueous volcanism. AGU Washington DC, pp 73-95
Clague DA, Davis AS (2003) Submarine Strombolian eruptions on the Gorda Mid-Ocean Ridge In: White JDL, Smellie JL, Clague DA (eds) Explosive subaqueous volcanism. AGU Washington DC, pp 111-128
Clague DA, Paduan JB, Davis AS (2009) Widespread strombolian eruptions of mid-ocean ridge basalt. Journal of Volcanology and Geothermal Research 180:171-188
Cole PD, Guest JE, Cuncan AM, Pacheco J-M (2001) Capelinhos 1957-1958, Faial, Axores: deposits formed by an emergent sursteyan eruption. Bulletin of Volcanology 63:204-220
De Rosa R (1999) Compositional models in the ash fraction of some modern pyroclstic deposits: their determination and significance. Bulletin of Volcanology 61:162-173
Deardorff ND, Cashman KV, W. CJW (2011) Observations of eruptive plume dynamics and pyroclastic deposits from submarine explosive eruptions at NW Rota- 1, Mariana arc. Journal of Volcanology and Geothermal Research 202:47-59
Dellino P, Isaia R, Vope LL, Orsi G (2001) Statistical analysis of textural data from complex pyroclastic sequences: implications for fragmental processes of the Agnano-Monte Spina Tephra (4.1 ka), Phlegraean Fields, southern Italy Bulletin of Volcanology 63:443-461
Dellino P, La Vope L (1996) Image processing analysis in recnostructing fragmentation and transportation mechanisms of pyroclastic deposits. THe case of Monte-Pilato-Rocche Rosse erutpions, Lipari (Aeolian islands, Italy). Journal of Volcanology and Geothermal Research 71:13-29
Dellino P, Liotino G (2002) The fractal and multifractal dimensions of volcanic ash particles contour: a test study of the utility and volcanological relevance Journal of Volcanology and Geothermal Research 113:1-19
Dimroth E, Pierre C, Leduc M, Sanshagrin Y (1978) Structure and organization of Archean subaqueous basalt flows, Rouyn-Noranda area, Quebec, Canada. Canadian Journal of Earth Science 15:902-918
Durig T, Mele D, Dellino P, Zimanowski B (2012) Comparative analyses of glass fragments from brittle fracture experiments and volcanic ash particles. Bulletin of Volcanology 74:691-704
Edwards BR, I.P. S, Cameron B, Haynes C, Lloyd A, Hungerford JHD (2009) Evolution of an englacial volcanic ridge: Pillow Ridge tindar, Mount Edziza volcanic complex, NCVP, British Columbia, Canada. Journal of Volcanology and Geothermal Research 185:251-275
Eissen J-P, Fouquet Y, Hardy D, Ondreas H (2003) Recent MORB volcaniclastic explosive deposits formed between 500 and 1750 m.b.s.l. on the axis of the Mid-Atlantic Ridge, South of the Azores. In: White JDL, Smellie JL, Clague DA (eds) Explosive Subaqueous Volcanism AGU, Washington DC, pp 143- 166
Ersoy O, Chinga G, Aydar E, Gourgaud A, Cubukcu HE, Ulusoy I (2006) Texture discrimination of volcanic ashes from different fragmentation mechansims: A case study, Mount Nemrut stratovolcano, eastern Turkey. Computers and Geosciences 32:936-946
Fowler AD, Berger B, Shore M, Jones MI, Ropchan J (2002) Supercooled rocks: develoment and significance of varioles, spherulites, dendrites and spinifex in Archean volcanic rocks, Abitibi Greenstone belt, Canada. Precambrain Research 115:311-328

1036 Fujibayashi N, Sakai U (2003) Vesiculation and eruption processes of submarine effusive and
1037 explosive rocks from the middle Miocene Ogi Basalt, Sado Island, Japan. In: White JDL, Smellie
1038 JL, Clague DA (eds) Explosive submarine volcansim. AGU Washington DC, pp 259-272
1039 Gorny C, F. , White JDL, Gudmundsson M (2012) Contorticlasts and shoaling subglacial
1040 intrusions. In: Volcano Ice Interactions III. Anchorage, Alaska
1041 Graettinger AH, Skilling IP, McGarvie DW, Hoskuldsson A (2012) Intrusion of basalt into
1042 frozen sediments and generation of Coheren-Margined Volcaniclastic Dikes (CMVD's). Journal
1043 of Volcanology and Geothermal Research 217-218:30-38
1044 Gregg TKP, Fink JH (1995) Quantification of submarine lava-flow morphology through analog
1045 experiements. Geology 23:73-76
1046 Gregg TKP, Keszthelyi L (2004) The emplacement of pahoehoe toes: field observations and
1047 comparison to laboratory simulations. Bulletin of Volcanology 66:381-391
1048 Gregg TKP, Smith D (2003) Volcanic investigations of the Puna Ridge, Hawai'i: relations of
1049 lava flow morphologies and underlying slopes. Journal of Volcanology and Geothermal
1050 Research 126:63-77
1051 Griffiths RW, Fink J (1992) Solidification and morphology of submarine lavas: A dependence on
1052 extrusion rate. Journal of Geophysical Research 97:19729-19737
1053 Grunewald U, Zimanowski B, Büttner R, Phillips LF, Heide K, Büchel G (2007) MFCI
1054 experiements on the influence of NaCl-saturated water on phreatomagmatic explosions. Journal
1055 of Volcanology and Geothermal Research 159:126-137
1056 Gudmundsson MT (2003) Melting of Ice by magma-ice-water interactions during subglacial
1057 eruptions an indicator of heat transfer in subaqueous eruptions. In: White JS, JL; Clague, DA
1058 (ed) Explosive Subaqueous Volcanism American Geophysical Union, Washington DC, pp 61-72
1059 Gudmundsson MT, Sigmundsson F, Björnsson H (1997) Ice-volcano interaction of the 1996
1060 Gjálp subglacial eruption, Vatnajökull, Iceland. Nature 389:954-957
1061 Harpel CJ, Kyle PR, Dunbar NW (2008) Englacial tephrostratigraphy of Erebus volcano,
1062 Antarctica. Journal of Volcanology and Geothermal Research 177:549-568
1063 Head JW, Wilson L (2003) Deep submarine pyroclastic eruptions: theory and predicted
1064 landforms and deposits. Journal of Volcanology and Geothermal Research 121:155-193
1065 Heiken GH (1971) Tuff Rings: Examples from the Fort Rock-Christmas Lake Valley Basin,
1066 South-Central Oregon. Journal of Geophysical Research 76(23):5615-5626
1067 Helo C, Longpre M-A, Shimizu N, Clague DA, Stix J (2011) Explosive eruptions at mid-ocean
1068 ridges driven by CO2- rich magmas. Nature Geoscience 4:260-263
1069 Höskuldsson A, Sparks RSJ, Carrol MR (2006) Constraints on the dynamics of subglacial basalt
1070 eruptions from geological and geochemical observations at Kverkfjoll, NE-Iceland. Bulletin of
1071 Volcanology 68:689-701
1072 Houghton BF, Gonnermann H (2008) Basaltic explosive volcanism: Constraints from deposits
1073 and models Chemie der Erde 68:117-140
1074 Houghton BF, Nairn IA (1991) The 1976-1982 Strombolian and phreatomagmatic eruptions of
1075 White Island, New Zeland: eruptive and depositional mechanisms at a 'wet' volcano. Bulletin of
1076 Volcanology 54:25-49
1077 Houghton BF, Schmincke H-U (1989) Rotenberg scoria cone, East Eifel: a complex Strombolian
1078 and phreatomagmatic volcano. Bulletin of Volcanology 52:28-48

Houghton BF, Smith RT (1993) Recycling of magmatic clasts during explosive eruptions: estimating the true juvenile content of phreatomagmatic volcanic deposits. Bulletin of Volcanology 55:414-420
Jones JG (1970) Intraglacial volcanoes of the Laugarvatn region, Southwest Iceland II. The Journal of Geology 78(2):127-140
Kokelaar P (1986) Magma-water interactions in subaqueous and emergent basaltic volcanism. Bulletin of Volcanology 48:275-289
Lautze NC, Taddeucci J, Andronico D, Cannata C, Tornetta L, Scarlato P, Houghton B, Lo Castro MD (2012) SEM-based methods for the analysis of basaltic ash from weak explosive activity at Etna in 2006 and the 2007 eruptive risis at Stromboli. Physica and Chemistry of the Earth 45-46:113-127
Maicher D, White JDL, Batiza R (2000) Sheet hyaloclastite: density-current deposits of quench and bubble-burst fragments from thin, glassy sheet lava fows, Seamount Six, Eastern Pacific Ocean. Marine Geology 171:75-94
Mastin LG, Christiansen RL, Thornber C, Lowenstern J, Beeson M (2004) What makes hydromagmatic eruptions violent? Some insights from the Keanakako'i Ash, Kilauea Volcano, Hawai'i. Journal of Volcanology and Geothermal Research 137:15-31
Mastin LG, Spieler O, Downey WS (2009) An experimental study of hydromagmatic fragmentation through energetic, non-explosive magma-water mixing. Journal of Volcanology and Geothermal Research 180:161-170
Mattox T, Mangan M (1997) Littoral hydrovolcanic explosions: a case study of lava-seawater interaction at Kilauea volcano Journal of Volcanology and Geothermal Research 75:1-17
Mattsson HB (2010) Textural variation in juvenile pyroclasts from an emergent, Surtseyan-type, volcanic eruption: The Capela tuff cone, Sao Miguel (Azores). Journal of Volcanology and Geothermal Research 189:81-91
Mattsson HB, Tripoli BA (2011) Depositional characteristics and volcanic landforms in the Lake Natron-Engaruka monogenetic field, northern Tanzania. Journal of Volcanology and Geothermal Research 203:23-34
Moitra P, Gonnerman HM, Houghton BF, Giachetti T (2013) Relating vesicle shapes in pyroclasts to eruption styles. Bulletin of Volcanology 75:691
Moore JG (1975) Mechansim of formation of pillow lava. American Scientist 63(3):269-277
Moore JG, Calk LC (1991) Degassing and differentiation in subglacial volcanoes, Iceland Journal of Volcanology and Geothermal Research 46:157-180
Moore JG, Hickson CJ, Calk LC (1995) Tholeiitic-alkalic transition at subglacial volcanoes, Tuya region, British Columbia, Canada. Journal of Geophysical Research 100(B12):24577-24592
Murtagh RM, White JDL, Sohn YK (2011) Pyroclast textures of the Ilchulbong 'wet' tuff cone, Jeju Island Journal of Volcanology and Geothermal Research 201:385-396
Nemeth K, Cronin SJ (2011) Drivers of explosivity and elevated hazard in basaltic fissure eruptions: The 1913 eruption of Ambrym Volcano, Vanuatu (SW-Pacific). Journal of Volcanology and Geothermal Research 201:194-209
Parcheta CE, Houghton BF, Swanson DA (2013) Contrasting patterns of vesiculation in low, intermediate, and high Hawaiian fountains: A case study of the 1969 Mauna Ulu eruption. Journal of Volcanology and Geothermal Research

1123 Parfitt E, A., Wilson L (2009) Fundamentals of Physical Volcanology In: Blackwell Publishing
1124 Malden, MA, p 230
1125 Polacci M, Baker DR, Bai L, Mancini L (2008) Large vesicles record pathways of degassing at
1126 basaltic volcanoes. Bulletin of Volcanology 70:1023-1029
1127 Portner RA, Daczko NR, Dickinson JA (2010) Vitiriclastic lithofacies from Macquarie Island
1128 (Southern Ocean): compositional influence on abyssal eruption explosivity in a dying Miocene
1129 spreading ridge. Bulletin of Volcanology 72:165-183
1130 Ross P-S, White JDL (2012) Quantification of vesicle characteristics in some diatreme-filling
1131 deposits and the explosivity levels of magma-water interactions within diatremes. Journal of
1132 Volcanology and Geothermal Research 245-246
1133 Ross PS, Delpit S, Haller MJ, Nemeth K, Corbella H (2011) Influence of the substrate on maar-
1134 diatreme volcanoes- An example of a mixed setting from the Pali Aike volcanic field, Argentina
1135 Journal of Volcanology and Geothermal Research 201:253-271
1136 Rosseel J-B, White JDL, Houghton BF (2006) Complex bombs of phreatomagmatic eruptions:
1137 Role of agglomeration and welding in vents of the 1886 Rotomahana eruption, Tarawera, New
1138 Zealand. Journal of Geophysical Research 111:B12205
1139 Schipper CI, Sonder I, Schmid A, White JDL, Dürig T, Zimanowski B, Büttner R (2013) Vapour
1140 dynamics during magma-water interaction experiments: hydromagmatic origins of submarine
1141 volcaniclastic particles (limu o Pele) Geophysical Journal International:1109-1115
1142 Schipper CI, White JDL (2010) No depth limit to hydrovolcanic limo o Pele: analysis of limu
1143 from Lō'ihi Seamount, Hawai'i Bulletin of Volcanology 72:149-164
1144 Schipper CI, White JDL, Houghton BF (2010) Syn- and post-fragmentation textures in
1145 submarine pyroclasts from Lo'ihi Seamount, Hawai'i. Journal of Volcanology and Geothermal
1146 Research 191:93-106
1147 Schipper CI, White JDL, Houghton BF (2011) Textural, geochemical, and volatile evidence for a
1148 Strombolian-like eruption sequence at Lo'ihi Seamount Hawai'i Journal of Volcanology and
1149 Geothermal Research 207:16-32
1150 Schipper CI, White JDL, Houghton BF, Shimizu N, Stewart RB (2010) Explosive submarine
1151 eruptions driven by volatile-coupled degassing at Lo'ihi Seamount, Hawai'i. Earth and Planetary
1152 Science Letters 295:497-510
1153 Schipper CI, White JDL, Houghton BF, Shimizu N, Stewart RB (2010) "Poseidic" explosive
1154 eruptions at Loihi Seamount, Hawaii. Geology 38:291-294
1155 Schipper CI, White JDL, Zimanowski B, Büttner R, Sonder I, Schmid A (2011) Experimental
1156 interaction of magma and "dirty" coolants. Earth and Planetary Science Letters 203:323-336
1157 Schmid A, Sonder I, Seegelken R, Zimanowski B, Büttner R, Gudmundsson MT, Oddsson B
1158 (2010) Experiments on the heat discharge at the dynamic magma-water-interface. Geophysical
1159 Research Letters 37:L.20311
1160 Scott CR, Richard D, Fowler AD (2003) An Archean submarine pyroclastic flow due to
1161 submarine dome collapse: The Hurd Deposit, Harker Township, Ontario, Canada. In: White
1162 JDL, Smellie JL, Clague DA (eds) Subaqueous Explosive Volcanism AGU Washington DC, pp
1163 317-327
1164 Shea T, Houghton BF, Gurioli L, Cashman KV, Hammer JE, Hobden B (2010) Textural studies
1165 of vesicles in volcanic rocks: An integrated methodology. Journal of Volcanology and
1166 Geothermal Research 190:271-289

Simpson K, McPhie J (2001) Fluidal-clast breccia generated by submarine fire fountaining, Trooper Creek Formation, Queensland, Australia. Journal of Volcanology and Geothermal Research 109:339-355
Skilling IP (2009) Subglacial to emergent basaltic volcanism at Hlöðufell, south-west Iceland: A history of ice-confinement. Journal of Volcanology and Geothermal Research 185:276-289
Skilling IP, Mercurio E, Cameron B (2009) Ice-confined basaltic eruptive fissure complexes in Iceland: Accessible analogs for understanding shallow submarine ridge construction. In: AGU. AGU, San Fransico
Smellie JL (2001) Lithofacies architecture and construction of volcanoes erupted in englacial lakes: Icefall Nunatak, Mount Murphy, Eastern Marie Byrd Land, Antarctica In: White JDL, Riggs NR (eds) Volcaniclastic Sedimentation in Lacustrine Settings. Blackwell Science Ltd, London, p 309
Smellie JL, Hole MJ (1997) Products and processes in Pliocene-Recent, subaqueous to emergent volcanism in the Antarctic Peninsula: examples of englacial Surtseyan volcano construction. Bulletin of Volcanology 58:628-646
Smellie JL, Johnson JS, McIntosh WC, Esser R, Gudmundsson MT, Hambrey MJ, van Wyk de Vries B (2008) Six million years of glacial history recorded in volcanic lithofacies of the James Ross Island Volcanic Group, Antarctic Peninsula. Palaeogeography, Palaeoclimatology, Palaeoecology 260:122-148
Sohn RA, Willis C, Humphris S, Shank TM, Singh H, Edmonds HN, Kunz C, Hedman U, Helmke E, Jakuba M, Liljebladh B, Linder J, Murphy C, Nakamura K-i, Sato T, Schlindwein V, Stranne C, Tausenfruen M, Upchurch L, Winsor P, Jakobsson M, Soule AA (2008) Explosive volcanism on the ultraslow-spreading Gakkel ridge, Arctic Ocean. Nature 453:1236-1238
Sohn YK (1995) Geology of Tok Island, Korea: eruptive and depositional processes of a shoaling to emergent island volcano. Bulletin of Volcanology 56:660-674
Solgevik H, Mattson HB, Hermelin O (2007) Growth of an emergent tuff cone: Fragmentation and depositional processes recorded in teh Capelas tuff cone, Sao Miguel, Azores. Journal of Volcanology and Geothermal Research 159:246-266
Sorrentino L, Cas RAF, Stilwell JD (2011) Evolution and facies architecture of Paleogene Surtseyan volcanoes on Chatham Islands, New Zealand, Southwest Pacific Ocean Journal of Volcanology and Geothermal Research 202:1-21
Staudigel H, Schmincke H-U (1984) The Pliocene Seamount Series of La Palma/Canary Islands. Journal of Geophysical Research 89(B13):11195-11215
Stovall WK, Houghton BF, Gonnermann H, Fagents S, Swanson DA (2011) Eruption dynamics of Hawaiian-style fountains: the case study of episde 1 of the Kilauea Iki 1959 eruption. Bulletin of Volcanology 73:511-529
Walker GPL (1992) Morphometric study of pillow-size specturm among pillow lavas. Bulletin of Volcanology 54:459-474
Walker GPL, Croasdale R (1971) Characteristics of some basaltic pyroclasts. Bulletin of Volcanology 35:303-317
Werner R, Schmincke H-U (1999) Englacial vs lacustrine origin of volcanic table mountains: evidence from Iceland. Bulletin of Volcanology 60:335-354
Werner R, Schmincke H-U, Sigvaldason GE (1996) A new model for the evolution of table mountains: volcanological and petrological evidence from Herdubreid and Herdubreidartögl volcanoes (Iceland) Geol Rundsch 85:390-397

White JDL (1996) Impure coolants and interaction dynamics of phreatomagmatic eruptions. Journal of Volcanology and Geothermal Research 74:155-170
White JDL (1996) Pre-emergent construction of a lacustrine basaltic volcano, Pahvant Butte, Utah (USA). Bulletin of Volcanology 58:249-262
White JDL (2000) Subaqueous eruption-fed density currents and their deposits. Precambrain Research 101:87-109
White JDL, Ross PS (2011) Maar-diatreme volcanoes: A review. Journal of Volcanology and Geothermal Research 201:1-29
Wohletz KH (1986) Explosive magma-water interactions: Thermodynamics, explosions mechansims, and field studies. Bulletin of Volcanology 48:245-264
Wohletz KH (2002) Water/magma interaction: some theory and experiments on peperite formation. Journal of Volcanology and Geothermal Research 114:19-35
Wohletz KH (2003) Water/magma interaction: physical considerations for the deep submarine environment. In: White JDL, Smellie JL, Clague DA (eds) Explosive Subaquous Volcanism AGU Washington DC, pp 25-49
Zimanowski B, Büttner R (2002) Dynamic mingling of magma and liquefied sediments Journal of Volcanology and Geothermal Research 114:37-44
Zimanowski B, Büttner R (2003) Phreatomagmatic explosions in subaqueous volcanism. In: White JDL, Smellie JL, Clague DA (eds) Explosive Subaqueous Volcansim. AGU, Washington DC, pp 51-60
Zimanowski B, Büttner R, Lorenz V (1997) Premixing of magma and water in MFCI experiements Bulletin of Volcanology 58:491-495
Zimanowski B, Wohletz KH (2000) Physics of Phreatomagmatism-1. Terra Nostra 6:515-523
Zimanowski B, Wohletz KH, Dellino P, Büttner R (2003) The volcanic ash problem. Journal of Volcanology and Geothermal Research 122:1-5

Figure captions

Figure 1 Location of Askja, Iceland including locations of pillow lava, breccia to lapilli tuff sequences. The shaded area represents the field area, Austurfjöll. Sample sites are located in major gullies incised into the base of the glaciovolcanic sequence of Askja. Sample locations from north to south are Drekagil (DG), Nautagil (NG), and Rosagil (RG).

Figure 2 Overview of Drekagil sequence including field image, annotated sketch of sampling sites and stratigraphic log.

Figure 3 Overview of the Nautagil sequence including field image, annotated sketch of sampling sites, and stratigraphic log.

Figure 4 Overview of the Rosagil sequence including field image, annotated sketch of sampling sites, and stratigraphic log.

Figure 5 Comparison of the two dominant pillow lava facies from Austurfjöll. Schematics of the pillow form outlines highlight the regularity of Pl1 and the irregularity of Pl2 lavas.

Figure 6 Field images and schematic characterizations of outsized clasts found within the three sequences described at Askja. A) Image of a broken pillow clast displaying typical rind and vesicle textures of a pillow. B) A fluidal bomb displaying irregular shape and vesicle distribution. Sketches of idealized clasts include a pillow in cross-section, a fluidal bomb in cross-section and an angular block.

Figure 7 Stratigraphic overview of a typical effusive to explosive transitional deposit from Askja. Three grain sizes (blocks/bombs, lapilli, and fine ash) were analyzed for size, morphology, and vesicularity as they trend up section. Bombs are described by maximum clast diameter. Vesicularity of both bombs and lapilli are presented as average values for a stratigraphic layer. Vesicle morphology is presented as representative shapes from actual lapilli measured. The fine ash morphologies are presented as percents of relative abundance through the sequence.

Figure 8 Examples of lapilli and fluidal bomb morphologies and textures that reflect ductile fragmentation of the magma. Images on the right hand side are field images. Images on the left hand side are from a binocular microscope. A) Ductile structures in a lapillus quench crust. B) Large coalesced vesicles in a fluidal bomb. C) Fluidal crust structures preserved on a lapillus by surrounding matrix (indicated by yellow line). D) Convolute bomb shape and vesicles. E) Large coalesced bubbles interacting with the clast surface. F) Fluidal bomb with intact quench rind (broken for sampling). G) Lapillus with stretched vesicles along glassy surface. H) Fluidal bomb with large randomly distributed vesicles. A brittle overprinting is present in images A, E and G, where the lapilli have been brittlely fractured.

Figure 9 SEM secondary electron images of example grain morphologies found in textural analysis of fine ash particles. Adhering particles and aggregate ash particles are common. Arrows are used to highlight features of interest. A) Blocky grain and (left) and fragile spine on margin of a vesicle influenced grain boundary (right) from DG. B) Tube vesicles from DG. C) Vesicles isolated within glassy ash particles from DG. Vesicles may intersect fracture surfaces they do not control the fracture shape. D) Limu o Pele from DG. E) A particle with vesicle-dominated fracture surfaces and fragile spines from NG. F) Ash particles dominated by vesicles From NG. G) Elongate bladed shaped vesicle free particles From DG. Note the micron scale crust flaking off the particle. H) Blocky particles exhibiting scalloped edges from NG. I) Chip and blocky shaped particles from NG. Note the stepped appearance of the conchoidal fracture.

Figure 100 Model of fragmentation mechanisms as they occur during the formation of the three transitional sequences at Askja. Solid lines represent relative dominance of a fragmentation style. Dotted lines indicate continued, but diminished fragmentation. The question mark indicates that the final position of magmatic fragmentation is an inference as the signature is muted by FCI activity by this stratigraphic level. The textures used to construct the model are described.

EFFrevisions.docx
Click here to view linked References

Subaqueous basaltic magmatic explosions trigger phreatomagmatism: a case study from Askja, Iceland

Alison H. Graettinger[1], Ian Skilling[2], Dave McGarvie[3], Ármann Höskuldsson[4]

1Alison H. Graettinger (corresponding author)
University of Pittsburgh, 200 SRCC, Pittsburgh PA, 15260
*Currently:
University at Buffalo, Center for Geohazard Studies, 411 Cooke Hall, Buffalo, NY 14260
Telephone: +17166454286
agraettinger@gmail.com

2Ian P. Skilling
University of South Wales, Pontypridd, RCT, CF37 4BD, UK
Telephone: +44 1443 654151
ipskilling@gmail.com

3Dave W. McGarvie
The Open University in Scotland, 10 Drumsheugh Gardens, Edinburgh, EH3 7QJ, UK
Telephone: +44 (0) 131 226 3851
Dave.mcgarvie@open.ac.uk

4Ármann Höskuldsson
The University of Iceland, Askja, Sturlagata 7, 101 Reykjavik, Iceland
Telephone +354-5254215
armh@hi.is

Abstract

Sequences of basaltic pillow lavas that transition upwards with systematic gradation from pillow fragment breccias to fluidal bomb-bearing breccia to bomb-bearing lapilli tuffs are common at Askja volcano, Iceland. Based on the detailed textural investigation of three of these sequences, we argue that they record temporally continuous transition from effusive to explosive products that were erupted from and deposited at or near a single subaqueous vent. The recognition of such sequences is important as they provide evidence for controls on the onset of explosive activity in subaqueous environments. Such investigations are complicated by the interplay of magmatic gas expansion, phreatomagmatic and mechanical granulation fragmentation mechanisms in the subaqueous eruptive environment.

~~The Askja sequences represent deposits resulting from the transition from effusive pillow eruption, to explosive magmatic gas expansion that in turn enabled more effective phreatomagmatic explosions.~~ All of the sequences studied at Askja have textural, componentry and sedimentological characteristics suggestive of a close genetic and spatial relationship between the pillow lavas and all of the overlying glassy clastic deposits. The identification of magma fragmentation signatures in pyroclasts was accomplished through detailed textural studies of pyroclasts within the full range of grain sizes of a given deposit i.e. bomb/blocks, lapilli and fine ash. These textural characteristics were compared and evaluated as discriminators of fragmentation in pyroclastic deposits. ~~The textures investigated include 2-D vesicle and microlite percentages, average vesicle dimensions, vesicle number density, vesicle morphology, sideromelane to tachylite proportions, clast size, clast shape and the nature of any sedimentary structures.~~ The presence of angular vitric clasts within the breccia and lapilli tuff displaying

fragile glassy projections indicates little or no post-depositional textural modification. ~~This observation and the fact that the clastic deposits are massive in nature, with no traction current structures, bedding or erosional contacts observed, is consistent with an interpretation as rapidly-emplaced fallout.~~ A shift in vesicle and clast textures between the pillow lavas and the large concentration of fluidal bombs in the breccia indicate that the phreatomagmatic explosions were initially triggered by magmatic vesiculation. The initial magmatic gas expansion may have been triggered by depressurization caused by the drainage of the ice-confined lake surrounding Askja. The Fuel Coolant Interactions (FCI) of the more efficient phreatomagmatic explosion was enabled by the increase in the surface area to volume ratio of the fluidal bombs in the water, producing a premix of magma and water. The onset and increasing influence of phreatomagmatic fragmentation is preserved in the presence of very fine blocky ash particles and diminished presence of larger particles such as fluidal bombs. The textural, sedimentological and environmental characteristics of these deposits suggest that phreatomagmatic explosions can be triggered by initial magmatic gas expansion, but that it is likely one of many mechanisms for triggering such explosions.

Keywords: magma fragmentation; phreatomagmatic explosions; basalt; subaqueous eruption

1.0 Introduction

The question of what controls the transition of basaltic effusive to explosive activity in water-rich environments, has been a matter of debate over the last 20 years (Houghton and Nairn 1991; Houghton and Schmincke 1989; Mastin et al. 2004; White 1996; Wohletz 1986; Wohletz 2002; Wohletz 2003; Zimanowski et al. 1997; Zimanowski et al. 2003). The answer to this question has

important implications for modeling volcanic hazards, such as the potential for explosions or the grain size distribution, height and duration of ash plumes in wet environments. Submarine exploration technology has advanced our ability to describe subaqueous explosive volcanic deposits from the submarine environment (Clague et al. 2003; Clague and Davis 2003; Clague et al. 2009; Eissen et al. 2003). However, the study of explosively generated deposits formed in an ice-confined (glaciovolcanic) environment offers much more accessible deposits that are commonly well preserved in three-dimensions. We argue that such centers preserve sequences that record in situ transitions from effusive to explosive activity at a single vent. The detailed textural and stratigraphic study of such sequences offers the best opportunity for understanding the onset of explosive activity and the interplay of fragmentation mechanisms in natural subaqueous settings.

The focus of this study is three ca. 30 m thick, glass-rich, incipiently palagonitized basaltic pyroclastic deposits that directly overlie pillow lavas from Askja volcano, Iceland (Fig. 1). All three clastic sequences are massive but display a systematic and continuous fining upward from pillow-fragment breccia to fluidly-shaped bomb-bearing breccia and then into vitric lapilli tuff. Ostensibly similar sequences of pillow lavas overlain by breccias, containing pillow fragments, capped by vitric lapilli tuffs, have been described from many areas, including ophiolite sequences (Carlisle 1963), Archean basalt provinces (Dimroth et al. 1978), ocean island settings (Fujibayashi and Sakai 2003) and several glaciovolcanic sequences (Jones 1970; Skilling 2009; Werner and Schmincke 1999). Such sequences could clearly be derived through many processes. Common interpretations for these sequences can be divided into those where the clastic deposits are (1) erupted from a different vent than that which produced the lavas, (2) were produced by the same vent that produced the lavas but not as part of a temporally continuous

eruption, (3) or were erupted from the same vent as lavas and were part of a continuous eruption. Mechanisms that produce unrelated sequences of pillow lavas and clastic deposits include deposition of density currents from nearby vents or post-emplacement collapse of deposits on top of the pillows. Similar sequences produced from the same vent without continuous eruption include flow related collapse (autoclastic breccias), intrusion of pillowed dikes into clastic deposits, or explosive activity instigated under already solidified lava. Based on a detailed textural analysis of the sequences from the Austurfjöll massif of Askja, we argue that the deposits were produced from the same vent over a brief eruption that transitioned from effusive activity to magmatic explosive, and then to phreatomagmatic explosive eruptive activity.

The interpretation of such clastic deposits relies heavily on the distinction of the influence of different fragmentation mechanisms in the formation of subaqueous basaltic pyroclasts along the contact between facies within the transitional sequences. Evidence for the mechanisms of fragmentation, transportation and deposition are preserved in the textures of subaqueous pyroclasts over the full range of grain sizes, including bombs, lapilli and fine ash, though most research has focused on fine ash textures (Büttner et al. 1999; De Rosa 1999; Dellino et al. 2001; Dellino and Liotino 2002; Durig et al. 2012; Ersoy et al. 2006; Heiken 1971; Mattox and Mangan 1997). These textural data can then be used to make inferences on the controls of the onset of subaqueous explosive activity and specifically phreatomagmatic activity. In this study we present data on textural characteristics of fine ash to block-sized clasts that could be used to help distinguish phreatomagmatic from magmatic fragmentation, and argue that the phreatomagmatic eruptions in our study area were generated following an initial mingling (premixing) of magma and water driven by magmatic fragmentation. It is not clear how important or common initial mingling by magmatic fragmentation might be in basaltic

phreatomagmatic sequences elsewhere, and is likely only one mechanism for instigating such eruptions. The uniquely dynamic nature of the ice-confined lakes may play a role in the initiation of magmatic gas expansion through depressurization caused by lake drainage. Nevertheless, similar textural investigations may be used to identify the mechanisms during the onset of exposivity in other basaltic phreatomagmatic systems.

1.1 Eruption setting

Basaltic glaciovolcanic systems under thick ice (>400 m) typically evolve into ice-confined lacustrine centers (Allen et al. 1982; Gudmundsson 2003; Gudmundsson et al. 1997; Werner and Schmincke 1999). Within the ice-confined lake the water level may change rapidly and repeatedly through time (Bjornsson 2002; Gudmundsson et al. 1997; Höskuldsson et al. 2006; Smellie et al. 2008). Simplified models of such centers include initial subaqueously emplaced effusive products, dominated by pillowed lavas, followed by a shift towards more explosive activity with deposition of glassy fragmental deposits (Allen 1980; Jones 1970; Moore et al. 1995; Werner et al. 1996). Within this model it is assumed that there is a decreasing fragmentation and dispersal of subaqueous eruptions as confining pressure or water depth increases, particularly above 400 m (Allen 1980; Clague et al. 2003; Zimanowski and Büttner 2003). However, investigations of submarine basaltic deposits are revealing the presence of explosively derived deposits at depths up to 3 km (Clague and Davis 2003; Fujibayashi and Sakai 2003; Helo et al. 2011; Portner et al. 2010; Schipper and White 2010; Schipper et al. 2010; Schipper et al. 2011; Sohn et al. 2008; Wohletz 2003). This uncertainty over the importance of controls other than confining pressure (Mastin et al. 2009; Schipper et al. 2011; White 1996) on

151 the triggering of subaqueous explosions emphasizes the importance for detailed studies of natural
152 deposits that may record the onset of basaltic explosions in water.
153
154 **1.2 Field area**
155 Askja is one of the largest and best-exposed formerly ice-confined volcanoes on Earth. Most
156 research to date has been on its Holocene (ice-free) evolution. It comprises a complex of basaltic
157 glaciovolcanic massifs that are dominated by pillow lavas and subaqueously emplaced vitric
158 lapilli tuff deposits. These massifs are cut by at least three calderas and surrounded by Holocene
159 subaerial lava flows (Fig. 1). The greatest volume of glaciovolcanic deposits at Askja is the
160 eastern mountain massif, Austurfjöll, which is truncated by the two youngest calderas.
161 Austurfjöll has been described briefly by Brown et al. (1991), Sigvaldason, (1968 and 2002) and
162 more recently in detail by Graettinger et al. (2012).
163 Austurfjöll is incised on its eastern side by large gullies that extend up to 3 km into the
164 massif. The vertical exposure within the gullies is between 10 and 100 m. These exposures are
165 dominated by pillow lava sheets, lava breccias and vitric lapilli tuff. Three of these gullies
166 contain well-exposed sequences that display gradual transitions up section between effusive
167 pillow lavas at their base, to an upward fining pillow fragment and bomb-bearing breccia and
168 vitric lapilli tuff sequence. The sequences have lateral continuity of tens of meters and can be
169 traced in multiple directions. The three gullies from north to south are named, Drekagil, Nautagil
170 and Rosagil (Fig. 1).
171
172 **2.0 Methods**

This study is based on field work conducted over two seasons at Austurfjöll. The three sequences of basaltic pillow lava, pillow-fragment breccia, fluidal bomb-bearing breccia and vitric lapilli tuffs were identified in 2010 and revisited in 2011 for more detailed sampling and study. Samples were collected from the top of the basal pillow units, the lowermost breccia at the contact with the pillow lavas and then progressively up through the section of overlying breccias and vitric lapilli tuffs, with an average sample interval of two meters. At each location a sample of matrix (lapilli and any ash present) and an outsized clast was collected. Outsized clasts are defined here as the largest clasts that exceed the visually estimated median grain size at a particular stratigraphic level. Measurements were taken of the average clast size and the outsized clasts. Measurements were limited to the longest axis of the largest outsized clasts with intact glassy chill rinds around their entire margins. Field measurements of vesicularity percentages of the core and glassy rim of outsized clasts were supported by measurements of field photographs. A minimum of five measurements of such clasts were taken at each site. If a secondary size mode of outsized clast was present, the largest clasts representative of both modes were studied.

A binocular microscope with mounted digital camera was used to estimate the vesicularity percentage of partially disaggregated matrix and clasts. Additional observations of vesicle shape, distribution, alignment and coalescence were recorded. These observations were also used to estimate the mean matrix grain sizes. The partial consolidation, high friability and fragile clast morphologies precluded full granulometric analyses. Digital images of thin sections were also used to quantify 2D vesicularity percentages and dimensions using ImageJ software. Vesicle number density (Nv) was calculated based on methods outlined in Shea et al. (2010). In addition to vesicle textures, the presence of microlites and rare phenocrysts, tachylite, sideromelane and mixed tachylite-sideromelane fragments were documented across matrix and

clast samples. Values represent 2D volume percent of each parameter calculated from image analysis.

Detailed logging of sedimentary structures and X-ray fluorescence (XRF) analyses of outsized clasts and pillows were completed for each sequence to investigate the genetic relationships between the facies of the sequence. XRF bulk rock major element analyses were conducted at Washington State University GeoAnalytical lab from pillow lavas, fluidal bombs in the breccia and outsized clasts in the lapilli tuff.

Textural analysis, using secondary electron images collected on a JEOL JSM-5900 at Dickinson College, of the fine ash fraction included study of grain mounts of loose grains, coated in carbon. Samples were sieved to isolate particles <50 μm to target potential 'active' particles (<130 μm) of fuel coolant interaction (FCI) experiments (Büttner, 2002). Textures described include ash morphology (blocky and equant, chips and blades, or spines and needles), conchoidal fracture, the presence of intact or broken vesicles, abrasion features (scalloped edges), coatings and adhering particles. Textures were recorded in a per grain basis, so percentages represent the abundance of a given texture, not volumetric presence of vesicles within the ash particles.

3.0 Overview of lithofacies

All three sequences are exposed in steep walled gullies incised into the base of the eastern margin of the 750 m high Austurfjöll massif of Askja volcano (Fig.1). The sequences have basal pillow lavas overlain by pillow-fragment and fluidal bomb-bearing breccias and capped by vitric lapilli tuffs. Fluidal bombs also occur within the lapilli tuff sequences, but decrease in abundance up section. The transition from breccia to lapilli tuff is defined as the point where the fluidal bomb presence is less than 30 vol.% of the deposit. The clastic deposits range from 15-35 m in

thickness and display gradational transitions between each lithofacies. Geomorphologic evidence, particularly the thickness of subaqueous sequences at Austurfjöll (700 m), and volatile saturation pressure data indicate the eruption of the basal lavas occurred in water ca. 700 m deep, or beneath some combination of water, ice and sediment with a confining pressure of ca. 7.7 MPa (Cameron, B. unpublished data). There is no structural or textural evidence that these three sequences include subaerially emplaced deposits.

Pillow lava flows at Askja can be subdivided into two main lithofacies, named Pl1 and Pl2. The distinction between the two lithofacies is the variability in the dimensions of the pillow tubes and the frequency of transitions into non-pillowed lavas. Pl1 lavas are comprised of highly regular tubes, both in shape and cross-sectional dimension with average diameters of 50 cm and a range of <20 cm in diameter per within a pillow lava sheet. Pl2 lavas contain a much greater diversity of pillow dimensions, with cross-sectional diameters ranging from 50–200 cm. They also commonly display transitions to columnar, curvi-columnar and blocky-jointed subaqueously emplaced lava flows without pillow forms. Pl2 lavas also have more distended pillow shapes and display less regular stacking (Fig. 5). Pillows measured in the basal lava of the three transitional sequences and apparently intact pillows in the lowermost pillow breccia, fall within observed range of the massif, where cross-sectional diameters are typically 60 cm and core vesicularities around 50 vol.%. Their internal variability and common occurrence of transitions to non-pillowed lavas means that the basal lavas of all three sequences described here are classed as Pl2 facies.

In all three sequences the breccia that immediately overlies the pillow lavas is initially entirely clast-supported, composed of apparently intact pillows and pillow fragments, with decreasing occurrence of obvious pillow forms (intact or otherwise) within 1-2 meters of the

contact. Clasts in the breccia become progressively more isolated in the vitric lapilli matrix (30-70 vol.% of the breccia) up section and pillow fragments are replaced by fluidal bombs within one meter of the pillow lava to breccia contact.

Pillows are distinguished by their regular, ellipsoidal cross-sectional shape and occasional presence of keels. Typical pillows exhibit vesicle bands and pipe vesicles (Fig. 6). Pillows typically have regular glassy rinds between 0.1 and 1.5 cm thick. Vesicles are typically round and undeformed in the vesicle bands that dominate the outer few cm of the pillow. Pillow cores may display coalesced vesicle morphologies and radial pipe vesicles are common at the core and rim of the pillow (Edwards et al. 2009; Fujibayashi and Sakai 2003; Höskuldsson et al. 2006). Pillow fragments display partial glassy quench rinds, interrupted vesicle bands, pipe vesicles and incomplete pillow forms. Fluidal bombs on the other hand display a wider range of cross-sectional morphologies, with convolute clast shapes and an irregular distribution of irregular vesicles. When not intact, bombs display a jig-saw fit fracture pattern. The average fluidal bomb vesicularity is on the order of 25% but can be as much as 60 %. Fluidal bombs have glassy rinds between 0.1 and 2 cm in diameter. Vesicles are also typically coalesced and polylobate, with an abundance of elongate vesicles parallel to the glassy rim. Radial pipe vesicles are absent. The distribution of vesicles within the bombs is irregular. Vesicle morphology within the bombs displays an increase in coalescence up section (Fig. 7). The breccia matrix comprises coarse, glassy and angular vitric lapilli (0.5-2 cm). All the vitric clasts within the breccias and lapilli tuffs except fluidal bombs are highly angular with fragile shapes.

The vitric lapilli tuff makes up the bulk of the sequences. The change from breccia into lapilli tuff is characterized by a gradual decrease in the abundance of fluidal bombs with height in all three sequences, from 30 vol.% in the top of the breccia unit to 5 vol.% at the top of lapilli

tuff (Fig. 2-4). Weak sub-parallel bedding develops only in the upper 3 m of the lapilli tuff in two of the sequences, NG and RG. The diameter of the bombs peaks in the lower portion of the lapilli tuff, frequently within 5-10 m of the facies transition (Fig. 7) and then decreases rapidly up section. Lapilli are 1-3 cm are dominantly equant and angular, but may have partial fluidal margins and display no systematic change in size up section. Vesicles in the vitric lapilli display a wide range of morphologies that include isolated ellipsoidal to irregularly shaped vesicles, high degrees of interconnectedness, and the presence of tube vesicle morphologies (Fig. 8). Lapilli vesicularity is internally consistent between 20-40% depending on the sequence. The microlite content of bombs increases up-section from 2% up to nearly 10%. The microlite content of lapilli however, peaks in the breccia, and remains low in the lapilli tuff <10%. Clasts greater than 2 cm have sideromelane rims that can reach up to 1 cm thick and microlite-bearing tachylite cores. Fragments below 2 cm in diameter are dominated by sideromelane. Consequently, the overall ratio of sideromelane to tachylite in the deposit increases up-section. Ash and lapilli are typically very angular with delicate spines and margins preserved (Fig. 8). The clasts display no rounding or removal of fragile spines from fine ash and the deposits exhibit no traction current structures, slump structures or other evidence of remobilization or lateral transport. While palagonitized deposits are common within Austurfjöll, the deposits described here have very limited and impersistent occurrence of palagonite.

The bulk rock chemistry for the sequences of the basal pillows, fluidal bombs of the breccia and lapilli tuff and lapilli clasts were analyzed for major and trace element abundances. The deposits are all tholeiitic basalts with limited internal variability between clast types in given sequence as highlighted in Table 1.

Fourteen fine ash samples were selected for SEM micro-textural analysis from the uppermost breccias and through the overlying lapilli tuff unit of the Drekagil and Nautagil localities. Between 100 and 180 grains <50 microns were counted for each sample and values are reported as abundance of grains with a target texture. Individual particles may display multiple textures. Less than 25% of the fine ash particles had any obvious vesicles (Fig. 9). Of the vesicles present, only about 3% had clast margins dominated by the presence of a vesicle (where the vesicle influences the shape of 40% or greater of the margin. The bulk of vesicles observed at this scale were small, round and isolated within significantly larger grains and dissected by planar or obviously stepped conchoidal fracture surfaces. Vesicle sizes recorded in the fine ash were mostly between 5 and 100 microns in diameter. A significant portion of fine ash grain shapes (35-40%) were chips (one small dimension, two equal dimensions), blade (one small, one long dimension), or needle-like (two small and one long dimension) (Fig. 9). Approximately 45% of fine ash grains were blocky and roughly equant or prismatic in shape (all dimensions are similar; Fig. 9A). The fine ash samples also include minor occurrences of tube vesicle rich clasts (<10 %) and limu o Pele (<5 %). Limu o Pele are thin (μm to mm) curved lenses of sideromelane glass (Fig. 9D). These curved sheets of glass are significantly thinner than the chips described above. The curvature of the limu o Pele suggests they were derived from vesicles with a diameter greater than the typical vesicles preserved (>60 μm) at this grain size. There are no crystals in the fine ash component of any of the sequences.

Fine ash particles with sharp edges showed evidence of minor abrasion, including rounding and scalloping (Fig. 9H), on less than 10% of all fine ash grains studied. In contrast convolute and fragile shapes, including thin spines of glass (Fig. 9A,D,E), were present on an average of 12% of the fine ash grains. The fine ash fraction of the NG and DG sections displays

some minor discoloration from a grey brown to yellow brown, commonly associated with palagonatization. Other evidence for chemical alteration of the fine ash fraction includes pitting of fracture surfaces and flakey coatings. Adhering finer particles are common on 50% of the fine ash grains, but rarely obscure the complete grain. Some particles have thin (micron) skins or coatings that are cracked and flaking away from the grain.

3.1 Individual sequences

The three sequences studied occur within deep gullies called Drekagil, Nautagil and Rosagil (Fig. 1). The sequence in Drekagil (DG) is exposed in a near vertical cliff within a 50 m deep east-west trending gully. Laterally, the sequence overlies a sharp erosional contact of the top of a sequence of well-bedded lapilli and ash tuffs that display significant palaeotopography on their upper surface (Fig. 2). The pillow lavas occur as a thick (30 m) valley-filling pillow lava sheet that abuts and overtops a paleo-cliff of ash and lapilli tuff. Due to the steep nature of the modern gully, sampling of the pillow unit was limited to the margins of the lensoid unit. The corresponding stratigraphic log follows a diagonal path from the margin of the transitional sequence to its center to access the lapilli tuff directly overlying the greatest thickness of the pillow unit (Fig. 2). The pillow unit is well exposed in the vertical wall, directly below the lapilli tuff. The breccia that overlies the pillow lavas is ca. 5 m thick and initially clast supported with intact and fragmented pillow clasts preserved in the basal 1 m. The clasts are replaced by fluidal bombs with increasing lapilli matrix presence (transitioning from 30-70 vol.% of the breccia) in the upper 4 m. The lapilli tuff has a thickness of 14 m with fluidal bombs throughout. Maximum bomb sizes are 50 cm, but are predominantly between 20-30 cm in the lapilli tuff. . The sequence

is capped by a convolute bedded ash that is overlain by a feldspar-phyric non-pillowed sheet lava. The contact between the lapilli tuff and the ash tuff is sharp, but there is no evidence of significant erosion. The sequence at Drekagil is the only one of the three studied that contains accidental lithics in the lapilli tuff, namely subangular porphyritic tholeiite lava lapilli (< 5 cm in diameter), which comprise <1 vol.% of the deposit and are too infrequent to have any obvious trend in occurrence.

Nautagil (NG) contains the thickest of the sequences (35 meters) where it forms the entire southern wall of the gully (Fig. 3). The thickness of the basal pillow lava unit is uncertain as the pillows are partially covered by unconsolidated deposits of pumice from the 1875 eruption of Askja and local talus, but the pillow lavas are at least 2 m thick. The overlying breccia is 7 m thick with pillow fragments dominating the lowest 2 m giving way to fluidal bombs and increasing (up to 60 vol.%) lapilli matrix the upper 5 m. This breccia is overlain by 24 meters of lapilli tuff. In the upper 3 m of the lapilli tuff a weak parallel ca. 10^0 bedding dipping to the northeast (away from Austurfjöll) develops. Laterally, the deposit displays some palagonitization, but typically displays only incipient palagonitization along the sampled southern wall of the valley. This sequence is cut by a basaltic dike that is one of the type examples of coherent margined volcaniclastic dikes (CMVDs) described from Askja and interpreted as having formed by dike emplacement into ice-cemented volcaniclastic sediments (Graettinger et al. 2012).

The exposure in Rosagil (RG) makes up a large portion of the southern wall of the gully, with a total thickness of 16 m. The basal pillow lava exposure is limited due to talus, but has a minimum thickness of 2 m (Fig. 4). The breccia is 4 m thick with pillow fragments dominating the lower 1 m and fluidal bombs occurring in the upper 3 m. The breccia is overlain by ten

meters of lapilli tuff. A weak parallel and shallow (10^0 dipping northeast, away from the summit of Austurfjöll) stratification develops in the upper meter of the tuff. The upper 1 m of the deposit is also locally more intensely palagonitized than the rest of the deposit. Laterally (2-5 away from sampling area) this sequence is intruded by pillowed intrusions with meter-wide peperitic margins.

4.0 Interpretation of deposits

Sequences of pillow lava, to pillow fragment and fluidal bomb breccias, to lapilli tuff sequences are not uncommon in subaqueous basaltic sequences (Carlisle 1963; Dimroth et al. 1978; Fujibayashi and Sakai 2003; Jones 1970; Skilling 2009; Werner and Schmincke 1999). Their gross similarities between these pillow lava, breccia, and tuff sequences belie the range of mechanisms that can produce outwardly similar deposits. The following discussion will use detailed stratigraphic and textural studies of the facies present at Askja to identify the eruptive history of these deposits.

The structure and components of the Austurfjöll sequences are indicative of a wholly subaqueous environment, including pillowed lavas, sideromelane dominate clastic deposits and the absence of bomb sags, oxidation, or other emergent textures. The morphology of the massif and dominance of subaqueous deposits up to 700 m above the local base and volatile analyses (see section 3.0) from pillow glass rinds indicate that the depth of water was likely on the order of 750 m. The sequences of pillowed lavas, to pillow fragment and fluidal bomb breccia to fluidal bomb-bearing lapilli tuff show consistent internal bulk rock geochemistry suggestive of a co-genetic origin for the pillows and clastic components of the deposits (Table 1). The vesicle

morphology of the lapilli is highly similar to that of the fluidal bombs supporting the related genesis of the pyroclasts.

The dominant feature of the three sequences is the massive nature of the lithofacies associated with a progressive upward fining from pillow breccia, through fluidal bomb breccia, to lapilli tuff. The lapilli show fairly consistent dimensions throughout the sequence. The transitions between the facies are gradational and show no sedimentary structures indicative of hiatuses in the eruption.

The gradational upward fining, associated poor sorting and random clast orientation of these sequences is likely the result of high sediment fallout rates possibly from direct deposition from subaqueous convective plumes (Maicher et al. 2000). Grading of outsized clasts may result from Stokes settling of larger particles before smaller particles; however, the lack of sorting present in the lapilli and ash sized particles, and initial increase in bomb size, does not support this mechanism for bomb distribution in these deposits. A weak parallel bedding is present only in the upper few meters of two of the three deposits. This bedding may be due to time gaps in deposition or delayed gravitational settling in the water column of the finer deposits in this case lapilli and fine ash late in the eruption. Loading structures, traction currents, slump structures and other structures suggesting lateral transport of the deposit are not present (Maicher et al. 2000; White 2000). The apparent lack of remobilization is also supported by the lack of alteration of sharp grain edges (Solgevik et al. 2007) and the preservation of fragile glassy spines and limu o Pele (Fig. 9A,D,E) that would be easily damaged if mobilized in any granular flow or slump (Sohn 1995). The massive nature and systematic grading of coarser clasts through the deposit supports continuous deposition of pyroclasts. This observation, the presence of significant bombs and the limited lateral extent of the deposits suggest that they are vent proximal.

If the deposits are interpreted as primary and vent proximal, it would imply that the sequence represents the inverse of what was expelled from the vent, suggesting that the eruption initially produced large and abundant blocks and bombs, that progressively decreased in size and abundance through the eruption, until a lapilli dominated deposit of consistent grain-size was formed. Based on the lack of remobilization, co-genetic origin and structureless nature of the deposits we interpret the sequences to represent in situ temporally continuous eruptions from a single vent that display a transition from effusive to explosive basaltic activity.

The identification of fragmentation mechanisms in subaqueous pyroclasts remains a challenging task, dependent on the presence of multiple collaborating pieces of evidence. Previous pyroclastic studies have put emphasis on VND and fine ash textures (Ersoy et al. 2006; Lautze et al. 2012; Murtagh et al. 2011; Shea et al. 2010), but these features are not consistent indicators of fragmentation (Mattsson 2010; Ross and White 2012). The basaltic pyroclastic textures useful for such studies are summarized in Table 2 and evaluated for the relative strength of different textural parameter historic uses.

4.1 Pillow lava

Pillow lava sheets of both Pl1 and Pl2 type are the dominant morphology of subaqueous lavas at Askja. The relationship between subaqueous lava flow morphology and effusion rate is established based on three major groups with pillow lavas representing the lowest effusion rate, lobate pillow-free lavas an intermediate effusion rate and sheet flows (highest effusion rate)(Gregg and Fink 1995; Gregg and Smith 2003; Griffiths and Fink 1992). Lava flow morphology can also be a factor of slope angle (Gregg and Fink 1995; Gregg and Keszthelyi 2004), but as the large pillow sheet flows at Askja occur on shallow slopes, except where they

abut paleotopography, slope effects can be ignored here. Pl1 lavas, that display regular pillow forms and stacking, are interpreted as the lowest effusion rate end-member of subaqueous lava flows. Pl2 lavas have a more complex internal structure and locally display textures of lobate subaqueous lava flows, including blocky and columnar jointing domains mingled with large irregular pillow lava tubes. These structures suggest that Pl2 lavas represent an intermediate step between low effusion rate pillow lavas and moderate effusion rate lobate flows (Bear and Cas 2007; Dimroth et al. 1978; Griffiths and Fink 1992; Walker 1992). All three sequences described here have these higher effusion rate pillowed lavas at their base.

4.2 Pillow fragments and fluidal bombs

The breccias that immediately overlie the pillow lavas are dominated by three main types of block-sized components: isolated intact pillow forms, pillow fragments and fluidal bombs. Pillows can become isolated or appear to be isolated in clastic matrix through an influx of fragmental material during effusion without significant interaction with the lava (Carlisle 1963; Dimroth et al. 1978; Schipper et al. 2011), intrusion of pillowed dikes through fragmental deposits (Carlisle 1963; Edwards et al. 2009; Gorny et al. 2012), by gravitational detachment and deposition away from the main lava flow (Bevins and Roach 1979; Dimroth et al. 1978; Gorny et al. 2012; Moore 1975), or as ballistic blocks into clastic deposits (Staudigel and Schmincke 1984). Well incised exposures, like at Askja, are useful to determine if pillow clasts are truly isolated, or if they can be traced to an intrusion or pillow lava tube. In the Askja deposits, intact isolated pillows are the least common block-sized component, and while intrusions are present, sampling was preferentially collected away from exposed intrusions. Consequently, at Austurfjöll apparently intact pillows in the breccias are interpreted as isolated clasts.

Angular pillow fragments can be formed through gravitational collapse of an advancing flow (Jones 1970; Moore 1975), or any other brittle break-up of partially or fully cooled pillow lavas such as slumping (Cas et al. 2003; Jones 1970) or through explosive disruption of an existing flow (Smellie and Hole 1997). Differentiation of these processes requires detailed investigation of the clast morphologies and three dimensional exposures of the deposit structure. The breccia clasts at Askja were described in detail and are dominated by apparently intact pillows, and within a few meters, fluidal bombs. Angular pillow fragments do occur along the contact with the pillow lavas, but are notably rare higher in the clastic sequences.

The deposits described here have significant lateral continuity and do not display any bedding, including slump structures, nor do they display any transitions into competent lava flows. Flow-generated "autoclastic" breccias are frequently observed within large pillow sheets at the Askja complex, but they occur as lenses between multiple lava flows and have both lateral and vertical gradational contacts with coherent pillowed lavas with a dominance of angular pillow fragment clasts. The Austurfjöll deposits however, contain an abundance of fragile glass features, including glassy rinds, complex fluidal shapes, spines on fine ash and the lack of sedimentary structures indicating lateral transport, all of which suggest that they are not reworked Additionally, if the deposit experienced collapse or transport a greater proportion of angular blocks would be expected rather than the dominance of fluidal bombs with intact rinds as observed at Askja. The componentry, fragile grain edges, and structureless upward fining of the transitional sequences of DG, NG and RG are suggestive of an explosive origin for the breccia with high rates of settling through a water column.

Fluidal bombs display convolute shapes reflecting ductile fragmentation of liquid magma (Houghton and Gonnermann 2008; Houghton and Nairn 1991; Houghton and Schmincke 1989;

Walker and Croasdale 1971). Similar clasts have been described in submarine sequences, where they have been misnamed “pillows” (Portner et al. 2010; Staudigel and Schmincke 1984) but have also been recognized as juvenile fluidal bombs in some sequences (Cole et al. 2001; Simpson and McPhie 2001; Sorrentino et al. 2011; Staudigel and Schmincke 1984). The fluidal bombs from Austurfjöll share significant similarities in morphology, vesicularity and coalescence of vesicles to the examples attributed to subaqueous fire fountaining (Cas et al. 2003; Simpson and McPhie 2001; Staudigel and Schmincke 1984). Bombs in subaerial Strombolian and Hawaiian and Surtseyan deposits can have fluidal shapes including fusiform, ribbon, or cow-pie morphologies that all result from the ductile disruption of liquid magma (Houghton and Gonnermann 2008; Houghton and Schmincke 1989; Murtagh et al. 2011; Sorrentino et al. 2011; Walker and Croasdale 1971). Fluidal shapes in subaerial environments are most commonly associated with fire fountaining (Cas et al. 2003; Houghton and Gonnermann 2008; Houghton and Schmincke 1989). The fluidal bombs at Austurfjöll are distinct from the angular blocks that are common in Surtseyan sequences (Brown et al. 1994; Sohn 1995; Sorrentino et al. 2011), which are derived from solidified lava, e.g. from cooled lava flows, larger fragmented bombs, vent walls, or intrusions. Unlike typical Surtseyan eruption deposits, fluidal bombs dominate the breccias and lower lapilli tuff of the Askja sequences and angular bombs (pillow fragments) are limited to absent. Juvenile bombs are also frequently subordinate in abundance to such accidental lithics in Surtseyan eruption deposits (Murtagh et al. 2011; Sohn 1995; Walker and Croasdale 1971). Descriptions of bombs are notably absent in numerous characterizations of deep submarine explosive eruptions, which may in part be due to sampling logistics (Clague et al. 2003; Clague and Davis 2003). However, the presence of these fluidal bombs, and the observation of fluidal ejecta in FCI experiments (Büttner et al. 2002; Grunewald

et al. 2007; Ross and White 2012; Zimanowski et al. 1997), have not yet been incorporated into models of fragmentation. Consequently, the fluidal bombs within the Austurfjöll sequences are interpreted as juvenile products of subaqueous explosive magmatic fragmentation, based on their initial abundance, morphology, intact glass rinds and distinctive vesicle pattern from the pillow lavas at the base of the sequence.

Subaerial Strombolian and Hawaiian bombs typically display a range of vesicularity of 30-60 and 60-90 vol.% respectively (Brown et al. 1994; Houghton and Schmincke 1989). These values are higher than what is observed at Askja (20-60 vol.%) or typical Surtseyan eruptions (5-40 vol.%)(Brown et al. 1994; Cas et al. 2003; Head and Wilson 2003; Murtagh et al. 2011; Sorrentino et al. 2011). Head and Wilson (2003) suggest that the vesicularity required for deep subaqueous explosive eruptions is 75%, but values are commonly reported significantly lower at mid-ocean ridges (Clague and Davis 2003). The boundaries between eruptions that are described as "Surtseyan" and "Strombolian" are fuzzy and both behaviors have been described within a single eruption (Houghton and Gonnermann 2008; Houghton and Nairn 1991; Houghton and Schmincke 1989). Similarly, the recognition of bombs or clasts generated in wetter versus drier environments can be difficult without contrasting textures revealing interaction with air (oxidization) vs. water (thick glassy rinds) within the same deposit (Brown et al. 1994; Sorrentino et al. 2011) and indeed the presence or absence of water in the environment does not automatically dictate the fragmentation style (Table 2). Bomb vesicularity is frequently one of the few characteristics used to differentiate between subaerial and phreatomagmatic eruption deposits, where typical Surtseyan bombs have lower average vesicularities than typical Strombolian bombs (Houghton and Gonnermann 2008). Fluidal bombs from Askja have low vesicularites (20-60%), thick glassy rinds (0.2-1.5 cm) and no apparent oxidization showing the

greatest similarity to Surtseyan bombs, but having irregular vesicle distributions and polylobate shapes typical of Strombolian subaerial bombs. The frequent presence of the bombs indicates a low efficiency of fragmentation relative to that of phreatomagmatic explosions low in the sequence.

4.3 Lapilli and coarse ash

Lapilli dominate the bulk of the deposit from the matrix of the breccia to the top of the lapilli tuff. The dominant lapilli size range is from 1 to 3 cm with vesicle morphologies and shapes similar to vesicles found in the fluidal bombs. ~~The lapilli may display partial quench rims up to 1 cm thick or be entirely glassy.~~ The bulk of lapilli are equant in size and serve as matrix for the larger blocks and bombs in the upper breccia and lapilli tuff. ~~The lapilli are nominally smaller in the upper lapilli tuff, but the range in lapilli size is limited (~ 1 cm).~~ The lapilli are interpreted as the products of the breakup of larger globules of melt (like fluidal bombs) and the disruption of melt directly at the vent. Fragmentation of the lapilli reflects a combination of magmatic degassing, quench granulation and brittle fragmentation from interaction with other particles or the conduit during transport and deposition. The low percentage of microlites and dominance of sideromelane glass are indicative of rapid cooling of smaller juvenile fragments, suggesting that there is greater primary fragmentation influencing lapilli formation.

4.4 Fine Ash

Fine ash first occurs within the sequences in the lapilli tuffs and progressively increases in abundance up section. In order to use fine ash textures to infer primary fragmentation mechanisms, it must be assumed that they are the result of molten magma break up, not post-

539 explosive mechanical fragmentation (Mattox and Mangan 1997) an assumption supported by
540 their very fine and blocky nature and preserved fragile textures. The fine ash component of the
541 DG and NG tuffs are dominated by chips, blades and needle shapes that are associated with
542 mechanical granulation in experimental magma-water interactions (Büttner et al. 1999) (Fig. 9).
543 Particles with these textural signatures of quench fragmentation are abundant (up to 40%) in the
544 fine ash fraction of the breccia and lapilli sequences. Evidence of the entrapment of external
545 water within the melt, is preserved in the presence of a small percentage (5%) of limu o Pele,
546 representing local ductile deformation in the formation of a large bubble wall fragment (Maicher
547 et al. 2000; Schipper et al. 2013; Schipper and White 2010; Schipper et al. 2011).

548 Blocky, equant fine ash grains with stepped features and an absence of significant vesicle
549 influence are frequently called 'active particles' (<130 microns) of FCI (Büttner et al. 2002;
550 Wohletz 2003; Zimanowski and Wohletz 2000). Blocky textures can also be produced in non-
551 explosive interactions with water and wet sediment, but the resulting grain size are coarse ash to
552 fine lapilli (Mastin et al. 2009; Schipper et al. 2011). These particles are all the product of rapid
553 thermal transfer from the particles to a coolant, resulting in the brittle fragmentation of the
554 magma.

555 Blocky/equant fine ash particles make up on average 45% of the fine ash fraction of the
556 Austurfjöll sequences. Lapilli within the breccias and tuffs of the sequence between 2-20 mm
557 also display blocky equant shapes, but have vesicularities up to 25 vol.% and crystal contents up
558 to 10 vol.%, whereas the blocky fine ash fraction are crystal free. The fine ash particles that do
559 contain vesicles were counted separately and display a much lower presence of vesicles in
560 general and notably fewer fracture surfaces that are clearly influenced by vesicle walls than
561 similarly sized particles from a purely magmatic eruption (Houghton and Gonnermann 2008). As

562 a result of the particle size investigated the vesicles preserved in the fine ash are much smaller
563 than were preserved in the lapilli and fluidal bombs. It is nevertheless important to acknowledge
564 the similarity in morphology of the fine ash particles with coarser grain fractions in the
565 sequences at Askja as well as with those in non-explosive thermal granulation experiments.
566 Scalloped edges, characterized by small ~1-2 micron curved gashes along the margins of grains
567 (Fig. 9H) and rounding of fine ash particles are indicative of physical alteration of fine ash
568 particles (Solgevik et al. 2007), but were only found on 10% of fine ash grains studied at
569 Austurfjöll. Fragile shapes, including thin spines of glass, were present on an average 12% of the
570 fine ash grains, such delicate features would be difficult to preserve in the event of any
571 remobilization of the deposit. Flakey coatings probably indicate minor alteration post-
572 fragmentation along with the orange discoloration of fine ash these indicate weak hydration,
573 incipient palagonatization, of the deposits (Büttner et al. 2002; Büttner et al. 1999; Harpel et al.
574 2008; Nemeth and Cronin 2011). Fine ash particles are a critical grain size for unraveling the
575 fragmentation mechanisms of the eruptions as they represent the most efficient fragmentation
576 and require the greatest energy to produce. The size of these grains means that they only preserve
577 the last stage of fragmentation, as interacting fragmentation mechanisms may destroy much of
578 the earlier evidence of less efficient fragmentation mechanisms. Such particles are also limited as
579 they do not make up more than 10% of the total deposit volume at any stratigraphic level. The
580 finest grains must be studied in the context of detailed analysis of the whole deposit including
581 larger pyroclasts, eruption, transport and depositional processes and their environments.

582 Mechanisms of magma fragmentation clearly impart textural characteristics to glass
583 particles at all scales. Vesicle size, shape and alignment and interconnectedness reflect magmatic
584 volatile exsolution, fragmentation and quenching with implications for the relative timing of all

585 of these processes (Murtagh et al. 2011; Stovall et al. 2011). Quench rind thickness,
586 sideromelane vs. tachylite ratios and microlite presence indicate the relative rate of cooling
587 (Schipper et al. 2011). However, the signatures of initial fragmentation can be altered by
588 subsequent fragmentation and shape modification during transport, deposition and chemical
589 alteration. The final deposition of subaqueous volcaniclastic material is commonly the result of
590 lateral transport mechanisms such as density currents (Maicher et al. 2000; Smellie and Hole
591 1997; White 2000), the collapse of over-steepened deposits (Jones 1970; Sohn 1995), or
592 suspension settling (Eissen et al. 2003; Maicher et al. 2000). Remobilization can cause additional
593 fragmentation and/or impart textures such as the chipping of edges or rounding through abrasion
594 (Solgevik et al. 2007), muting or destroying textural signatures of initial fragmentation. The
595 introduction of accidental clasts during transport also complicates interpretations. Recycling of
596 clasts has been noted as a common process in subaerial and emergent/near surface
597 phreatomagatic eruptions, but has not been discussed much in the subaqueous literature
598 (Houghton and Smith 1993; Rosseel et al. 2006). Although numerous textures have been used to
599 distinguish magmatic from phreatomagmatic eruption products no one texture can be used in
600 isolation (Table 2). A full interpretation of the textures displayed by glassy pyroclasts should
601 include magma state prior to fragmentation, fragmentation, eruption mechanism(s), transport,
602 deposition, environment and any subsequent post-depositional changes (Harpel et al. 2008).
603
604 **4.5 Vesicle textures as a record of fragmentation mechanism**
605 Vesicles textures are the product of a combination at least six processes: nucleation, diffusive
606 growth, decompressive expansion, coalescence, collapse, deformation and escape (Schipper et al.
607 2010). The overall vesicularity of the deposits described here (25-60 vol.%) is comparable to

subaqueous to emergent (i.e. phreatomagmatic) basaltic deposits (10-60 vol.%) (Houghton and Gonnermann 2008; Houghton and Schmincke 1989; Murtagh et al. 2011; Schipper et al. 2011; Simpson and McPhie 2001). The dominance of coalescence and vesicle growth in the lapilli and fluidal bombs is suggestive of decoupled gas within the magma (Schipper et al. 2011), rather than continuous nucleation and exsolution.

The differences observed in vesicularity between the three grain size groups (ash, lapilli and blocks/bombs) are clearly influenced by the size of vesicles that can be observed, and the method of calculating vesicularity. The vesicularity of bombs and lapilli were calculated both in the field and with image analysis using ImageJ, both methods are two dimensional. ~~, and converted to three dimensions based on the~~These values are assumed to be ~~ption~~ of representative ~~distribution~~of three dimensional distributions. The vesicularity of fine ash was not calculated as a vesicle percent, but rather a binary value of presence of vesicles in part due to the small size and low abundance of vesicles at this grain size. Vesicle textures can be described as young (pre-fragmentation) textures or mature (post-fragmentation) textures. Young textures are small, sub-spherical and abundant vesicles. Rim to core vesicle coarsening is a sign of post-fragmentation vesiculation in subaerial and subaqueous bombs (Moitra et al. 2013; Parcheta et al. 2013; Schipper et al. 2011; Stovall et al. 2011). This mature texture results from a residence time ~~for~~ of the melt in a shallow chamber or the conduit for gases to exsolve~~d~~ and be distributed through the melt (Schipper et al. 2011). In the case of mature textures in pillow lavas, the distribution of large coalesced vesicles is typical found at the center of the pillow, away from rapidly cooling and apparently young vesicle textured rims.

The overall distribution of the vesicles in fluidal bombs indicates that they are not post-fragmentation bubble textures, or at least the process of coalescence had commenced prior to

631 fragmentation as they are well distributed throughout the bombs. Smaller vesicles are also
632 present, but a consistent alignment or distribution is absent, and thus no evidence of continued
633 nucleation of vesicles after bomb formation. Stretched vesicles along the bomb margins may be
634 ellipsoidal in morphology and represent deformation of pre-fragmentation vesicles during and
635 after bomb formation. Vesicle textures in pillows and fluidal bombs can be compared to reveal
636 the relative timing of vesicle coalescence to fragmentation. The pillows are early stage eruption
637 products with rounded vesicles (pre-fragmentation) and including radial pipe vesicles and an
638 inward coarsening of vesicle diameter (post-fragmentation), which are also preserved in pillow
639 fragments.

640 Lapilli vesicle morphology and distribution is nearly identical to that of the fluidal bombs
641 suggesting the vesicles of both grain sizes have the same pre-fragmentation origin. In very fine
642 ash, those vesicles observed isolated within a particle and smaller than the fracture planes formed
643 prior to fragmentation. The <50 μm size of fine ash particles studied precludes the preservation
644 of vesicles larger than 100 μm. Those vesicles that are present, however, are indicative of pre-
645 fragmentation vesiculation.

646 The similarity of vesicle coalescence and other textures between bomb and lapilli clasts
647 suggests that similar processes were controlling vesicle formation in the breccia and lapilli tuff.
648 However, a comparison of initial pillow lava vesicle textures with fluidal bombs and lapilli
649 suggests a change in the behavior of magmatic gasses during the eruption. The vesicles in the
650 bombs display increased coalescence relative to the uppermost pillow lava flows and minor (~5-
651 10%) increase in vesicularity, indicating an increase in gas exsolution within the melt, and
652 suggest that the bombs were formed by explosive magmatic gas expansion (Fig. 7). The fluidal
653 morphology of the bombs also indicates ductile deformation during transport through the vent

and the overlying water column, which is in agreement with a magmatic, rather than phreatomagmatic origin for the generation of the bombs. While fluidal bombs are observed in some phreatomagmatic deposits, they do not occur with the concentration observed at Askja or other subaqueous magmatic settings (Simpson and McPhie 2001). However, the more complex textures of the lapilli and ash indicate multiple fragmentation mechanisms were contributing to the formation of these finer particles including FCI and mechanical granulation (Fig.7).

5.0 Magma fragmentation at the onset of basaltic phreatomagmatic explosions

The kinetic disruption of a magma is accomplished in two main ways: ductile deformation of the melt and brittle deformation of the cooling glass/lava. Ductile, or inertial fragmentation, is the breakup of magma during decompression in the form of inertial stretching and breakup of the liquid magma (Houghton and Gonnermann, 2008; and references within). Basaltic magmatic explosions predominantly involve the ductile disruption of the melt through the nucleation and growth and buoyant rise of vesicles (Parfitt and Wilson 2009; Zimanowski et al. 2003). The fluidal texture of bombs, with elongate vesicles in the glassy rim and convolute vesicle morphologies is a result of the ductile deformation of magma driven by the expansion and coalescence of magmatic water (Büttner et al. 1999; Eissen et al. 2003; Kokelaar 1986; Mastin et al. 2009; Parcheta et al. 2013; Zimanowski and Büttner 2003; Zimanowski and Wohletz 2000). Vesicle morphologies and distributions are distinct in the pillow lavas and pillow lava fragments, relative to the later pyroclasts (fluidal bombs and lapilli), and suggest coalescence of magmatic gas bubbles prior to the formation of the pyroclasts but not during pillow extrusion. This accumulation of magmatic gas could lead to the initial formation of fluidal bombs and possibly some lapilli, generated by expansion of these bubbles (Fig. 7 & 8). There is, however, limited

677 evidence of ductile deformation preserved in the fine ash scale in the form of tube vesicles and
678 rare fine ash with large vesicle walls preserved along fractures. This supports the evidence that
679 magmatic gas expansion is recorded in the large polylobate vesicles representing existing
680 degassing pathways, and not nucleation of new vesicles.

681 While it is reasonable to indicate the onset of magmatic gas expansion driven explosivity
682 in these deposits it is exceedingly difficult to identify when, if at all, the magmatic gas expansion
683 stops. Rather, the fragmentation mechanism that dominates pyroclast formation changes, and
684 may then mask the signature of magmatic fragmentation. The polylobate highly coalesced
685 vesicles of are also present in the lapilli tuff, but the influence of magmatic fragmentation
686 becomes less evident with the rapid decrease in fluidal bombs within a meter or so of the top of
687 the breccia, suggesting a more effective fragmentation mechanism.

688 Brittle fragmentation of magma occurs when the material fails as a solid. In order for
689 liquid magma to deform in a brittle fashion the strain rate must be high enough to prevent liquid
690 relaxation of the melt (Büttner et al. 2002; Büttner et al. 1999; Dellino et al. 2001; Zimanowski
691 et al. 2003). Fragmentation of basaltic magma by brittle processes include: FCI, quench
692 granulation and other mechanical fracture through impact upon landing or transportation
693 (Maicher et al. 2000). Most studies that distinguish between phreatomagmatic and magmatic
694 fragmentation focus on the fine ash grain size fraction (<64 μm) as it records the most efficient
695 fragmentation mechanism involved in the creation of the deposit, i.e. the mechanism that
696 requires the greatest energy (Büttner et al. 1999; Dellino and La Vope 1996; Durig et al. 2012;
697 Heiken 1971; Mattsson and Tripoli 2011; Zimanowski et al. 2003). Phreatomagmatic explosions
698 driven by FCI occur where vapor is produced through the rapid heating of the water interacting
699 with the surface of the melt. This vapor film must be disrupted to bring the melt in direct contact

700 with the water. The disruption of the vapor film can be an internal or external process, where
701 changes in the system, including other mechanisms of melt fragmentation, can initiate FCI
702 explosions. (Kokelaar 1986; Schipper et al. 2013; Wohletz 1986; Wohletz 2003; Zimanowski
703 and Büttner 2003; Zimanowski and Wohletz 2000). The resulting explosion can then create
704 pressure variations and fragment country rock or cooling crusts and result in the exposure of
705 fresh magma to the system. The violence of these interactions produces deposits that are
706 characterized by lithic blocks and abundant fine ash. Disruption of melt by FCI shockwaves can
707 result in the rapid depressurization of a degassing melt and encourage magmatic explosivity.
708 Similarly magmatic explosions can engender the formation of a fuel coolant premix and enable a
709 phreatomagmatic interaction. The dynamic interplay of pressure, heat and coolant can result in a
710 feedback loop where one or both of these fragmentation mechanisms may engender the
711 conditions required to trigger the other. Simultaneously, both of these mechanisms result in the
712 exposure of new melt which subsequently cools and contracts resulting in quench granulation.
713 This complex interplay of magma fragmentation mechanisms only highlights the challenge of
714 interpreting sequences like those at Austurfjöll.

715 Quench granulation is due to contraction during cooling and the brittle failure of the outer
716 contracted layers of melt that is accentuated in wet environments (Cas et al. 2003; Schipper et al.
717 2010; Wohletz 1986; Wohletz 2003). This secondary fracture occurs at a variety of scales
718 including jig-saw fit bombs, angular blocks and chip and needle-shaped fine ash particles. Lapilli
719 that have incomplete sideromelane rims reflect the brittle fragmentation of cooled melt. Particles
720 associated with this type of fragmentation are typically dominated by wholly sideromelane
721 clasts. Quench granulation only releases 10% of the thermal energy available (Schmid et al.
722 2010) and creates larger particles (coarse ash and lapilli) than FCI. Additional fragmentation can

occur through clast to clast interaction, impact with the ground and during transportation. The preservation of large fluidal clasts and intact glassy margins on lapilli and bombs indicate that these secondary fragmentation mechanisms, including post-depositional transport, are limited. Fine ash grain textures also support this lack of transportation through the preservation of fragile spines and limited grain abrasion.

The role of ductile deformation in FCI explosions is poorly understood. Ductiley deformed clasts are observed in limited quantities in phreatomagmatic deposits, including limu o Pele (Clague et al. 2009; Maicher et al. 2000; Schipper and White 2010) and fluidal bombs (Mattsson and Tripoli 2011; Ross et al. 2011). The formation of limu o Pele involves the ductile deformation of melt as a result of trapping external water within the melt. The trapped water rapidly expands as vapor stretching the melt into a thin film (bubble wall), in a processes documented in littoral, submarine and subglacial environments (Clague et al. 2009; Maicher et al. 2000; Schipper and White 2010). Limu o Pele are not a dominant feature within the Askja deposits (never more than 4 vol %), but are frequent enough (Fig. 9) to indicate that trapping of external water by molten magma did occur in this fully subaqueous environment, further indicating the complexity of subaqueous melt water interactions.

It is very important to note that none of these fragmentation processes occur in isolation, as each individual mechanism disrupts the magma and may enable the decompression of internal volatiles, increase the surface area for interaction with external water and disrupt insulating vapor films (Maicher et al. 2000) triggering other mechanisms of fragmentation enabling feedback loops between magmatic and phreatomagmatic explosions. Quench granulation, in particular, can occur in any wet eruptive environment and contributes to all subaqueous eruptions (Cas et al. 2003; Mastin et al. 2009; Schipper et al. 2010; Wohletz 1986; Wohletz 2003).

The interpretation of pillow, fluidal bomb, lapilli and fine ash particle textures from the three transitional sequences at Askja clearly reflect a complex interplay of several fragmentation mechanisms that evolve throughout the eruption sequence. The shape of clasts and fine particles reflect the ductile or brittle nature of these mechanisms. The interrelated nature of mechanisms of fragmentation results in the modification, overprinting and even destruction of earlier textural signatures of the fragmentation (Ersoy et al. 2006). It is therefore, critical to use multiple parameters, such as sedimentary structures, vesicularity, grain size and grain shape at multiple grain sizes to reconstruct the mechanisms of fragmentation for pyroclastic deposits generated in wet environments. For the sequences described here, we suggest that the evolution of the fragmentation mechanisms producing the deposits started with initial magmatic fragmentation in a subaqueous environment which then enabled more efficient FCI explosions. This progressive shift does not imply that magmatic fragmentation was shut down by the onset of phreatomagmatic activity, rather the more effective process rapidly dominated the production of pyroclasts with magmatic gas expansion becoming a subordinate process. At the same time fragmentation by mechanical process (dominantly quench granulation) and the entrapment of external water (limu o Pele) accompanied the more dominant fragmentation mechanisms (Fig. 10).

5.1 What triggers explosive activity in subaqueous eruptions?

Potential triggers for a transition from effusive to explosive activity in a subaqueous environment include: depressurization by a decrease in confining pressure, access/infiltration of water to the rising magma, and internal dynamics of the magma due to changes in the magma flux, volatile content or crystallization. In a glaciovolcanic setting a reduction of confining pressure can result

769 from a decrease in the overburden, such as water or ice or wet sediment due to the dynamic
770 nature of the environment. Ice-confined lake water levels are highly dynamic and can drain
771 slowly or rapidly during and after an eruption (Bjornsson 1985; Höskuldsson et al. 2006; Skilling
772 et al. 2009; Smellie 2001; Smellie and Hole 1997). Decompression would also occur as a result
773 of increasing the elevation of a vent relative to the water level through the construction of a
774 massif (Edwards et al. 2009; Moore and Calk 1991; Zimanowski and Büttner 2003). A sudden
775 collapse of the growing massif or collapse of the vent itself could also result in rapid
776 decompression over the vent area (Fujibayashi and Sakai 2003; Scott et al. 2003; Wohletz 2003).
777 The initiation of external water-magma interaction may further instigate decompression
778 and facilitate further explosive activity (White 1996; Wohletz 1986; Wohletz 2002). This may be
779 accomplished through the trapping of external water under an advancing flow over wet
780 sediments, or between pillows, or the infiltration of water into the vent, or fractured lava flow
781 crusts (Brown et al. 1994; Clague et al. 2009; Eissen et al. 2003; Maicher et al. 2000; Schipper
782 and White 2010; White 1996; Zimanowski and Büttner 2002). In the case of the completely
783 subaqueous sequence at Askja, ample volumes of water are available for interaction with
784 erupting magma indicating that the volume of water was not a limiting variable for triggering the
785 explosions. The presence of effusive pillow lavas during the early phase of the eruption indicates
786 that melt was interacting with abundant water, but conditions were not conducive for melt/water
787 pre-mix generation and FCI explosions (Wohletz 2002; Zimanowski et al. 1997). The pillow
788 fragment breccia indicates that the pillow lava was partially mechanically disrupted, likely
789 through the onset of explosive magmatic activity which formed juvenile fluidal bombs that then
790 progressively dominate the breccia up-section. Vesicle morphologies and their distribution in the
791 fluidal bombs points to an increase in magmatic volatile expansion and accumulation of vesicles

through coalescence after pillow formation and during bomb formation. During the initial explosive phase lapilli were also produced in small quantities to form the matrix of the breccia. As the eruption continued lapilli became the dominant pyroclast size, producing a massive lapilli tuff. This upward fining of the deposit, as expressed by the increase in ash presence and decrease in outsized clasts and the accompanying increasing abundance of very fine blocky ash particles indicates that conditions became more favorable for FCI explosions. The initial magmatic fragmentation enabled the dynamic mingling of magma and water to enable FCI and increased quench granulation. The threshold between passive and explosive fragmentation in these cases is loosely constrained by laboratory scale experiments defining a range of the greatest potential for explosive interaction, where the mass ratios of coolant to magma is between $1>R>0.1$ (Wohletz 2002). However, this mass ratio does not occur in isolation and the other variables, including confining pressure, and magma viscosity have not been sufficiently investigated. In this case the increased surface area to volume ratio of the 20-50 cm bombs needed to occur with sufficient volume to maintain a mass ratio of water to magma below 1. Based on the 4-7 m of fluidal bomb-bearing breccia it seems feasible that the ratio of heat to coolant in the resulting mix was favorable to trigger a FCI explosion. This then suggest that explosive magmatic fragmentation can facilitate explosive fuel coolant interactions that dominate pyroclast formation for the remainder of the eruption. While not the only mechanism to instigate FCI explosions, this may represent a common mechanism for FCI initiation. If this model is valid, one important question still remains, namely what controlled the initial increase in magmatic gas expansion for the Austurfjöll eruptions?

Variations of internal eruption dynamics could initiate magmatic explosive activity through an increase in eruption rate (Clague et al. 2009; Fujibayashi and Sakai 2003), changes in

volatile content, or viscosity (composition or crystallization) (Fowler et al. 2002; Wohletz 2003). The abundance of crystals within a melt will also directly affect the gross vesicularity and play a role in the potential explosivity of a melt (Houghton and Gonnermann 2008).

The presence of textures reflecting magmatic gas expansion and coalescence in the Austurfjöll deposits indicates that internal volatiles play a critical role in the first stages of fragmentation, and thus it is reasonable to consider internal drivers for the initiation of explosivity, such as eruption rate. The presence of pillow lavas of Pl2 type at the base of the Austurfjöll sequences indicates that effusion occurred at a higher rate than would form typical (i.e. Pl1) pillow lava forms. Deformed sideromelane glass quenched particles and elongated vesicles on clast rims in the overlying breccias/lapilli tuffs suggest a high strain rate that is also associated with a high eruption rate (Parcheta et al. 2013). This may suggest that the onset of explosivity coincided with an increased eruption rate from pillowed lavas to magmatic gas driven jetting of magma globules into the water column. Other internal factors such as melt viscosity and volatile saturation pressures do not seem to change dramatically between the pillows and the bombs. The crystal content of the lapilli and bomb samples is below 10 vol.% This suggests that the formation of crystals is not a significant contributor behavior of the melt. Additionally the chemistry of the pillows and clastic samples shows a high degree of internal consistency.

Alternatively, the shift in eruptive behavior may have been due to factors external to the melt where the increase in internal volatile expansion and coalescence between the pillow lavas and the fluidal bombs could have been the result of decompression from a reduction of confining pressure over the vent. Investigations of glaciovolcanic deposits have sought geologic textures that preserve the evidence of rapid syn-eruptive decompression through environmental changes,

and suggest that dramatic changes in bulk vesicularity may be a key to identifying this process (Höskuldsson et al. 2006). The first fluidal bombs at Austurfjöll have different morphology and distribution of vesicles from the underlying lavas, reflecting an increase in vesicle coalescence, not an increase in nucleation as might be expected during a decompression event. However, there is geologic evidence within nearby areas of Austurfjöll massif for voluminous drainage of water, as indicated by deeply eroded channels in similar lapilli tuffs that are infilled with stream flow and debris flow deposits. Such a large drainage event may have rapidly decreased the lake level volume, resulting in a rapid pressure change over the massif. The timing and duration of such an event is not well constrained, but at least one drainage event is stratigraphically correlated within the same eruptive unit as the NG transitional sequence (Graettinger unpublished data). Large ice sheets like would have been present at Askja are less susceptible to rapid drainage events than thinner, more localized ice bodies; however, the volume of water drained may not need to be significant to influence eruptive conditions of an actively degassing magma, particularly if the eruption rate was already high as evidenced by the presence of Pl2 lavas.

The internal compositional and textural consistency of the sequences at Askja suggests that there was little change in melt properties during the eruption of these deposits. While a change in mass flux at the vent may be responsible for the onset of magmatic gas decompression at all three sites, in similar fashions, it seems more likely that environmental conditions would produce such similar processes at different vents. Drainage events are frequent at glaciovolcanic centers (Bennett et al. 2006; Carrivick et al. 2004; Gudmundsson et al. 1997; Höskuldsson et al. 2006), and are a likely the strongest candidate to trigger the onset of explosive activity at an actively effusing vent.

5.2 Eruption Style

The discussion of eruption mechanics in fully subaqueous environments is complicated by the terminology, particularly with regard to comparisons that are often made with subaerial eruption styles. Comparisons with Strombolian (Clague and Davis 2003; Clague et al. 2009; Deardorff et al. 2011; Head and Wilson 2003; Schipper et al. 2011) and Hawaiian (Cas et al. 2003; Head and Wilson 2003; Schipper et al. 2010), eruption styles typically are focused on the decoupled or coupled nature of magmatic gas, but belies the underlying complexity of subaqueous fragmentation. Deep (ca. 1 km), gas-coupled submarine eruptions have also recently been given the term Poseidic (Schipper et al. 2010) to highlight some of the variations present in subaqueous eruptions. Surtseyan eruptions are considered to be the 'wet' equivalent of Strombolian eruptions, but the term is predominantly applied to emergent or limited water environments, not fully subaqueous systems (Brand and Clarke 2009; Skilling 2009; Sohn 1995; Sorrentino et al. 2011; White and Ross 2011).

Fluidal bombs have been used to suggest the occurrence of submarine basaltic fire fountaining at ocean islands (Simpson and McPhie 2001), but the nature of vesicles in the Austurfjöll deposits is more suggestive of decoupled gas, that is characteristic of Strombolian eruptions (Clague and Davis 2003; Clague et al. 2009; Polacci et al. 2008; Schipper et al. 2011; Schipper et al. 2010). The vesicularity of Hawaiian eruption deposits is typically high, and pyroclasts are dominated by ragged clasts with uniformly distributed vesicles, suggested that the gas bubbles are coupled to the magma during eruption and a more continuous eruption. Strombolian eruptions of basaltic magma have a variety of fluidal and ragged clasts are that are produced in a non-continuous 'unsteady' eruption, but occur as discrete eruptions, due to the decoupled gas (Houghton and Gonnermann 2008). Surtseyan eruptions can display discrete

bursts and continuous uprush behavior. The Askja deposits lack some of the more distinctive Surtseyan deposit characteristics including lithic blocks, bomb sags and stratigraphy indicative of pulsatory behavior. The sequences at Austurfjöll are predominantly massive with a gradual upward fining and weak bedding only in the upper meters of the larger deposits. This indicates a more continuous eruptive behavior resulting in continuous deposition.

The erosional history and complex overlapping facies of adjacent fissure eruptions at Askja make the identification of exact vent locations for each sequence very difficult. Without sufficient exposure vent position is estimated to be roughly located within the deposit itself, and therefore within 10-50 m of sample location based on the scope of the deposit and the lack of evidence for remobilization. Deposit volume is calculated from lateral extent, estimated by observation of the three-dimensional dissection of the deposit and from lithofacies mapping of DK, NG and RG. Original volume estimates are clearly approximate due to the degree of deposit overlap and erosion. The estimated volume of the individual deposits is between 0.0004-0.003 km^3. Typical Strombolian eruptions and Icelandic fissure eruptions have extrusion rates between 10 and 100 m^3/s (Parfitt and Wilson 2009). These explosive eruptive rates are also similar in range to the values estimated for subaqueous lobate lava flows (Griffiths and Fink 1992). Estimates for eruption duration can be established from these values to be minutes to a few hours for each sequence ~~(Table 5)~~.

~~Our model of the transition from effusion to explosion at Austurfjöll is based on the interpretation of the three deposits as representing a temporally continuous co-genetic sequence of deposits from a single vent and detailed textural study of the four major components (pillows, bombs, lapilli to coarse ash and fine ash).~~

We have suggested above that the first formation of fluidal bombs is the result of rapid extrusion of magma driven by internal volatiles, jetting the magma into the water column. The shear stress imparted on the surface of the magma exceeds the surface tension causing a separation into magma globules, forming the fluidal bombs (Cas et al. 2003; Head and Wilson 2003; Wohletz 2003). The presence of pillow fragments mixed with fluidal bombs suggests that the pillows were disrupted during the onset of explosivity, but the absence of frothy pillows or pillow fragments suggests that the transition occurred in the vent and not in a growing pillow tube. The coalescence of vesicles and vesicle size indicate decoupled volatile behavior (Clague and Davis 2003; Head and Wilson 2003; Schipper et al. 2011). The ejection of this first globule then exposes a greater surface area of magma to interact with external water. The bomb-bearing lapilli tuff is interpreted as representing the shift from subaqueous magmatic fragmentation to FCI fragmentation. The increased efficiency of the fragmentation is recorded in the overall decreasing grain size of the deposits through the increase in the proportion of lapilli and ash. The sequences described here would be insufficiently characterized by only one grain size faction due to the limitations of each particle type to record the interplay of fragmentation mechanisms observed through this more comprehensive textural study.

The interplay of phreatomagmatic fragmentation (FCI) with magmatic fragmentation is not unique to fully submerged eruptions (Houghton and Schmincke 1989; Skilling 2009; Solgevik et al. 2007; White 1996). However, the initiation of a phreatomagmatic eruption by a decoupled gas magmatic eruption has not yet been described in a completely subaqueous environment. Deposits preserving a magmatic trigger for FCI explosions at Askja likely do not represent an exclusive series of events, but instead represents the dynamic nature of subaqueous

928 explosive eruptions and reinforces the potential for feedback loops of basaltic magma
929 fragmentation mechanisms.
930
931 **6.0 Conclusion**
932 Pyroclast textures in three subaqueous basaltic sequences from Askja reveal the interaction of
933 magmatic and FCI fragmentation mechanisms as the eruption transitioned from effusive to
934 explosive behavior. The identification of the signature of different fragmentation mechanisms in
935 natural subaqueous phreatomagmatic eruptions remains a challenge. However, the comparison of
936 textures in multiple grain sizes across important facies transitions as in this study can reveal
937 subtle changes in internal volatile expansion and fragment cooling history as preserved in vesicle
938 morphology, distribution and size as well as glass type and microlite abundances. By using an
939 integrated approach it is possible to compensate for challenges such as textural overprinting and
940 limited sedimentary structures. We propose an eruption history for the three sequences described
941 here where the initial disruption of the effusively erupting magma by decoupled magmatic
942 volatile expansion was the result of decompression that may have been the result of drainage or
943 partial drainage of overlying water in the ice-confined lake. This magmatic explosive behavior
944 subsequently enabled FCI, as well as minor trapping of external water and quench granulation.
945 All of these fragmentation mechanisms influenced the final grain size distribution and pyroclast
946 textures of the sequences. The initial disruption of the magma that was driven by volatile
947 expansion is preserved in the form of the fluidal bombs up to 50 cm in diameter and the large,
948 irregularly distributed, polylobate vesicles of the lapilli and bombs that were no present in the
949 underlying pillows. The role of phreatomagmatic explosions is recorded predominantly in the
950 fine ash fraction of the deposit in the form of blocky, vesicle free grains and the increase and

dominance of sideromelane dominated lapilli and fine ash up section. The combination of low efficiently magmatic fragmentation and FCI explosions in the same eruptive sequence highlights the complexity of magma water interactions in wet environments. Given the close genetic and spatial relationship between the pillows and clastic deposits we suggest that the deposits were produced through the continuous eruption of effusive to transitionally explosive behavior. The recognition of such transitional sequences is important as they provide evidence for controls on the onset of explosive activity in subaqueous environments. It is critical to continue to investigate the conditions and triggers of fuel coolant interactions to better model violent phreatomagmatic eruptions.

7.0 Acknowledgments

This work was made possible by a National Science Foundation grant to IPS, DG and AH. Our gratitude goes to Háskóli Íslands, NORVOLK and the Vatnajökull National Park, for field logistics and permits. Dickinson College is acknowledged for the use of the SEM and Robert Dean should be thanked for his assistance using the equipment. Field assistance from R. Wham, R. Lee, A. Lema and M. Ellis was invaluable. This manuscript was improved greatly by two anonymous reviewers.

8.0 References

Allen CC (1980) Icelandic subglacial volcanism: thermal and physical studies The Journal of Geology 88:108-117

974 Allen CC, Jercinovic MJ, Allen JSB (1982) Subglacial volcansim in North-Central British
975 Columbia and Iceland The Journal of Geology 90:699-715
976 Bear AN, Cas RAF (2007) The complex facies architecture and emplacement sequene of a
977 Miocene submarine mega-pillow lava flow system, Muriwai, North Island, New Zealand.
978 Journal of Volcanology and Geothermal Research 160:1-22
979 Bennett MR, Huddart D, Waller RI (2006) Diamict fans in subglacial water-filled cavities- a new
980 glacial environment. Quaternary Science Reviews 25:3050-3069
981 Bevins RE, Roach RA (1979) Pillow lava and isolated-pillow breccia of rhyodacite composition
982 from the Fishguard Volcanic Group, Lower Ordovician, S.W. Wales, United Kingdom. The
983 Journal of Geology 87(2):193-201
984 Bjornsson A (1985) Dynamics of crustal rifting in NE Iceland. Journal of Geophysical Research
985 90:10151-10162
986 Bjornsson H (2002) Subglacial lakes and jokulhlaups in Iceland. Global and Planetary Change
987 35:255-271
988 Brand BD, Clarke AB (2009) The architecture, eruptive history, and evolution of the Table Rock
989 Complex, Oregon: From a Surtseyan to an energetic maar eruption. Journal of Volcanology and
990 Geothermal Research 180:203-224
991 Brown SJA, Smith RT, Cole JW, Houghton BF (1994) Compositional and textural
992 characteristics of the strombolian and surtseay K-Trig basalts, Taupo Volcanic Centre, New
993 Zealand: Imlications for eruption dynamics. New Zealand Journal of Geology and Geophysics
994 37:113-126
995 Büttner R, Dellino P, La Volpe L, Lorenz V, Zimanowski B (2002) Thermohydraulic explosions
996 in phreatomagmatic eruptions as evidenced by the comparison between pyroclasts and products
997 from Molten Fuel Cooland Interaction experiments. Journal of Geophysical Research 107:2277
998 Büttner R, Dellino P, Zimanowski B (1999) Identifying magma-water interaction from the
999 surface features of ash particles. Nature 401:688-690
1000 Carlisle D (1963) Pillow breccias and their aquagene tuffs, Quadra Island, British Columbia. The
1001 Journal of Geology 71(2):48-71
1002 Carrivick JL, Russell AJ, Tweed FS (2004) Geomorphological evidence for jokulhlaups from
1003 Kverkfjoll volcano, Iceland. Geomorphology 63:81-102
1004 Cas RAF, Yamagishi H, Moore L, Scutter C (2003) Miocene submarine fire fountain deposits,
1005 Ryugazaki Headland, Oshoro Peninsula, Hokkaido, Japan: implications for submarine fountain
1006 dynamics and fragmentation processes. In: White JDL, Smellie JL, Clague DA (eds) Subaqueous
1007 Explosive Volcanism AGU Washington DC, pp 299-316
1008 Clague DA, Batiza R, Head JW, Davis AS (2003) Pyroclastic and hyrdoclastic deposits on Loihi
1009 Seamount, Hawaii. In: White JDL, Smellie JL, Clague DA (eds) Explosive subaqueous
1010 volcanism. AGU Washington DC, pp 73-95
1011 Clague DA, Davis AS (2003) Submarine Strombolian eruptions on the Gorda Mid-Ocean Ridge
1012 In: White JDL, Smellie JL, Clague DA (eds) Explosive subaqueous volcanism. AGU
1013 Washington DC, pp 111-128
1014 Clague DA, Paduan JB, Davis AS (2009) Widespread strombolian eruptions of mid-ocean ridge
1015 basalt. Journal of Volcanology and Geothermal Research 180:171-188
1016 Cole PD, Guest JE, Cuncan AM, Pacheco J-M (2001) Capelinhos 1957-1958, Faial, Axores:
1017 deposits formed by an emergent sursteyan eruption. Bulletin of Volcanology 63:204-220

De Rosa R (1999) Compositional models in the ash fraction of some modern pyroclstic deposits: their determination and significance. Bulletin of Volcanology 61:162-173
Deardorff ND, Cashman KV, W. CJW (2011) Observations of eruptive plume dynamics and pyroclastic deposits from submarine explosive eruptions at NW Rota- 1, Mariana arc. Journal of Volcanology and Geothermal Research 202:47-59
Dellino P, Isaia R, Vope LL, Orsi G (2001) Statistical analysis of textural data from complex pyroclastic sequences: implications for fragmental processes of the Agnano-Monte Spina Tephra (4.1 ka), Phlegraean Fields, southern Italy Bulletin of Volcanology 63:443-461
Dellino P, La Vope L (1996) Image processing analysis in recnostructing fragmentation and transportation mechanisms of pyroclastic deposits. THe case of Monte-Pilato-Rocche Rosse erutpions, Lipari (Aeolian islands, Italy). Journal of Volcanology and Geothermal Research 71:13-29
Dellino P, Liotino G (2002) The fractal and multifractal dimensions of volcanic ash particles contour: a test study of the utility and volcanological relevance Journal of Volcanology and Geothermal Research 113:1-19
Dimroth E, Pierre C, Leduc M, Sanshagrin Y (1978) Structure and organization of Archean subaqueous basalt flows, Rouyn-Noranda area, Quebec, Canada. Canadian Journal of Earth Science 15:902-918
Durig T, Mele D, Dellino P, Zimanowski B (2012) Comparative analyses of glass fragments from brittle fracture experiments and volcanic ash particles. Bulletin of Volcanology 74:691-704
Edwards BR, I.P. S, Cameron B, Haynes C, Lloyd A, Hungerford JHD (2009) Evolution of an englacial volcanic ridge: Pillow Ridge tindar, Mount Edziza volcanic complex, NCVP, British Columbia, Canada. Journal of Volcanology and Geothermal Research 185:251-275
Eissen J-P, Fouquet Y, Hardy D, Ondreas H (2003) Recent MORB volcaniclastic explosive deposits formed between 500 and 1750 m.b.s.l. on the axis of the Mid-Atlantic Ridge, South of the Azores. In: White JDL, Smellie JL, Clague DA (eds) Explosive Subaqueous Volcanism AGU, Washington DC, pp 143- 166
Ersoy O, Chinga G, Aydar E, Gourgaud A, Cubukcu HE, Ulusoy I (2006) Texture discrimination of volcanic ashes from different fragmentation mechansims: A case study, Mount Nemrut stratovolcano, eastern Turkey. Computers and Geosciences 32:936-946
Fowler AD, Berger B, Shore M, Jones MI, Ropchan J (2002) Supercooled rocks: develoment and significance of varioles, spherulites, dendrites and spinifex in Archean volcanic rocks, Abitibi Greenstone belt, Canada. Precambrain Research 115:311-328
Fujibayashi N, Sakai U (2003) Vesiculation and eruption processes of submarine effusive and explosive rocks from the middle Miocene Ogi Basalt, Sado Island, Japan. In: White JDL, Smellie JL, Clague DA (eds) Explosive submarine volcansim. AGU Washington DC, pp 259-272
Gorny C, F. , White JDL, Gudmundsson M (2012) Contorticlasts and shoaling subglacial intrusions. In: Volcano Ice Interactions III. Anchorage, Alaska
Graettinger AH, Skilling IP, McGarvie DW, Hoskuldsson A (2012) Intrusion of basalt into frozen sediments and generation of Coheren-Margined Volcaniclastic Dikes (CMVD's). Journal of Volcanology and Geothermal Research 217-218:30-38
Gregg TKP, Fink JH (1995) Quantification of submarine lava-flow morphology through analog experiements. Geology 23:73-76
Gregg TKP, Keszthelyi L (2004) The emplacement of pahoehoe toes: field observations and comparison to laboratory simulations. Bulletin of Volcanology 66:381-391

1063 Gregg TKP, Smith D (2003) Volcanic investigations of the Puna Ridge, Hawai'i: relations of
1064 lava flow morphologies and underlying slopes. Journal of Volcanology and Geothermal
1065 Research 126:63-77
1066 Griffiths RW, Fink J (1992) Solidification and morphology of submarine lavas: A dependence on
1067 extrusion rate. Journal of Geophysical Research 97:19729-19737
1068 Grunewald U, Zimanowski B, Büttner R, Phillips LF, Heide K, Büchel G (2007) MFCI
1069 experiements on the influence of NaCl-saturated water on phreatomagmatic explosions. Journal
1070 of Volcanology and Geothermal Research 159:126-137
1071 Gudmundsson MT (2003) Melting of Ice by magma-ice-water interactions during subglacial
1072 eruptions an indicator of heat transfer in subaqueous eruptions. In: White JS, JL; Clague, DA
1073 (ed) Explosive Subaqueous Volcanism American Geophysical Union, Washington DC, pp 61-72
1074 Gudmundsson MT, Sigmundsson F, Björnsson H (1997) Ice-volcano interaction of the 1996
1075 Gjálp subglacial eruption, Vatnajökull, Iceland. Nature 389:954-957
1076 Harpel CJ, Kyle PR, Dunbar NW (2008) Englacial tephrostratigraphy of Erebus volcano,
1077 Antarctica. Journal of Volcanology and Geothermal Research 177:549-568
1078 Head JW, Wilson L (2003) Deep submarine pyroclastic eruptions: theory and predicted
1079 landforms and deposits. Journal of Volcanology and Geothermal Research 121:155-193
1080 Heiken GH (1971) Tuff Rings: Examples from the Fort Rock-Christmas Lake Valley Basin,
1081 South-Central Oregon. Journal of Geophysical Research 76(23):5615-5626
1082 Helo C, Longpre M-A, Shimizu N, Clague DA, Stix J (2011) Explosive eruptions at mid-ocean
1083 ridges driven by CO2- rich magmas. Nature Geoscience 4:260-263
1084 Höskuldsson A, Sparks RSJ, Carrol MR (2006) Constraints on the dynamics of subglacial basalt
1085 eruptions from geological and geochemical observations at Kverkfjoll, NE-Iceland. Bulletin of
1086 Volcanology 68:689-701
1087 Houghton BF, Gonnermann H (2008) Basaltic explosive volcanism: Constraints from deposits
1088 and models Chemie der Erde 68:117-140
1089 Houghton BF, Nairn IA (1991) The 1976-1982 Strombolian and phreatomagmatic eruptions of
1090 White Island, New Zeland: eruptive and depositional mechanisms at a 'wet' volcano. Bulletin of
1091 Volcanology 54:25-49
1092 Houghton BF, Schmincke H-U (1989) Rotenberg scoria cone, East Eifel: a complex Strombolian
1093 and phreatomagmatic volcano. Bulletin of Volcanology 52:28-48
1094 Houghton BF, Smith RT (1993) Recycling of magmatic clasts during explosive eruptions:
1095 estimating the true juvenile content of phreatomagmatic volcanic deposits. Bulletin of
1096 Volcanology 55:414-420
1097 Jones JG (1970) Intraglacial volcanoes of the Laugarvatn region, Southwest Iceland II. The
1098 Journal of Geology 78(2):127-140
1099 Kokelaar P (1986) Magma-water interactions in subaqueous and emergent basaltic volcanism.
1100 Bulletin of Volcanology 48:275-289
1101 Lautze NC, Taddeucci J, Andronico D, Cannata C, Tornetta L, Scarlato P, Houghton B, Lo
1102 Castro MD (2012) SEM-based methods for the analysis of basaltic ash from weak explosive
1103 activity at Etna in 2006 and the 2007 eruptive risis at Stromboli. Physica and Chemistry of the
1104 Earth 45-46:113-127
1105 Maicher D, White JDL, Batiza R (2000) Sheet hyaloclastite: density-current deposits of quench
1106 and bubble-burst fragments from thin, glassy sheet lava fows, Seamount Six, Eastern Pacific
1107 Ocean. Marine Geology 171:75-94

1108 Mastin LG, Christiansen RL, Thornber C, Lowenstern J, Beeson M (2004) What makes
1109 hydromagmatic eruptions violent? Some insights from the Keanakako'i Ash, Kilauea Volcano,
1110 Hawai'i. Journal of Volcanology and Geothermal Research 137:15-31
1111 Mastin LG, Spieler O, Downey WS (2009) An experimental study of hydromagmatic
1112 fragmentation through energetic, non-explosive magma-water mixing. Journal of Volcanology
1113 and Geothermal Research 180:161-170
1114 Mattox T, Mangan M (1997) Littoral hydrovolcanic explosions: a case study of lava-seawater
1115 interaction at Kilauea volcano Journal of Volcanology and Geothermal Research 75:1-17
1116 Mattsson HB (2010) Textural variation in juvenile pyroclasts from an emergent, Surtseyan-type,
1117 volcanic eruption: The Capela tuff cone, Sao Miguel (Azores). Journal of Volcanology and
1118 Geothermal Research 189:81-91
1119 Mattsson HB, Tripoli BA (2011) Depositional characteristics and volcanic landforms in the Lake
1120 Natron-Engaruka monogenetic field, northern Tanzania. Journal of Volcanology and Geothermal
1121 Research 203:23-34
1122 Moitra P, Gonnerman HM, Houghton BF, Giachetti T (2013) Relating vesicle shapes in
1123 pyroclasts to eruption styles. Bulletin of Volcanology 75:691
1124 Moore JG (1975) Mechansim of formation of pillow lava. American Scientist 63(3):269-277
1125 Moore JG, Calk LC (1991) Degassing and differentiation in subglacial volcanoes, Iceland
1126 Journal of Volcanology and Geothermal Research 46:157-180
1127 Moore JG, Hickson CJ, Calk LC (1995) Tholeiitic-alkalic transition at subglacial volcanoes,
1128 Tuya region, British Columbia, Canada. Journal of Geophysical Research 100(B12):24577-
1129 24592
1130 Murtagh RM, White JDL, Sohn YK (2011) Pyroclast textures of the Ilchulbong 'wet' tuff cone,
1131 Jeju Island Journal of Volcanology and Geothermal Research 201:385-396
1132 Nemeth K, Cronin SJ (2011) Drivers of explosivity and elevated hazard in basaltic fissure
1133 eruptions: The 1913 eruption of Ambrym Volcano, Vanuatu (SW-Pacific). Journal of
1134 Volcanology and Geothermal Research 201:194-209
1135 Parcheta CE, Houghton BF, Swanson DA (2013) Contrasting patterns of vesiculation in low,
1136 intermediate, and high Hawaiian fountains: A case study of the 1969 Mauna Ulu eruption.
1137 Journal of Volcanology and Geothermal Research
1138 Parfitt E, A., Wilson L (2009) Fundamentals of Physical Volcanology In: Blackwell Publishing
1139 Malden, MA, p 230
1140 Polacci M, Baker DR, Bai L, Mancini L (2008) Large vesicles record pathways of degassing at
1141 basaltic volcanoes. Bulletin of Volcanology 70:1023-1029
1142 Portner RA, Daczko NR, Dickinson JA (2010) Vitiriclastic lithofacies from Macquarie Island
1143 (Southern Ocean): compositional influence on abyssal eruption explosivity in a dying Miocene
1144 spreading ridge. Bulletin of Volcanology 72:165-183
1145 Ross P-S, White JDL (2012) Quantification of vesicle characteristics in some diatreme-filling
1146 deposits and the explosivity levels of magma-water interactions within diatremes. Journal of
1147 Volcanology and Geothermal Research 245-246
1148 Ross PS, Delpit S, Haller MJ, Nemeth K, Corbella H (2011) Influence of the substrate on maar-
1149 diatreme volcanoes- An example of a mixed setting from the Pali Aike volcanic field, Argentina
1150 Journal of Volcanology and Geothermal Research 201:253-271

1151 Rosseel J-B, White JDL, Houghton BF (2006) Complex bombs of phreatomagmatic eruptions:
1152 Role of agglomeration and welding in vents of the 1886 Rotomahana eruption, Tarawera, New
1153 Zealand. Journal of Geophysical Research 111:B12205
1154 Schipper CI, Sonder I, Schmid A, White JDL, Dürig T, Zimanowski B, Büttner R (2013) Vapour
1155 dynamics during magma-water interaction experiments: hydromagmatic origins of submarine
1156 volcaniclastic particles (limu o Pele) Geophysical Journal International:1109-1115
1157 Schipper CI, White JDL (2010) No depth limit to hydrovolcanic limo o Pele: analysis of limu
1158 from Lō'ihi Seamount, Hawai'i Bulletin of Volcanology 72:149-164
1159 Schipper CI, White JDL, Houghton BF (2010) Syn- and post-fragmentation textures in
1160 submarine pyroclasts from Lo'ihi Seamount, Hawai'i. Journal of Volcanology and Geothermal
1161 Research 191:93-106
1162 Schipper CI, White JDL, Houghton BF (2011) Textural, geochemical, and volatile evidence for a
1163 Strombolian-like eruption sequence at Lo'ihi Seamount Hawai'i Journal of Volcanology and
1164 Geothermal Research 207:16-32
1165 Schipper CI, White JDL, Houghton BF, Shimizu N, Stewart RB (2010) Explosive submarine
1166 eruptions driven by volatile-coupled degassing at Lo'ihi Seamount, Hawai'i. Earth and Planetary
1167 Science Letters 295:497-510
1168 Schipper CI, White JDL, Houghton BF, Shimizu N, Stewart RB (2010) "Poseidic" explosive
1169 eruptions at Loihi Seamount, Hawaii. Geology 38:291-294
1170 Schipper CI, White JDL, Zimanowski B, Büttner R, Sonder I, Schmid A (2011) Experimental
1171 interaction of magma and "dirty" coolants. Earth and Planetary Science Letters 203:323-336
1172 Schmid A, Sonder I, Seegelken R, Zimanowski B, Büttner R, Gudmundsson MT, Oddsson B
1173 (2010) Experiments on the heat discharge at the dynamic magma-water-interface. Geophysical
1174 Research Letters 37:L.20311
1175 Scott CR, Richard D, Fowler AD (2003) An Archean submarine pyroclastic flow due to
1176 submarine dome collapse: The Hurd Deposit, Harker Township, Ontario, Canada. In: White
1177 JDL, Smellie JL, Clague DA (eds) Subaqueous Explosive Volcanism AGU Washington DC, pp
1178 317-327
1179 Shea T, Houghton BF, Gurioli L, Cashman KV, Hammer JE, Hobden B (2010) Textural studies
1180 of vesicles in volcanic rocks: An integrated methodology. Journal of Volcanology and
1181 Geothermal Research 190:271-289
1182 Simpson K, McPhie J (2001) Fluidal-clast breccia generated by submarine fire fountaining,
1183 Trooper Creek Formation, Queensland, Australia. Journal of Volcanology and Geothermal
1184 Research 109:339-355
1185 Skilling IP (2009) Subglacial to emergent basaltic volcanism at Hlöðufell, south-west Iceland: A
1186 history of ice-confinement. Journal of Volcanology and Geothermal Research 185:276-289
1187 Skilling IP, Mercurio E, Cameron B (2009) Ice-confined basaltic eruptive fissure complexes in
1188 Iceland: Accessible analogs for understanding shallow submarine ridge construction. In: AGU.
1189 AGU, San Fransico
1190 Smellie JL (2001) Lithofacies architecture and construction of volcanoes erupted in englacial
1191 lakes: Icefall Nunatak, Mount Murphy, Eastern Marie Byrd Land, Antarctica In: White JDL,
1192 Riggs NR (eds) Volcaniclastic Sedimentation in Lacustrine Settings. Blackwell Science Ltd,
1193 London, p 309

Smellie JL, Hole MJ (1997) Products and processes in Pliocene-Recent, subaqueous to emergent volcanism in the Antarctic Peninsula: examples of englacial Surtseyan volcano construction. Bulletin of Volcanology 58:628-646
Smellie JL, Johnson JS, McIntosh WC, Esser R, Gudmundsson MT, Hambrey MJ, van Wyk de Vries B (2008) Six million years of glacial history recorded in volcanic lithofacies of the James Ross Island Volcanic Group, Antarctic Peninsula. Palaeogeography, Palaeoclimatology, Palaeoecology 260:122-148
Sohn RA, Willis C, Humphris S, Shank TM, Singh H, Edmonds HN, Kunz C, Hedman U, Helmke E, Jakuba M, Liljebladh B, Linder J, Murphy C, Nakamura K-i, Sato T, Schlindwein V, Stranne C, Tausenfruen M, Upchurch L, Winsor P, Jakobsson M, Soule AA (2008) Explosive volcanism on the ultraslow-spreading Gakkel ridge, Arctic Ocean. Nature 453:1236-1238
Sohn YK (1995) Geology of Tok Island, Korea: eruptive and depositional processes of a shoaling to emergent island volcano. Bulletin of Volcanology 56:660-674
Solgevik H, Mattson HB, Hermelin O (2007) Growth of an emergent tuff cone: Fragmentation and depositional processes recorded in teh Capelas tuff cone, Sao Miguel, Azores. Journal of Volcanology and Geothermal Research 159:246-266
Sorrentino L, Cas RAF, Stilwell JD (2011) Evolution and facies architecture of Paleogene Surtseyan volcanoes on Chatham Islands, New Zealand, Southwest Pacific Ocean Journal of Volcanology and Geothermal Research 202:1-21
Staudigel H, Schmincke H-U (1984) The Pliocene Seamount Series of La Palma/Canary Islands. Journal of Geophysical Research 89(B13):11195-11215
Stovall WK, Houghton BF, Gonnermann H, Fagents S, Swanson DA (2011) Eruption dynamics of Hawaiian-style fountains: the case study of episde 1 of the Kilauea Iki 1959 eruption. Bulletin of Volcanology 73:511-529
Walker GPL (1992) Morphometric study of pillow-size specturm among pillow lavas. Bulletin of Volcanology 54:459-474
Walker GPL, Croasdale R (1971) Characteristics of some basaltic pyroclasts. Bulletin of Volcanology 35:303-317
Werner R, Schmincke H-U (1999) Englacial vs lacustrine origin of volcanic table mountains: evidence from Iceland. Bulletin of Volcanology 60:335-354
Werner R, Schmincke H-U, Sigvaldason GE (1996) A new model for the evolution of table mountains: volcanological and petrological evidence from Herdubreid and Herdubreidartögl volcanoes (Iceland) Geol Rundsch 85:390-397
White JDL (1996) Impure coolants and interaction dynamics of phreatomagmatic eruptions. Journal of Volcanology and Geothermal Research 74:155-170
White JDL (1996) Pre-emergent construction of a lacustrine basaltic volcano, Pahvant Butte, Utah (USA). Bulletin of Volcanology 58:249-262
White JDL (2000) Subaqueous eruption-fed density currents and their deposits. Precambrain Research 101:87-109
White JDL, Ross PS (2011) Maar-diatreme volcanoes: A review. Journal of Volcanology and Geothermal Research 201:1-29
Wohletz KH (1986) Explosive magma-water interactions: Thermodynamics, explosions mechansims, and field studies. Bulletin of Volcanology 48:245-264
Wohletz KH (2002) Water/magma interaction: some theory and experiments on peperite formation. Journal of Volcanology and Geothermal Research 114:19-35

Wohletz KH (2003) Water/magma interaction: physical considerations for the deep submarine environment. In: White JDL, Smellie JL, Clague DA (eds) Explosive Subaquous Volcanism AGU Washington DC, pp 25-49
Zimanowski B, Büttner R (2002) Dynamic mingling of magma and liquefied sediments Journal of Volcanology and Geothermal Research 114:37-44
Zimanowski B, Büttner R (2003) Phreatomagmatic explosions in subaqueous volcanism. In: White JDL, Smellie JL, Clague DA (eds) Explosive Subaqueous Volcansim. AGU, Washington DC, pp 51-60
Zimanowski B, Büttner R, Lorenz V (1997) Premixing of magma and water in MFCI experiements Bulletin of Volcanology 58:491-495
Zimanowski B, Wohletz KH (2000) Physics of Phreatomagmatism-1. Terra Nostra 6:515-523
Zimanowski B, Wohletz KH, Dellino P, Büttner R (2003) The volcanic ash problem. Journal of Volcanology and Geothermal Research 122:1-5

Figure captions

Figure 1 Location of Askja, Iceland including locations of pillow lava, breccia to lapilli tuff sequences. The shaded area represents the field area, Austurfjöll. Sample sites are located in major gullies incised into the base of the glaciovolcanic sequence of Askja. Sample locations from north to south are Drekagil (DG), Nautagil (NG), and Rosagil (RG).

Figure 2 Overview of Drekagil sequence including field image, annotated sketch of sampling sites and stratigraphic log.

Figure 3 Overview of the Nautagil sequence including field image, annotated sketch of sampling sites, and stratigraphic log.

Figure 4 Overview of the Rosagil sequence including field image, annotated sketch of sampling sites, and stratigraphic log.

Figure 5 Comparison of the two dominant pillow lava facies from Austurfjöll. Schematics of the pillow form outlines highlight the regularity of Pl1 and the irregularity of Pl2 lavas.

Figure 6 Field images and schematic characterizations of outsized clasts found within the three sequences described at Askja. A) Image of a broken pillow clast displaying typical rind and vesicle textures of a pillow. B) A fluidal bomb displaying irregular shape and vesicle distribution. Sketches of idealized clasts include a pillow in cross-section, a fluidal bomb in cross-section and an angular block.

Figure 7 Stratigraphic overview of a typical effusive to explosive transitional deposit from Askja. Three grain sizes (blocks/bombs, lapilli, and fine ash) were analyzed for size, morphology, and vesicularity as they trend up section. Bombs are described by maximum clast diameter. Vesicularity of both bombs and lapilli are presented as average values for a stratigraphic layer. Vesicle morphology is presented as representative shapes from actual lapilli measured. The fine ash morphologies are presented as percents of relative abundance through the sequence.

Figure 8 Examples of lapilli and fluidal bomb morphologies and textures that reflect ductile fragmentation of the magma. Images on the right hand side are field images. Images on the left hand side are from a binocular microscope. A) Ductile structures in a lapillus quench crust. B) Large coalesced vesicles in a fluidal bomb. C) Fluidal crust structures preserved on a lapillus by surrounding matrix (indicated by yellow line). D) Convolute bomb shape and vesicles. E) Large coalesced bubbles interacting with the clast surface. F) Fluidal bomb with intact quench rind

(broken for sampling). G) Lapillus with stretched vesicles along glassy surface. H) Fluidal bomb with large randomly distributed vesicles. A brittle overprinting is present in images A, E and G, where the lapilli have been brittlely fractured.

Figure 9 SEM secondary electron images of example grain morphologies found in textural analysis of fine ash particles. Adhering particles and aggregate ash particles are common. Arrows are used to highlight features of interest. A) Blocky grain and (left) and fragile spine on margin of a vesicle influenced grain boundary (right) from DG. B) Tube vesicles from DG. C) Vesicles isolated within glassy ash particles from DG. Vesicles may intersect fracture surfaces they do not control the fracture shape. D) Limu o Pele from DG. E) A particle with vesicle-dominated fracture surfaces and fragile spines from NG. F) Ash particles dominated by vesicles From NG. G) Elongate bladed shaped vesicle free particles From DG. Note the micron scale crust flaking off the particle. H) Blocky particles exhibiting scalloped edges from NG. I) Chip and blocky shaped particles from NG. Note the stepped appearance of the conchoidal fracture.

Figure 10~~1~~0 Model of fragmentation mechanisms as they occur during the formation of the three transitional sequences at Askja. Solid lines represent relative dominance of a fragmentation style. Dotted lines indicate continued, but diminished fragmentation. The question mark indicates that the final position of magmatic fragmentation is an inference as the signature is muted by FCI activity by this stratigraphic level. The textures used to construct the model are described.

Table 1 XRF bulk rock major element analyses for basal pillows and clastic samples. The results show that there is little variability internally in the sequence.

	Nautagil			Drekagil	
wt %	Basal Pillow	Breccia Fluidal Bomb	LT Lapilli clast	Basal Pillow	LT Fluidal bomb
SiO2	50.51	50.43	50.70	50.28	50.16
TiO2	2.492	2.506	2.509	1.939	1.911
Al2O3	13.22	13.23	13.24	14.35	14.06
FeOx	13.79	14.09	14.04	12.10	12.59
MnO	0.239	0.241	0.237	0.211	0.214
MgO	5.42	5.00	5.37	6.36	6.58
CaO	9.95	9.89	9.84	11.81	11.38
Na2O	2.56	2.58	2.59	2.33	2.23
K2O	0.48	0.48	0.49	0.31	0.30
P2O5	0.270	0.276	0.273	0.212	0.207
Total	98.92	98.73	99.28	99.90	99.63

1313

1314

1315

Table 2 of parameters used for the distinction of magmatic vs. phreatomagmatic fragmentation of basaltic magma. Focus is placed on pyroclast textures and properties. Some references refer to more evolved melts. Relevant details on the glassy clasts at Askja is included. One of the major challenges with all of the methods listed above is they focus on 'ideal' textural parameters from pure end member fragmentation, however, natural eruptions show variable eruptive styles and intensity even without the added variable of external water. In order to discriminate fragmentation methods in any natural deposit it is best to assume that fragmentation styles likely overlap and overprint their signature on the deposit under study. The greatest number of corroborating parameters (type of geologic evidence) then serves as the strongest argument for the dominant mechanism of fragmentation producing a deposit.

Parameters	Magmatic	Phreatomagmatic	Grain size	References	Askja	Value as a discriminator
Vesicularity (volume %)	>75%	<40% (as low as 6%)	Lapilli and >64 mm	Brown et al. 1994; Cas et al. 2003; DeRosa 1999; Ersoy et al. 2006; Head and Wilson 2003; Houghton and Schmincke 1989; Houghton and Wilson 1989; Houghton and Gonnerman 2008; Lautze and Houghton2007; Murtagh et al. 2011; Ross and White 2012	Variable 20-60%	**Low** Indicates whether a magma experienced degassing. Only records part of the degassing history. Degassing history can be further elucidated with the use of melt inclusion data and volatile analyses.
Lithic presence	Low to none	Typically high	Lapilli and >64 mm	Ersoy et al. 2006; Houghton and Schmincke 1989; Mutagh et al. 2011; Ross and White 2012 ; Sohn 1995; Walker and Crossdale 1971	Less than 1% of one of three deposits	**Moderate to High** The absence of lithic materials does not preclude the phreatomagmatic activity.
Sideromelane vs. tachylite	Dominated by tachylite	Dominated by sideromelane	Fine ash, coarse ash and lapilli	Heiken 1971; DeRosa 1999; Murtagh et al. 2011; Schipper et al. 2011a	Sideromelane dominated ash & lapilli	**Moderate** Useful at some grain sizes and is dependent on preservation
Vesicle Number Density (VND)	10^3-10^8	10^2 -10^5	Ash and fine lapilli	Houghton and Gonnermann 2008; Lautz et al. 2012; Murtagh, et al. 2011; Parcheta et al. 2013; Shea et al. 2010; Stovall et al. 2011	10^3 reflecting a high degree of coalescence	**Low** Recent studies suggest there is no correlation between these fragmentation mechanisms and VND (Ross and White 2012; Mattsson 2010).
Vesicle morphology	Spherical to polylobate or tube vesicles (variable sizes)	Spherical (small) BUT may preserve vesicle textures of a previously degassed magma.	Lapilli	Büttner et al. 1999; Houghton and Gonnerman 2008; Kokelaar 1986; Mastin et al. 2009; Moitra.et al. 2013; Murtagh et al. 2011; Parcheta et al. 2013; Polacci et al. 2008; Stovall et al. 2011; Zimanowski et al. 2003	Polylobate (vesicles up to 1-2 cm) , elongate at clast margins	**Moderate** Reflects the relative timing of degassing and cooling. As well as whether or not the gas is coupled with the magma. May indicate post-fragmentation degassing.
Vesicle textures at clast margins	Deformed vesicles at margins	Fractured with no trend in vesicles	>64 mm	Büttner et al. 1999; Eissen et al. 2003; Kokelaar 1986; Lautze and Houghton 2007; Mastin et al. 2009; Zimanowski and Büttner 2003; Zimanowski and Wohletz 2000	Deformed vesicles at margins	**High** Indicates the timing of deformation relative to fragmentation.
Ash clast morphology	Fractures at margins controlled by vesicles	Blocky – no obvious control of vesicles on fracture position	Very fine ash	Büttner and Zimanowski 1998; Durig et al 2012; Dellino and Liotino 2002; Dellino et al., 2001; Dellino and La Volpe 1996; Heiken 1971; Mattson 2010; Mattox and Mangan 1997; Zimanowski et al 1997	Increasing blocky fine ash presence up section	**Moderate** Can provide supporting information. May be over emphasized as an independent discriminator.
Juvenile Lapilli morphology	Fluidal, achnelith, ragged, blocky	Equant and blocky to fluidal (globules), accretionary lapilli	Lapilli	Lautze and Houghton 2007; Houghton and Gonnerman 2008; Houghton and Smith 1993; Mastin et al. 2009; Portner et al. 2010; Schipper et al. 2010a; Stovall et al. 2011	Narrow grain size (1-3 cm) and fluidal to equant.	**Low** While lapilli are the dominant grain size in basaltic magmatic and phreatomagmatic deposits. Not many studies have focused on

						the grain shape of this size. Quench granulation produces blocky grain sizes in the lapilli range.
Juvenile bomb morphology	Diverse shapes, rough edges, breadcrust textures, varieties of fluidal shapes (ribbon, cow pie etc.)	Cored bombs, Limited fluidal shapes Juvenile bombs are subordinate to finer fractions and lithic blocks.	>64 mm	Cas et al. 2003; Dellino et al. 2001; Heiken 1971;Houghton and Gonnermann 2008; Houghton and Nairn 1991; Houghton and Schmincke 1989; Houghton and Smith1994; Mattox and Mangan 1997; Murtagh et al. 2011; Rosseel et al. 2006; Ross et al. 2011; Ross and White, 2012; Simpson and McPhie 2001; Sorrentino et al. 2011; Staudigel and Schmincke 1984; Walker and Croasdale 1971	Fluidal at bomb and lapilli scale Initially bomb dominant, lapilli dominates within a few meters	**Low to Moderate** Useful in context and concentration
Crystal content (microlites by volume %)	0-50%	3-20%	Lapilli to ash	De Rossa 1999; Mattsson 2010; Murtagh et al. 2011; Ross and White 2012; Sable et al. 2006	<15% No free crystals	**Low** Higher crystalinity is typically associated with greater cooling time (slower ascent rates, slower decompression), but no trends have been observed indicative of these fragmentation processes. Free crystals may be indicative of more efficient fragmentation according to DeRosa (1999).
Deformation regime	Ductile (exceptions with high viscosity and high strain rate)	Brittle (time is less than viscous relaxation time)	All (perdominantly lapilli and ash)	Dürig et al. 2012a; Dürig et al. 2012b; Zimanowski et al. 2003; Mattsson 2010; Mattsson and Tripoli 2011	Shift of ductile dominated particles to brittle dominated particles	**Low to Moderate** Indicates rate of strain relative to viscosity of a fluid. In basaltic fluids FCI explosions occur at a higher rate than internal gas expansion. Dependent on rate of eruption, vent geometries and fluid viscosity.
Abundance of very fine ash	Low to moderate	Moderate to high	Fine ash	Houghton and Nairn 1991; Zimanowski et al. 1997 FCI 1-10% of the deposit Dellino and La Volpe 1996	Increase in presence of fine ash	**Moderate** Useful when stratigraphy is available. The presence of finer grain sizes indicates the efficiency of fragmentation. In FCI only a small portion of the material is actively involved in the explosion to reflect this efficiency.
Welding	Low to high	Low (emergent) to none (subaqueous)	Bombs	Rosseel et al. 2006	None	**High** Only when present. The absence of welding does not exclude magmatic fragmentation.
Limu o Pele	5%	5%	Fine ash to lapilli	Clague et al. 2009; Maicher et al. 2000; Schipper and White 2009; Schipper et al. 2013	Minor <4% in fine ash	**Low** The presence of limu oPele indicates the presence of water, but the significance as it relates to the nature of fragmentation is yet unknown (Schipper et al. 2013).

1316

1317
1318
1319
1320
1321

Table 1.docx
Click here to download Table: Table 1.docx

Table 1 XRF bulk rock major element analyses for basal pillows and clastic samples. The results show that there is little variability internally in the sequence.

	Nautagil			Drekagil	
wt %	Basal Pillow	Breccia Fluidal Bomb	LT Lapilli clast	Basal Pillow	LT Fluidal bomb
SiO2	50.51	50.43	50.70	50.28	50.16
TiO2	2.492	2.506	2.509	1.939	1.911
Al2O3	13.22	13.23	13.24	14.35	14.06
FeOx	13.79	14.09	14.04	12.10	12.59
MnO	0.239	0.241	0.237	0.211	0.214
MgO	5.42	5.00	5.37	6.36	6.58
CaO	9.95	9.89	9.84	11.81	11.38
Na2O	2.56	2.58	2.59	2.33	2.23
K2O	0.48	0.48	0.49	0.31	0.30
P2O5	0.270	0.276	0.273	0.212	0.207
Total	98.92	98.73	99.28	99.90	99.63

Table 2.docx
Click here to download Table: Table 2.docx

Table 2 of parameters used for the distinction of magmatic vs. phreatomagmatic fragmentation of basaltic magma. Focus is placed on pyroclast textures and properties. Some references refer to more evolved melts. Relevant details on the glassy clasts at Askja is included. One of the major challenges with all of the methods listed above is they focus on 'ideal' textural parameters from pure end member fragmentation, however, natural eruptions show variable eruptive styles and intensity even without the added variable of external water. In order to discriminate fragmentation methods in any natural deposit it is best to assume that fragmentation styles likely overlap and overprint their signature on the deposit under study. The greatest number of corroborating parameters (type of geologic evidence) then serves as the strongest argument for the dominant mechanism of fragmentation producing a deposit.

Parameters	Magmatic	Phreatomagmatic	Grain size	References	Askja	Value as a discriminator
Vesicularity (volume %)	>75%	<40% (as low as 6%)	Lapilli and >64 mm	Brown et al. 1994; Cas et al. 2003; DeRosa 1999; Ersoy et al. 2006; Head and Wilson 2003; Houghton and Schmincke 1989; Houghton and Wilson 1989; Houghton and Gonnerman 2008; Lautze and Houghton2007; Murtagh et al. 2011; Ross and White 2012	Variable 20-60%	**Low** Indicates whether a magma experienced degassing. Only records part of the degassing history. Degassing history can be further elucidated with the use of melt inclusion data and volatile analyses.
Lithic presence	Low to none	Typically high	Lapilli and >64 mm	Ersoy et al. 2006; Houghton and Schmincke 1989; Mutagh et al. 2011; Ross and White 2012 ; Sohn 1995; Walker and Crossdale 1971	Less than 1% of one of three deposits	**Moderate to High** The absence of lithic materials does not preclude the phreatomagmatic activity.
Sideromelane vs. tachylite	Dominated by tachylite	Dominated by sideromelane	Fine ash, coarse ash and lapilli	Heiken 1971; DeRosa 1999; Murtagh et al. 2011; Schipper et al. 2011a	Sideromelane dominated ash & lapilli	**Moderate** Useful at some grain sizes and is dependent on preservation
Vesicle Number Density (VND)	10^3-10^8	10^2 -10^5	Ash and fine lapilli	Houghton and Gonnermann 2008; Lautz et al. 2012; Murtagh, et al. 2011; Parcheta et al. 2013; Shea et al. 2010; Stovall et al. 2011	10^3 reflecting a high degree of coalescence	**Low** Recent studies suggest there is no correlation between these fragmentation mechanisms and VND (Ross and White 2012; Mattsson 2010).
Vesicle morphology	Spherical to polylobate or tube vesicles (variable sizes)	Spherical (small) BUT may preserve vesicle textures of a previously degassed magma.	Lapilli	Büttner et al. 1999; Houghton and Gonnerman 2008; Kokelaar 1986; Mastin et al. 2009; Moitra.et al. 2013; Murtagh et al. 2011; Parcheta et al. 2013; Polacci et al. 2008; Stovall et al. 2011; Zimanowski et al. 2003	Polylobate (vesicles up to 1-2 cm) , elongate at clast margins	**Moderate** Reflects the relative timing of degassing and cooling. As well as whether or not the gas is coupled with the magma. May indicate post-fragmentation degassing.
Vesicle textures at clast margins	Deformed vesicles at margins	Fractured with no trend in vesicles	>64 mm	Büttner et al. 1999; Eissen et al. 2003; Kokelaar 1986; Lautze and Houghton 2007; Mastin et al. 2009; Zimanowski and Büttner 2003; Zimanowski and Wohletz 2000	Deformed vesicles at margins	**High** Indicates the timing of deformation relative to fragmentation.
Ash clast morphology	Fractures at margins controlled by vesicles	Blocky – no obvious control of vesicles on fracture position	Very fine ash	Büttner and Zimanowski 1998; Durig et al 2012; Dellino and Liotino 2002; Dellino et al., 2001; Dellino and La Volpe 1996; Heiken 1971; Mattson 2010; Mattox and Mangan 1997; Zimanowski et al 1997	Increasing blocky fine ash presence up section	**Moderate** Can provide supporting information. May be over emphasized as an independent discriminator.
Juvenile Lapilli morphology	Fluidal, achnelith, ragged, blocky	Equant and blocky to fluidal (globules), accretionary lapilli	Lapilli	Lautze and Houghton 2007; Houghton and Gonnerman 2008; Houghton and Smith 1993; Mastin et al. 2009; Portner et al. 2010; Schipper et al. 2010a; Stovall et al. 2011	Narrow grain size (1-3 cm) and fluidal to equant.	**Low** While lapilli are the dominant grain size in basaltic magmatic and phreatomagmatic deposits. Not many studies have focused on the grain shape of this size. Quench granulation produces blocky grain sizes in the

						lapilli range.
Juvenile bomb morphology	Diverse shapes, rough edges, breadcrust textures, varieties of fluidal shapes (ribbon, cow pie etc.)	Cored bombs, Limited fluidal shapes Juvenile bombs are subordinate to finer fractions and lithic blocks.	>64 mm	Cas et al. 2003; Dellino et al. 2001; Heiken 1971;Houghton and Gonnermann 2008; Houghton and Nairn 1991; Houghton and Schmincke 1989; Houghton and Smith1994; Mattox and Mangan 1997; Murtagh et al. 2011; Rosseel et al. 2006; Ross et al. 2011; Ross and White, 2012; Simpson and McPhie 2001; Sorrentino et al. 2011; Staudigel and Schmincke 1984; Walker and Croasdale 1971	Fluidal at bomb and lapilli scale Initially bomb dominant, lapilli dominates within a few meters	**Low to Moderate** Useful in context and concentration
Crystal content (microlites by volume %)	0-50%	3-20%	Lapilli to ash	De Rossa 1999; Mattsson 2010; Murtagh et al. 2011; Ross and White 2012; Sable et al. 2006	<15% No free crystals	**Low** Higher crystalinity is typically associated with greater cooling time (slower ascent rates, slower decompression), but no trends have been observed indicative of these fragmentation processes. Free crystals may be indicative of more efficient fragmentation according to DeRosa (1999).
Deformation regime	Ductile (exceptions with high viscosity and high strain rate)	Brittle (time is less than viscous relaxation time)	All (perdominantly lapilli and ash)	Dürig et al. 2012a; Dürig et al. 2012b; Zimanowski et al. 2003; Mattsson 2010; Mattsson and Tripoli 2011	Shift of ductile dominated particles to brittle dominated particles	**Low to Moderate** Indicates rate of strain relative to viscosity of a fluid. In basaltic fluids FCI explosions occur at a higher rate than internal gas expansion. Dependent on rate of eruption, vent geometries and fluid viscosity.
Abundance of very fine ash	Low to moderate	Moderate to high	Fine ash	Houghton and Nairn 1991; Zimanowski et al. 1997 FCI 1-10% of the deposit Dellino and La Volpe 1996	Increase in presence of fine ash	**Moderate** Useful when stratigraphy is available. The presence of finer grain sizes indicates the efficiency of fragmentation. In FCI only a small portion of the material is actively involved in the explosion to reflect this efficiency.
Welding	Low to high	Low (emergent) to none (subaqueous)	Bombs	Rosseel et al. 2006	None	**High** Only when present. The absence of welding does not exclude magmatic fragmentation.
Limu o Pele	5%	5%	Fine ash to lapilli	Clague et al. 2009; Maicher et al. 2000; Schipper and White 2009; Schipper et al. 2013	Minor <4% in fine ash	**Low** The presence of limu oPele indicates the presence of water, but the significance as it relates to the nature of fragmentation is yet unknown (Schipper et al. 2013).

Figure1(f2).tif
Click here to download high resolution image

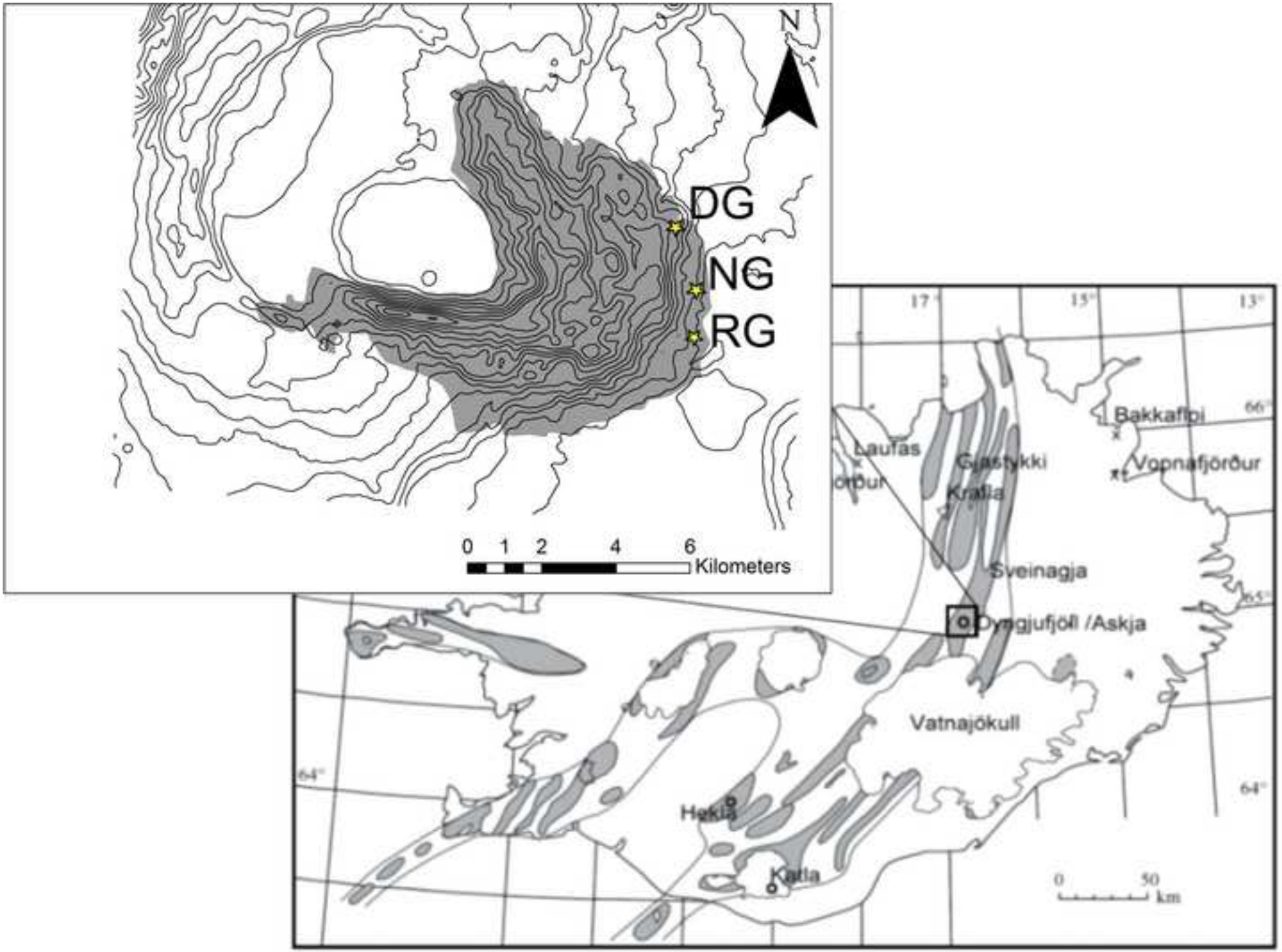

Figure2(f).tif
Click here to download high resolution image

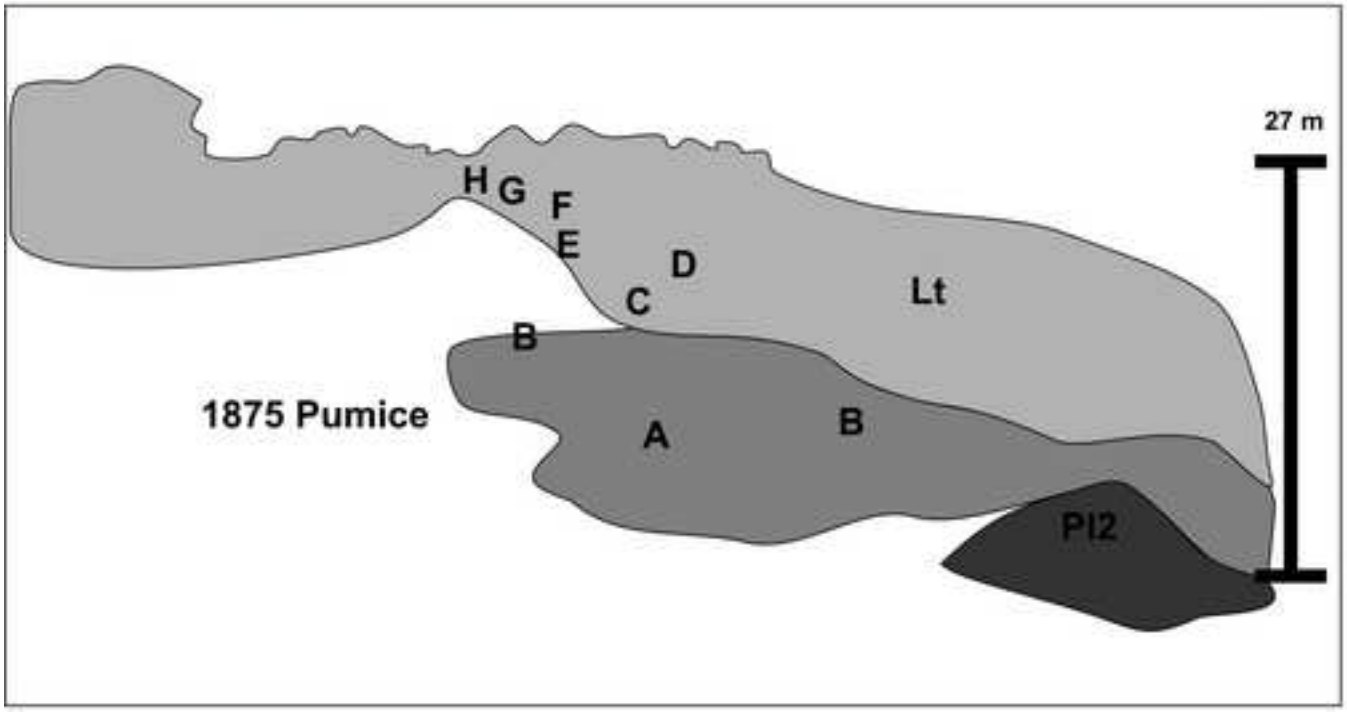

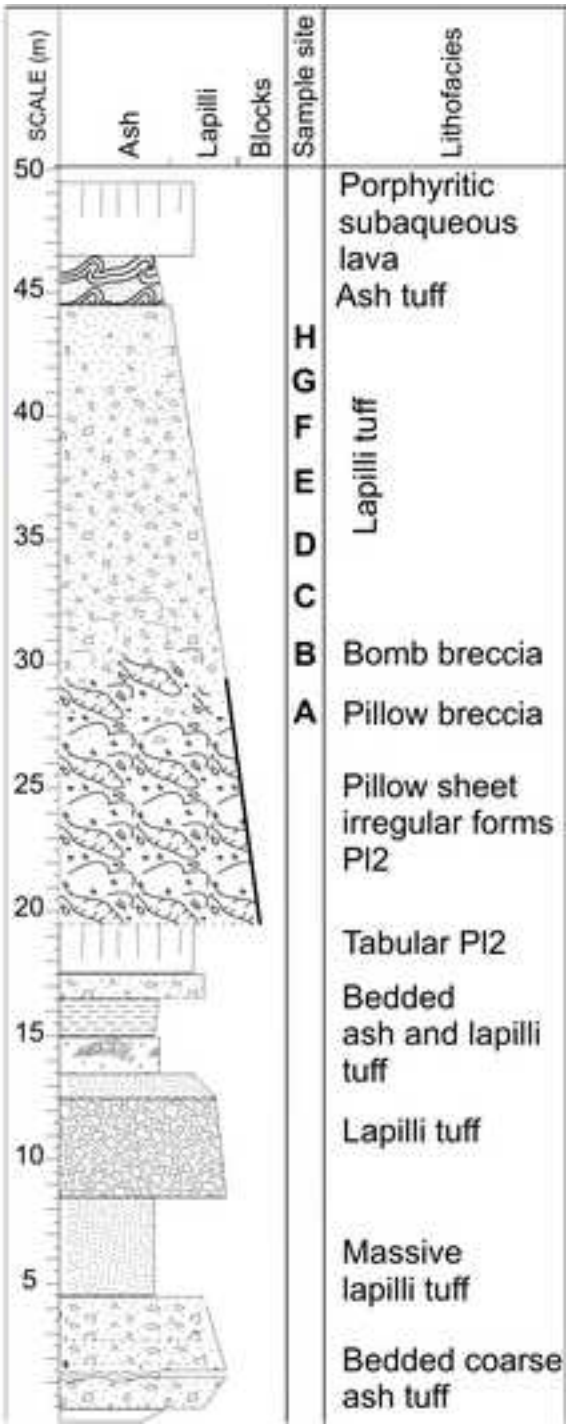

Figure3(f).tif
Click here to download high resolution image

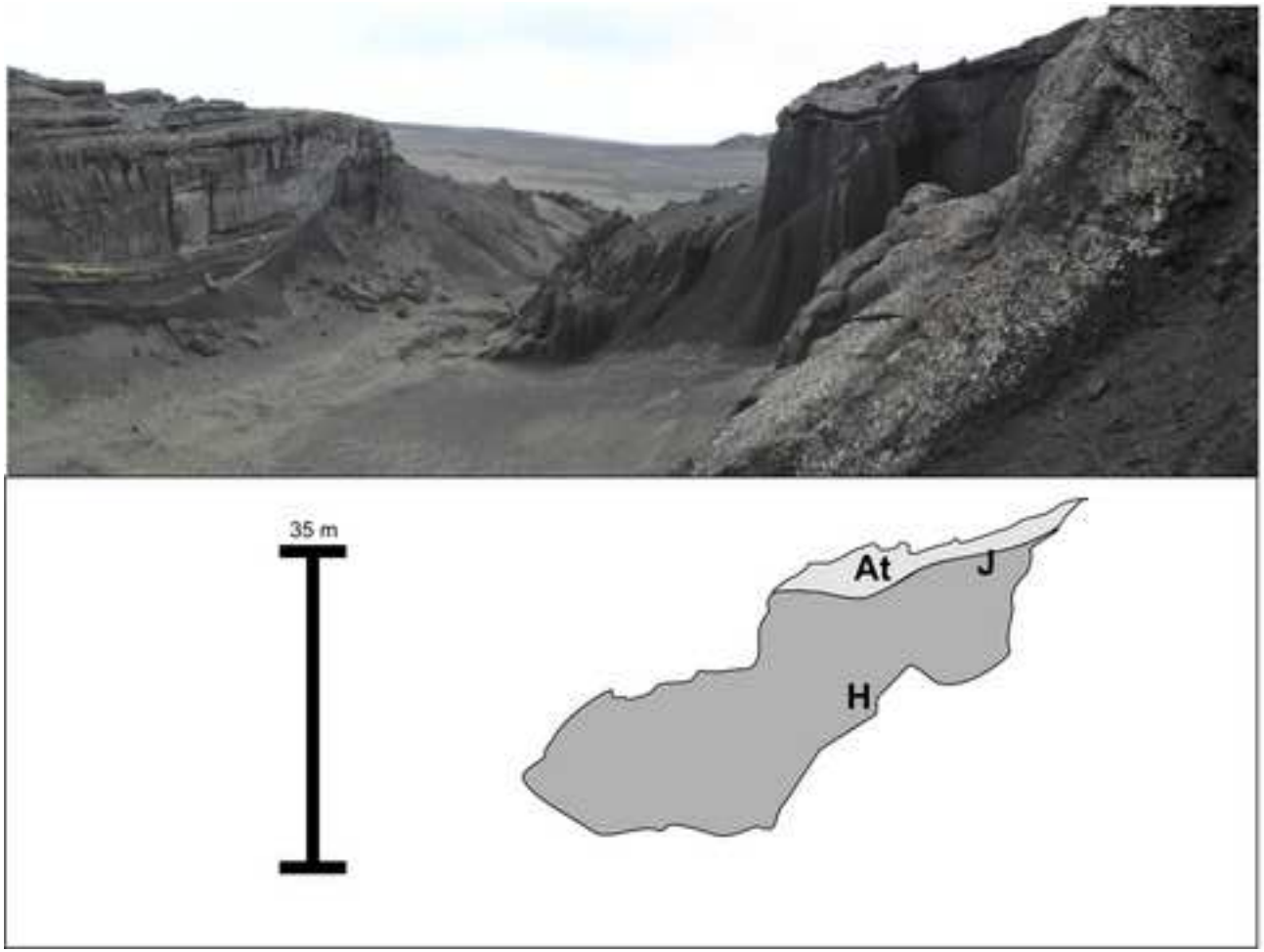

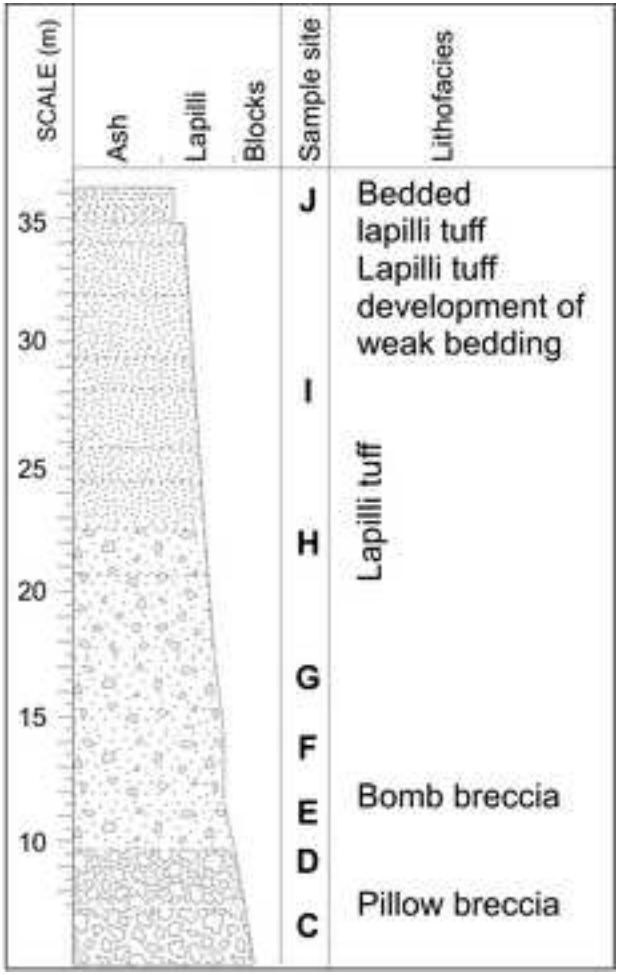

figure4(f).tif
Click here to download high resolution image

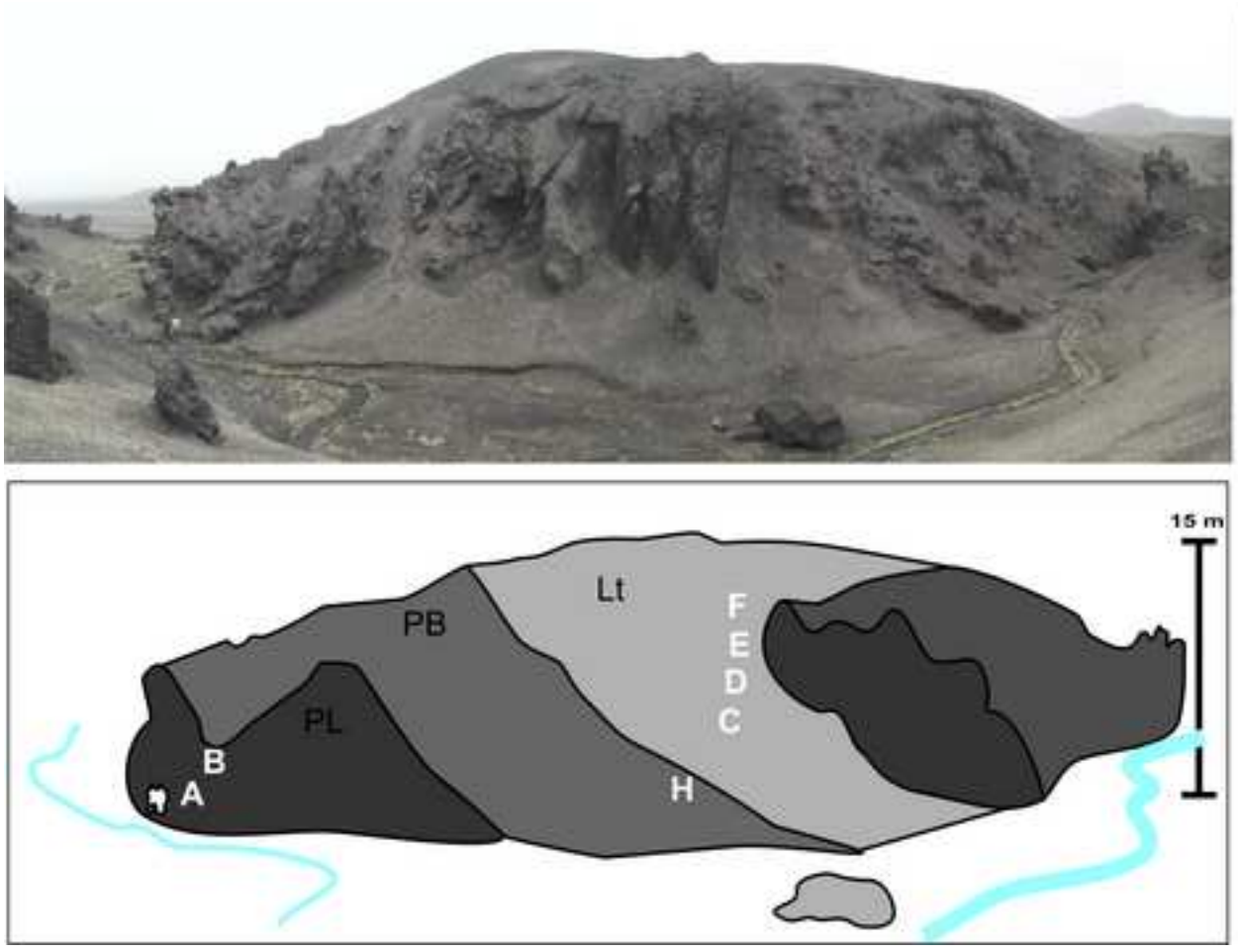

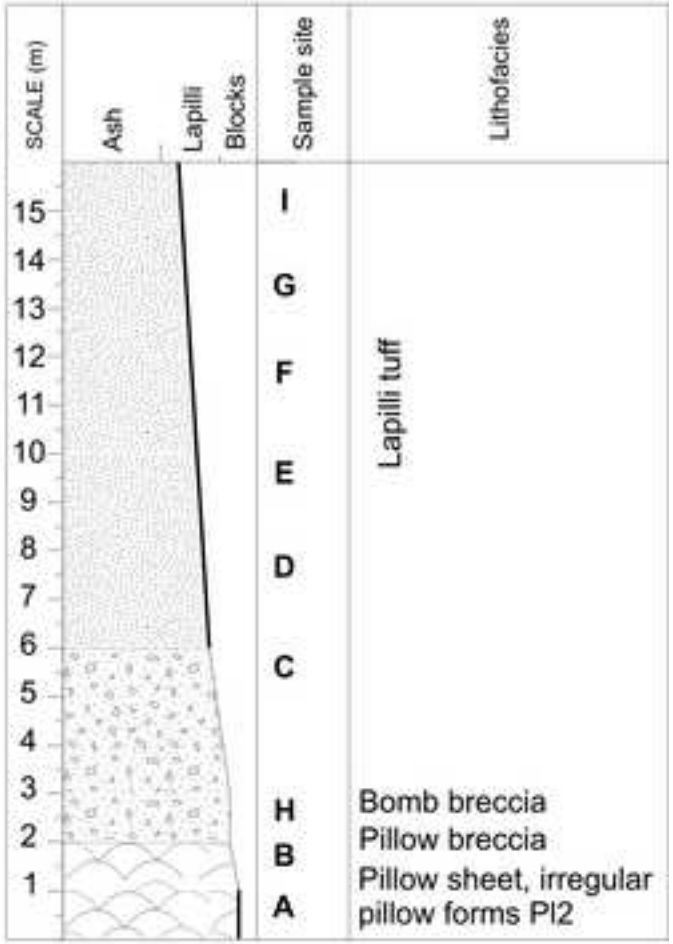

figure5(f).tif
Click here to download high resolution image

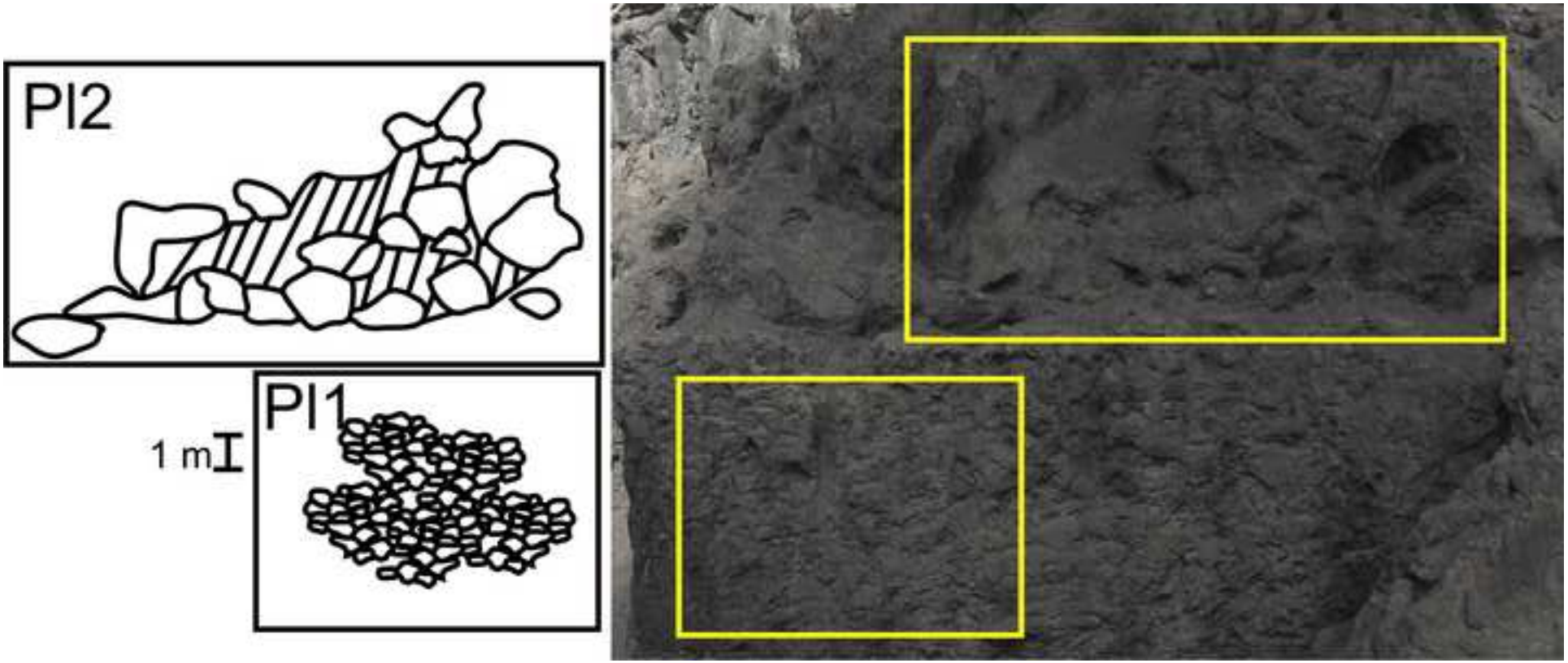

figure6(3).tif
Click here to download high resolution image

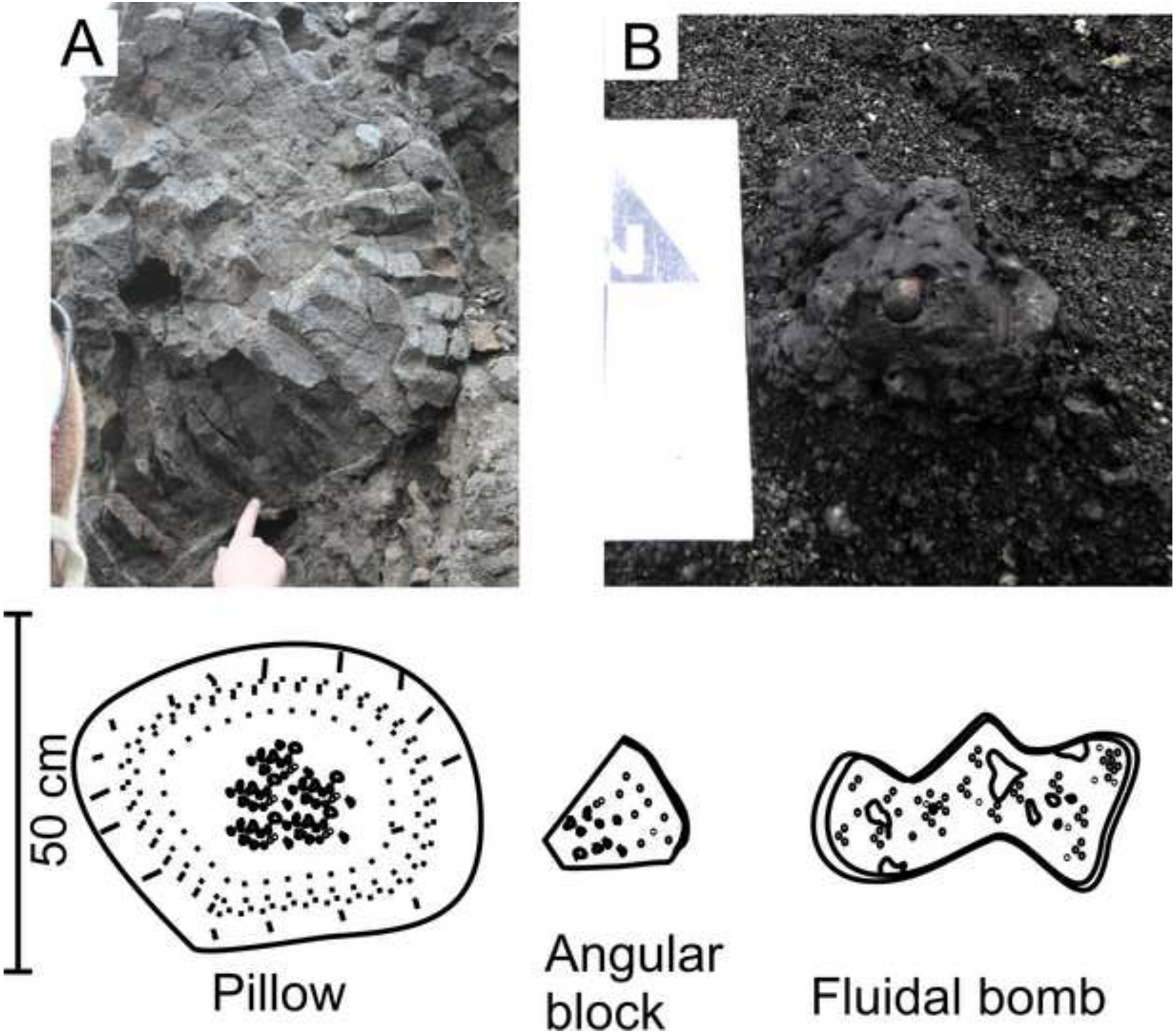

figure7(3).tif
Click here to download high resolution image

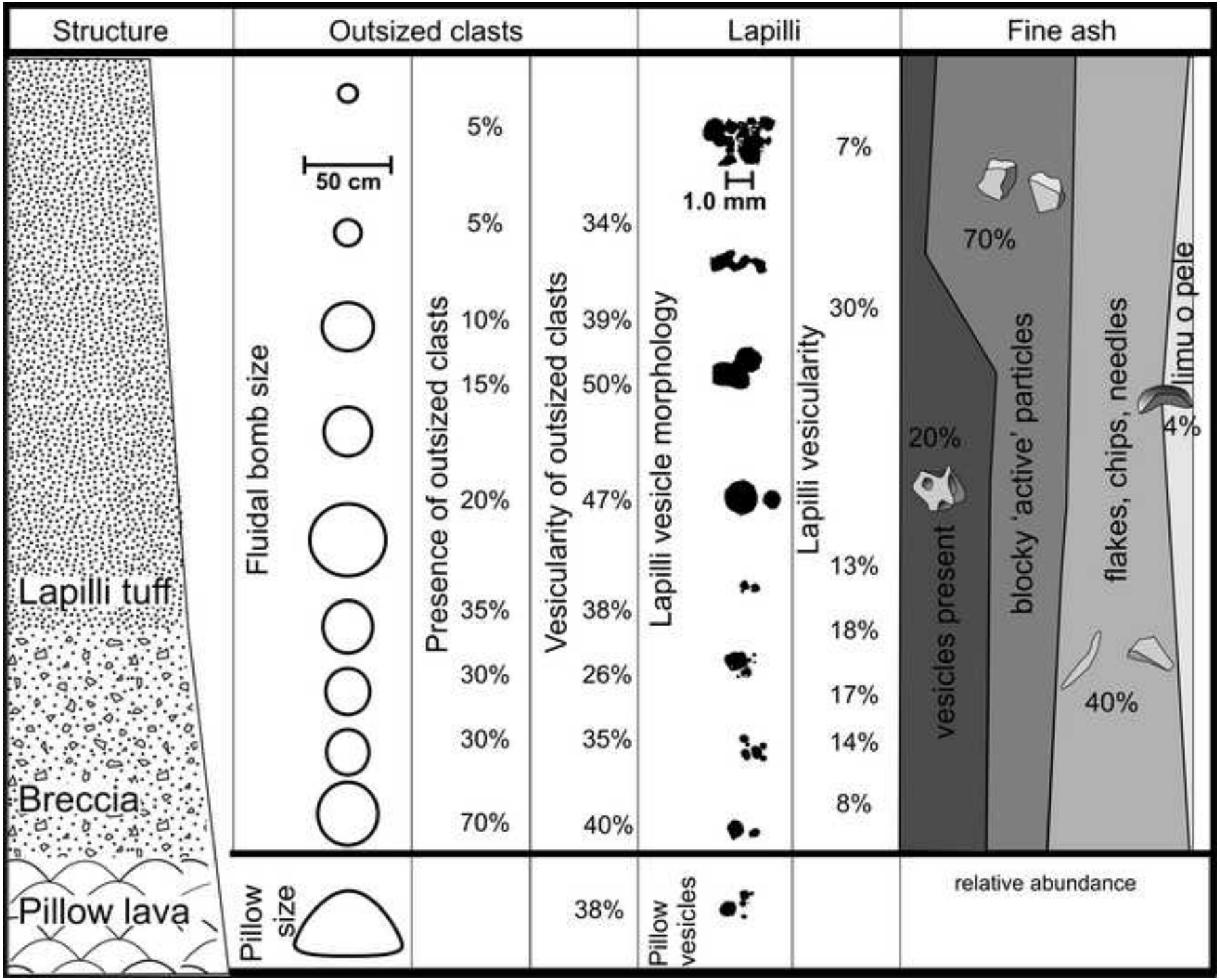

Figure8(3).tif
Click here to download high resolution image

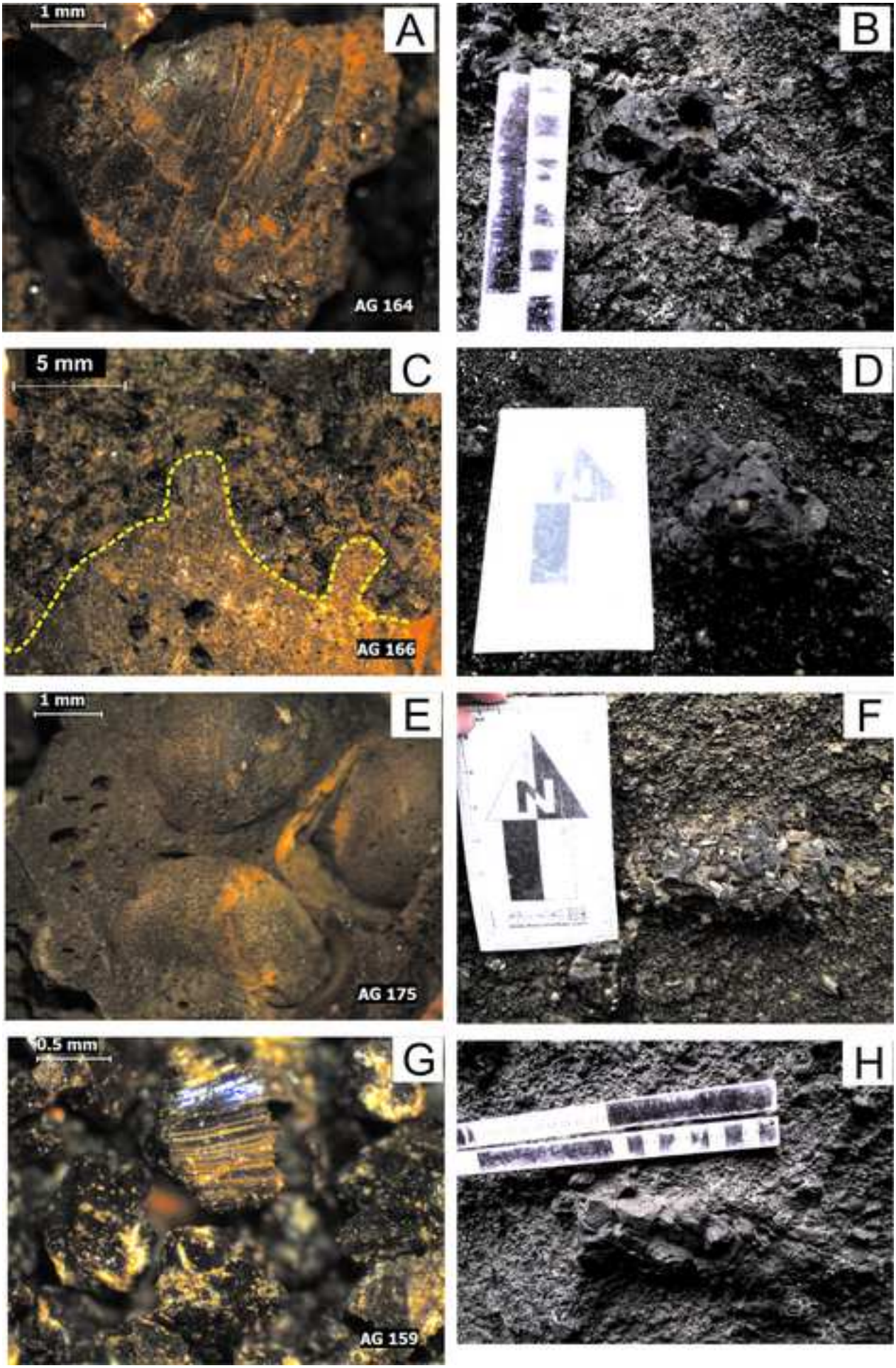

figure9(f).tif
Click here to download high resolution image

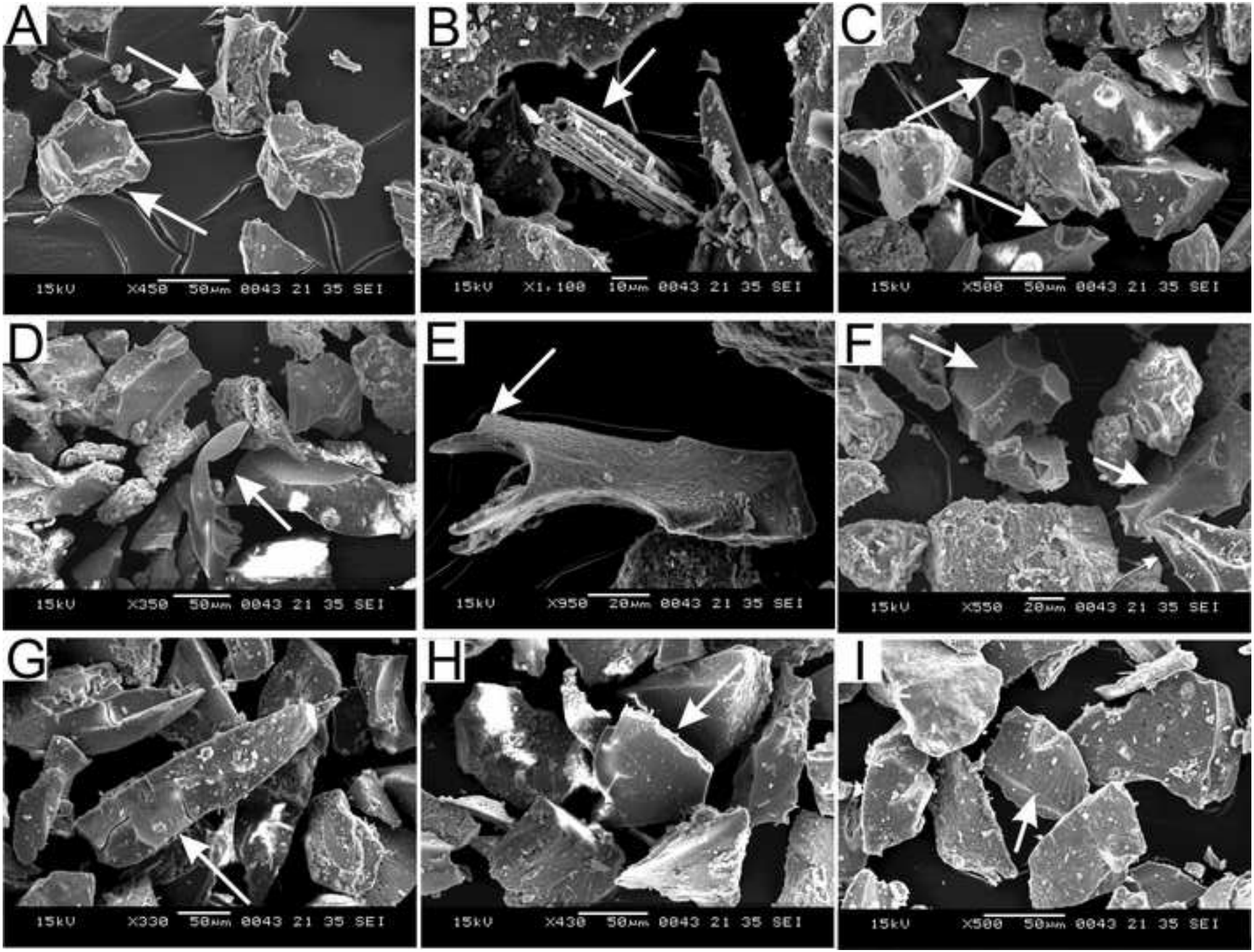

figure10(f).tif
Click here to download high resolution image